Master's thesis

NTNU
Norwegian University of Science and Technology
Faculty of Engineering
Department of Manufacturing and Civil Engineering

Zeid Sherpour

Development of CT-based Finite Element Modeling for Timber Board Stiffness Prediction

Master's thesis in Civil and Environmental Engineering - Digital Building Processes
Supervisor: Guomin Ji
Co-supervisor: Johannes Huber
June 2023

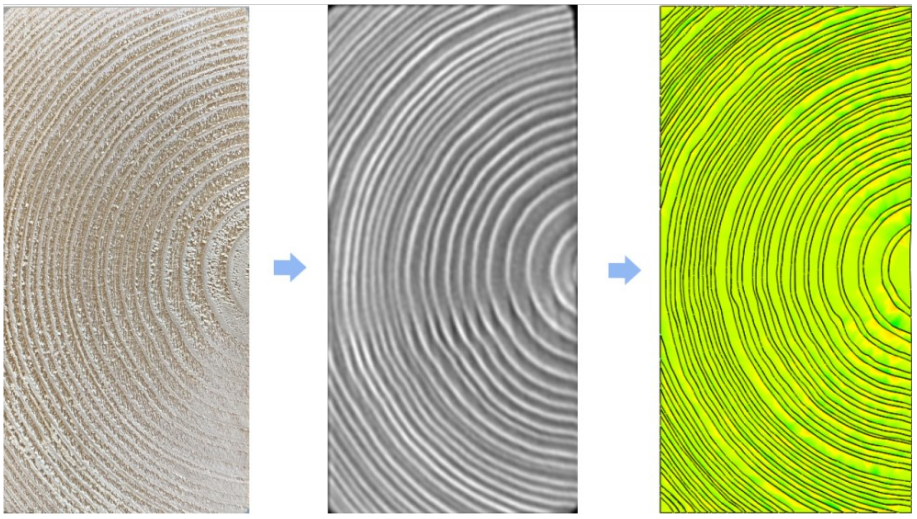

NTNU
Norwegian University of Science and Technology

Zeid Sherpour

Development of CT-based Finite Element Modeling for Timber Board Stiffness Prediction

Master's thesis in Civil and Environmental Engineering - Digital Building Processes
Supervisor: Guomin Ji
Co-supervisor: Johannes Huber
June 2023

Norwegian University of Science and Technology
Faculty of Engineering
Department of Manufacturing and Civil Engineering

NTNU
Norwegian University of Science and Technology

Preface

This master's thesis is written during the spring semester 2023 and corresponds to 30 credits. The assignment represents the final work of the master's degree in Civil and Environmental Engineering, specializing in Digital Building Processes and Structural Engineering at the Norwegian University of Science and Technology (NTNU).

I took a Finite Element Modeling course during my exchange semester at UC Berkeley in the spring of 2022. I found this course interesting and wanted to explore more about it. During the fall semester of 2022, my supervisor, Guomin Ji, proposed writing about using Finite element Modeling and CT scanning to predict the stiffness of timber board. The idea stuck in my head; the more I thought about it, the more interested I became. This topic would allow me to learn more about the FEM while learning about something new, CT scanning, an area in which I had very limited knowledge.

Many people stand behind the completion of this thesis, and I express my gratitude to all of them. First, I sincerely appreciate my supervisors, Guomin Ji (NTNU) and Johannes Huber (Luleå University). I learned immensely from you two; at the beginning of the semester, i struggled to keep up with our discussions, but later on, when my learning increased, I enjoyed those discussions alot. Thank you for your guidance, all the meetings we had, and helping me to overcome the challenges I faced during this thesis.

I thank Johannes Huber for hosting me at Luleå University and letting me experience their CT scanning machine. It was a pleasant experience, and I would also like to thank José Couceiro and Olof Broman for teaching me how to do CT scanning.

I am grateful to Kristine Nore (Omtre) and Wendy Wuyts (Omtre) for providing the materials and financing the trip to Sweden.

I want to express my appreciation to Tor Kristoffer Klethagen (NTNU) and Kenneth Kalvåg (NTNU) for facilitating the lab and helping me do the mechanical compressive testing.

To all professors I had the privilege to have during these years at NTNU, each of you contributed a lot to my learning about various aspects of the digitalization of building processes and structural engineering. I extend my appreciation to all of you.

Lastly, I would like to express my deep gratitude to my family members, who have always encouraged and stood by me. Thank you so much for your patience and sacrifices; even though I don't express it that often, I always admire each of you from the bottom of my heart. This thesis is dedicated to you.

Zeid Sherpour

Abstract

Stiffness is an important mechanical property, and it's about how much a material can resist deformation under loading. It influences the serviceability limit state, an essential factor in designing structures.

Wood is an anisotropic material whose material property differs across its axis; even in the same direction, its mechanical properties differ. The effects of knots, reaction wood, cracks, or other irregularities make it even more complex. CT scanning will be used to understand the wood's mechanical properties and internal structure.

CT scanning is a non-destructive density measure equipment used in hospitals for medical purposes. Using it at wood, it measures the density of the earlywood, latewood, and knots and illustrates how they are formed.

The thesis aims to develop a finite element model based on CT scans of wood that enables the prediction of its local stiffness. The research problem of the thesis is,

"***How can FE models be created based on CT scans of timber to predict the local stiffness of board sections?"***

The research method for the thesis is quantitative. Eleven timber board is CT scanned at Luleå University. Three software is used for developing the finite element modeling. The first two are 3D slicer and Fusion 360, which are utilized for creating the 3D model of the samples. The third software is FEBio studio, and it is used for doing the meshing, boundary condition, applying the displacement, and executing the finite element analysis.

Only two samples are created from the CT scan images, and they are called specimen 1 and specimen 2. The dimensions are 98 mm in height, 48 mm in weight, and 40 mm in length. FEA is applied at two sides of the specimens, called highside and lowside. Highside is the height side of the specimen, and the lowside is the weight side of the specimen. In addition, the sample is mechanically compressive tested to compare them with FEA results and to see their validity.

After FEA and mechanical testing are conducted, the FEA stiffness value for specimen 1 highside results in 145.86 N/mm^2 and mechanical testing yielded 135.87 N/mm^2. The FEA stiffness value is slightly higher than the mechanical stiffness value, indicating they are close. The FEA stiffness value for specimen 1 lowside is calculated at 163.01 N/mm^2, and the mechanical testing resulted in 202.72 N/mm^2. The FEA value is lower than the mechanical stiffness value, and they are 80 percent proximate to each other.

Moving to specimen 2, the FEA stiffness value for the highside is computed at 211.68 N/mm^2, and the mechanical testing result is at 247.27 N/mm^2. The FEA value is lower than the mechanical testing result, but they are close to each other. The stiffness value for lowside is computed at 200.93 N/mm^2, while the mechanical stiffness calculation is at 172.62 N/mm^2. The FEA stiffness value is higher than the mechanical value, and they are 86 percent coinciding.

The limitation of this procedure is that it's tested with only a few samples, which doesn't give a proper conclusion on the reliability and validity of it. Therefore, to draw a reasonable conclusion, further tests are needed for future work.

Sammendrag

Stivhet er en viktig mekanisk egenskap som beskriver et materiales evne til å motstå deformasjon under belastning. Det påvirker bruksgrensetilstanden, som er en viktig faktor ved prosjektering av konstruksjoner.

Tre er et anisotropt materiale, hvor de materielle egenskapene varierer langs forskjellige akser. Selv i samme retning er dens mekaniske egenskaper forskjellige. Effekten av kvister, reaksjonsved, sprekker eller andre uregelmessigheter gjør det enda mer komplekst. CT-skanning vil bli brukt for å forstå treets mekaniske egenskaper og indre struktur.

CT-skanning er et ikke-destruktivt tetthetsmålingsutstyr som brukes på sykehus for medisinske formål. Ved å bruke den på treverk, måler den tettheten til vårved, sommerved og kvister og illustrerer hvordan de er dannet.

Målet med oppgaven er å utvikle en finite element-modell basert på CT-skanninger av tre, som gjør det mulig å forutsi det lokale stivheten til trevirke. Forskningsspørsmålet for oppgaven er,

"Hvordan kan FE-modeller opprettes basert på CT-skanninger av trevirke for å forutsi den lokale stivheten til bordseksjoner?"

Forskningsmetoden i oppgaven er kvantitativ. Elleve trevirke er blitt CT-skannet ved Luleå universitet. Tre programvarer er brukt til å utvikle finite element-modellering. De to første programvarene er 3D Slicer og Fusion 360, som brukes til å lage 3D-modellen av prøvene. Den tredje programvaren er FEBio Studio, og den brukes til å utføre meshing, definere randbetingelser, påføre forskyvninger og gjennomføre finite element-analysen.

Bare to prøver er blitt generert fra CT-skanningsbildene, og de kalles for prøve 1 og prøve 2. Dimensjonene er 98 mm i høyde, 48 mm i bredde og 40 mm i lengde. FEA blir anvendt på to sider av prøvene, kalt høykant og lavkant. Høykant er prøvens høydeside, og lavkanten er prøvens breddeside. I tillegg blir prøvene trykktestet for å sammenligne resultatene med FEA-resultater.

Etter at FEA og mekanisk testing er gjennomført, viser FEA-stivhetsverdien for prøve 1 høykant 145,86 N/mm^2, mens den mekaniske testingen resulterte 135,87 N/mm^2. FEA-stivhetsverdien er litt høyere enn den mekaniske stivhetsverdien, men de er nære til hverandre. FEA-stivhetsverdien for prøve 1 lavkant er beregnet til 163,01 N/mm^2, og mekaniske testingen resulterte til 202,72 N/mm^2. FEA-verdien er lavere enn den mekaniske stivhetsverdien, og de er 80 prosent sammenfallende.

For prøve 2, FEA-stivhetsverdien for høykanten er beregnet til 211,68 N/mm^2, mens det mekaniske testresultatet ga en verdi på 247,27 N/mm^2. FEA-verdien er lavere enn det mekaniske testresultatet, men de er ganske nære til hverandre. Stivhetsverdien for lavkanten er beregnet til 200,93 N/mm^2, mens den mekaniske stivhetsberegningen er på 172,62 N/mm^2. FEA-stivhetsverdien er høyere enn den mekaniske verdien, og de er 86 prosent tilnærmet til hverandre.

Begrensningen ved denne prosedyren er at den er testet med begrenset antall prøver, noe som ikke gir en tilstrekkelig konklusjon om påliteligheten og gyldigheten av den. Derfor, for å trekke en rimelig konklusjon, er det nødvendig med ytterligere tester for fremtidig arbeid.

Table of Contents

List of Figures

List of Tables

1. Introduction

Throughout history, human beings used different materials for building small or large construction, such as rocks, stones, clay, concrete, steel, and wood. Among these materials, wood has always been an essential building material with an estimated building history of 10 000 years (Buildings, 2019). Today, the oldest standing wooden building is Horyuji. It is a Buddhist temple in Ikaruga, Japan, built in 607 AD, over 1400 years ago. The temple also includes a five-stories pagoda (Abundance, 2023). The oldest wooden building in Norway, probably one of the oldest in Europe, is Stålekleivloftet in Eidsborg. It was a storehouse belonging to a rich woman called Åse Stålekleiv. The exact date for when it was built is unknown, but according to archeologists, the wood on the building indicates that it was sawed shortly after 1167 AD (Norway, 2023).

Figure 1: Horyuji temple (Cool, 2023)

Figure 2: Stålekleivloftet (Telemarkshistorier, 2023)

Furthermore, wood is still somehow used a little bit today, not widely used as steel and concrete. In Norway, most single-family homes, some of the apartments, churches, schools, and sports halls are built of wood. In recent years it is getting popular to construct tall structures from wood such as Mjøstårnet, located in Brumunddal, Norway, with a height of 85.4 meters. Wood is not only used in buildings. It's also used in infrastructure such as bridges. For example, 250 of 283 bridges in Norway are wooden bridges. Over fifty percent are built for pedestrians and cyclists, and the remaining are for vehicles. Flisa Bridge is 196 meters long with two driving lanes and got the award for being the most beautiful national wooden bridge in the country (KLEPPE, 2023).

Figure 3: Mjøstårnet, tallest wooden building (Arkitekter, 2023)

Figure 4: Flisa bridge (Folkebladet, 2023)

There are several reasons why wood is a popular building material. First, it's an abundant and accessible material that is available in most regions around the globe. It is lightly weighted and easy to shape in different dimensions and forms. Also, it naturally gives that insulating factor that gives indoor comfort without regulating the heating or cooling temperature. Aesthetically, it looks beautiful and gives the feeling of harmony with nature. But the fundamental reason is its strength. Wood is inherently a strong material. It's strong as steel regarding the strength-to-weight ratio (Deng, Li, & Chen, 2012). Its unique cellular structure, made up of long fibers, provides strength into tension so that that material won't break or deform easily. And its annual rings provide resistance and stability, so that it won't split. With modern engineering, such as laminating and gluing, and better persevering technique, its life span and durability increases even more.

Along with so many benefits, wood is a sustainable and environmentally friendly material as well, which in recent years, due to climate change, its popularity has gained even more. Using wood as a building material contributes directly and indirectly to 7 out of 17 UN sustainable development goals.

1. Goal 8 Decent work and economic growth: Using more wood will increase the wood industry's growth, provide more jobs in the countryside, and reduce poverty (Nations, Goal 8, 2023).

2. Goal 9 Industry, innovation and infrastructure: Demand for wood leads the innovation of it in the wood industry, such as laminated wood, plywood, and modules. Which improves strength and building efficiency (Nations, Goal 9, 2023).

3. Goal 11 Sustainable cities and communities: Wood is a sustainable material; using it makes the buildings more energy efficient and reduces air pollution and other types of waste, ultimately making the cities and communities more sustainable (Nations, Goal 11, 2023).

4. Goal 12 Responsible consumption and production: Wood is a reusable material; with better engineering techniques and responsible forest management, overconsumption, and waste would decrease (Nations, Goal 12, 2023).

5. Goal 13 Climate action: Wood is a material that absorbs CO_2 during its lifespan; using it in buildings will help to decrease climate change and greenhouse gas emissions (Nations, Goal 13, 2023).

6. Goal 15 Life on land: The forest covers 30% of the earth's surface, and it provides food and shelter for over 80% of the animals. Unfortunately, humans destroy the health and ecosystem of the forest, which the entirety is dependent on. Consuming wood from sustainable forest management will protect the health and ecosystem of the forest, deforestation, and forest habitats. It also encourages using more wood building materials than steel and concrete, which are not that eco-friendly (Nations, Goal 15, 2023).

7. Goal 17 Partnerships for the goals: It creates partnerships with the government, wood industries, and society to achieve innovative wood materials, sustainable forest management, and reduce climate change (Nations, Goal 17, 2023).

Figure 5: UN's 17 sustainable development goals (Nations, The 17 Sustainable Development Goals, 2023)

Although wood is a sustainable building material, there are numerous benefits of using it. But there are also some limitations as well, such as the risk of fire, decay, uncertain durability, infestation of insects, etc. But one of the main limitations of wood is that it's considered an anisotropic material. This means its material property, stiffness, and strength are diverse in different directions. It even differ in the same direction. The effects of knots, reaction wood, cracks, or other irregularities makes it even more complex.

Here comes CT scanning; it is an essential piece of equipment that can be used to visualize the internal structure of the wood with high accuracy. It measures the density of the wood and shows all the defects and irregularities. Additionally, it gives information about the position of these defects and how these affect the wood's overall structure.

So many complexities and problems of the wood would be solved and understood if CT scanning were implemented. It would be interesting to dive into all these problems. But, for the sake of time and content of this thesis, it will only be focused on the stiffness part.

Stiffness is an important property; it is about how much a material can resist force before it deforms and breaks. Regarding serviceability limit state (SLS), stiffness plays a significant role; it keeps a construction stable, which helps contribute to the structure's comfort, functionality, and persistence.

1.1 Objective

The thesis aims to develop a Finite element model based on CT images to predict the wood's local stiffness. The plan is to create 3D model of samples from CT images, and with using the 3D slicer and Fusion 360 software. Later, the model will be imported into FEBio Studio to perform the Finite element analysis. The outcome of that will be used to calculate the stiffness value. In addition, the samples will be mechanically compressive tested so that the FEA results can be compared to that and see how close the results are to each other. The research problem of the thesis is,

"***How can FE models be created based on CT scans of timber to predict the local stiffness of board sections?"***

For future work, this thesis lays the fundament for doing the FE analysis of multiple CT images or the whole CT scanned board simultaneously. It also gives a new life to reclaimed wood because, through CT scanning, it can easily identify and see the effect of decay, nail, and screws, and it will help how the material can be recycled. This would reduce waste and produce better-quality boards. So, research in this area will open many doors and solve many environmental issues.

1.2 Limitations

- The majority part of the thesis is spent on developing this procedure, using CT scanning and Finite element modeling for local stiffness prediction of wood. However, it is essential to note that this procedure is only conducted on two samples. More tests are needed to provide more results so that the procedure's reliability and validity get better.

- FEA and mechanical testing are conducted on the sample of reclaimed wood, Norway spruce. The choice of samples was random. And, this doesn't exclude using this procedure on the other wood types. The internal structure of most wood has some resemblances, so this procedure is open and can be used for almost all kinds of wood.

2. Theory

2. 1 Wood anatomy

Most of the wood in the world originates from Angiospermae and Gymnospermae plants, called hardwood and softwood. Hardwood (Angiospermae) comes from deciduous trees, where they lose their leaves annually, and softwood (Gymnospermae) comes from conifer, where they are evergreen. The expected differences between the two are that hardwood appears darker, is usually denser, grows slower, and is more expensive than softwood. On the other hand, 80 percent of used timber in the world is softwood. Some examples of hardwood are Oak, Teak, and Mahogany. And some examples of softwood are Pine, Spruce, and Fir. This thesis will mainly use softwood for its experiment, especially Norway Spruce (Dahl, 2009) and (Laver, 2022).

The inner part of the tree is called the pith, and the outer part is called the bark. The bark is made up of dead cells, which protects the inward growth. The inner layer next to the bark is called the cambium, it is the layer where the growth of annual rings and cell formation happens, and the cambium is not that visible to the naked eye. And then comes the sapwood and the heartwood. 50-80 percent of the softwood is heartwood. Heartwood is made up of dead cells. Heartwood was once sapwood, and the conversion of sapwood to heartwood starts after 14-18 years of age. The purpose of sapwood is to transport water, minerals, and nutrients. And the purpose of heartwood is to give strength and stability. The visibility of sapwood and heartwood differs from wood type to wood type. For example, you can easily identify the difference in Pine, but in Spruce, you can't easily see it; it is almost invisible. The structure of sapwood is more open and permeable, making them easier to impregnate. As the tree grows, the sapwood turns into heartwood (PERSSON, 2000) and (Dahl, 2009).

Annually a tree grows a ring around it called a growth ring or annual ring, and it consists of two types of growth, called earlywood and latewood. The earlywood starts during spring, the growth rate is high, and it has a larger radial diameter, but its cell walls are thinner. Its color appears brighter compared to latewood, but the density is lower. The latewood grows during late summer, and the growth rate is slow, the rings appear darker, the lumen and its radial diameter are smaller, and their density is much higher than earlywood (PERSSON, 2000).

The distance between two growth rings is called ring width, and its distance is usually from 1 to 10 mm, and for rapid growth, the width of rings is even greater. Studying the annual rings provides information about their age, for example, by counting them. And it also tells about the environmental condition in the past, for example, how the growth was during that year, was the seasons dry or rainy, whether the forest fire happened, etc (PERSSON, 2000).

There are many types of Spruce in the world, but in Norway, the Norway spruce is the dominant one, and it's the most widely planted spruce compared to the other spruce types. Its species are found in European countries and even in North America. Its popularity is because its bark is thin, and the knots are tiny, making them hard and stiff. Due to its structure, it is not easy to absorb moisture, increasing its longevity. Its weight is not that heavy either, and they are easy to glue (Dahl, 2009).

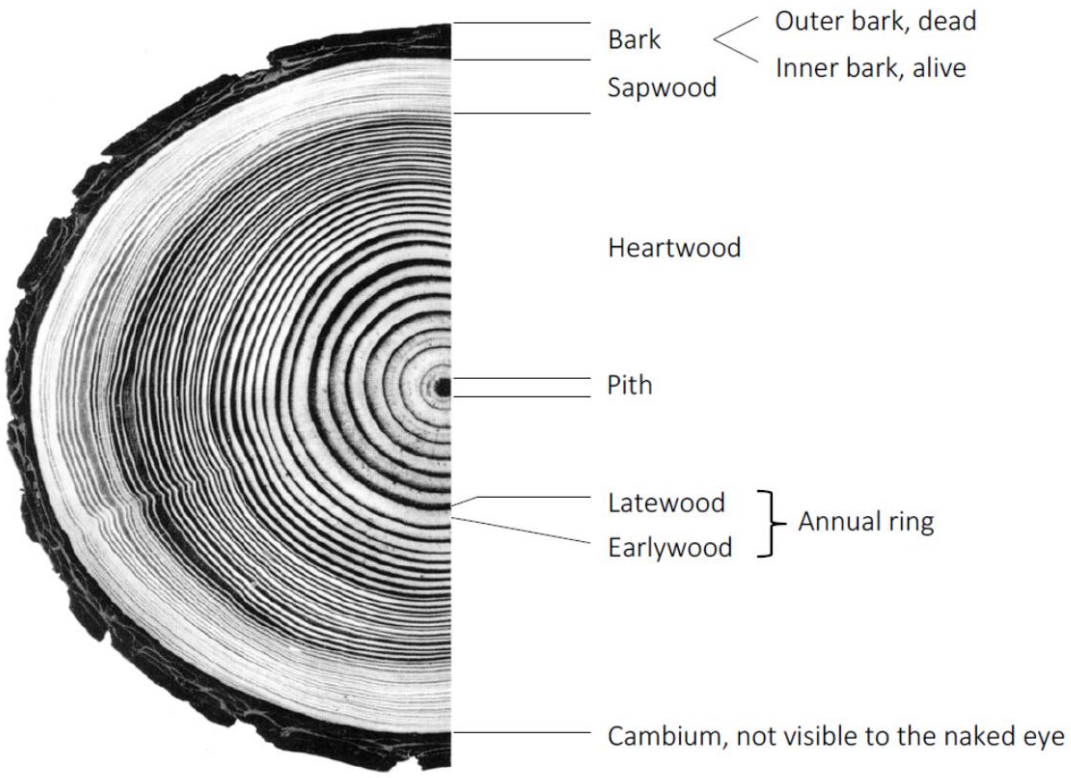

Figure 6: Cross-section of a tree (Blaß & Sandhaas, 2017)

The three axes of the wood have a lot to say about determining its mechanical properties, and they are called longitudinal, radial, and tangential directions. The longitudinal is along the fibers. The radial is toward the annual rings, and the tangential is along the annual rings. The longitudinal direction is 10-15 times stronger than the radial direction and 20-30 times stronger than the tangential (Dahl, 2009).

Due to the thin cell walls of earlywood, the shear stiffness for most softwood in the radial and tangential plane is about 5 percent of the radial stiffness. The same ratio applies to the strength as well. Therefore, one of the causes for failure perpendicular to the grain is due to that (Dahl, 2009).

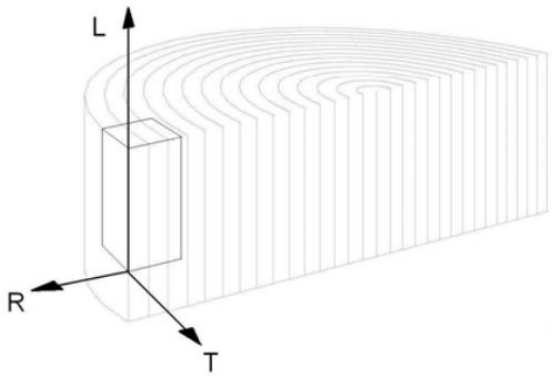

Figure 7: Orthogonal material axis system, Longitudinal, Radial and Tangential (Dahl, 2009)

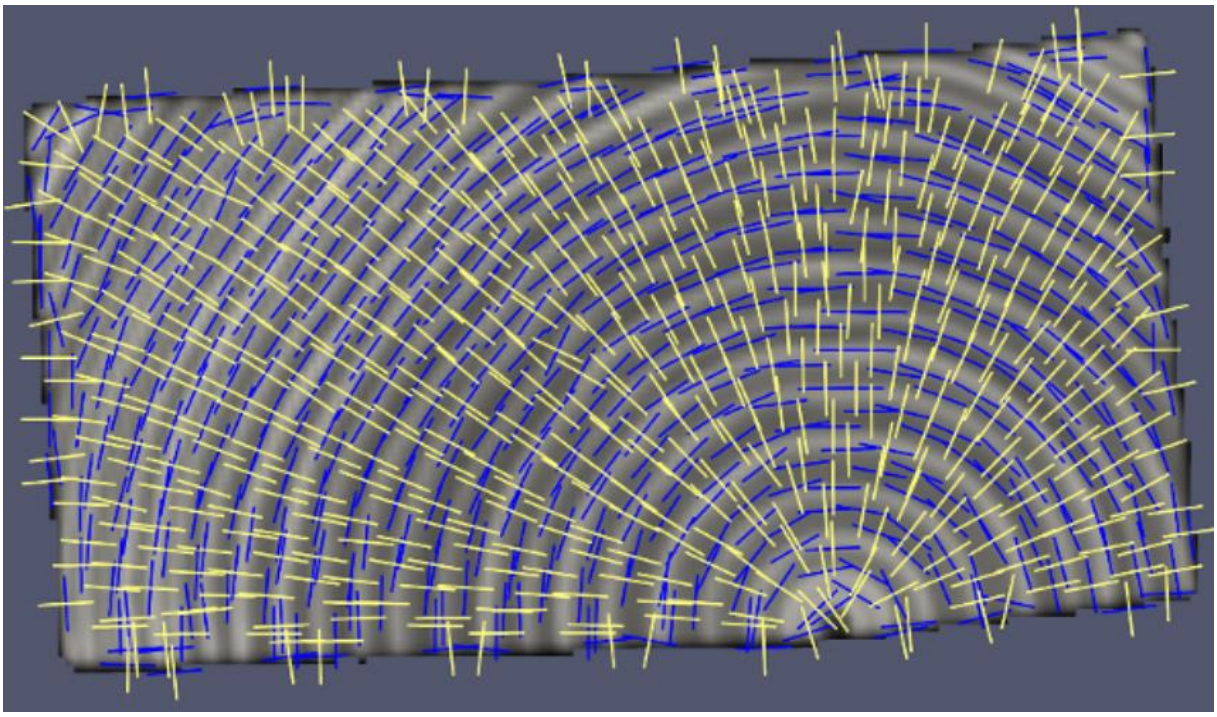

Figure 8: Radial(yellow) and tangential(blue) directions of clear wood slice (HUBER, EKEVAD, & BROMAN, 2021)

2.1.1 Cell wall

90-95% of the volume of the wood is made up of long slender cells called tracheids. Their cross-section looks like merged hollow rectangles with a central cavity called the lumen. The typical diameter of softwood tracheids is 20-40 μm, and the length is 2-4 mm. Earlywood tracheids are bigger than latewood tracheids, but their walls are thinner, and their function is to transport water and nutrients. The latewood tracheids are mainly used for strength, stiffness, and holding the tree straight. The cell walls are built of primary walls and secondary walls. And the secondary wall is made of three layers. They are called outer layer (S1), middle layer (S2), and inner layer (S3). Among all layers, S2 is the thickest one. It is 70-80% thick and carries most of the strength. The cell walls are made up of cellulose, hemicelluloses, and lignin, which make microfibrils. Microfibrils in the S2 are not built straight; it has an angle from 5° to 45° compared to the longitudinal direction. The lower the angle is, the stiffer the material is. Among the layers, one extra layer is called the middle lamella, made of lignin. It works like glue to keep the cell walls together with its neighboring cells (Dahl, 2009) and (PERSSON, 2000).

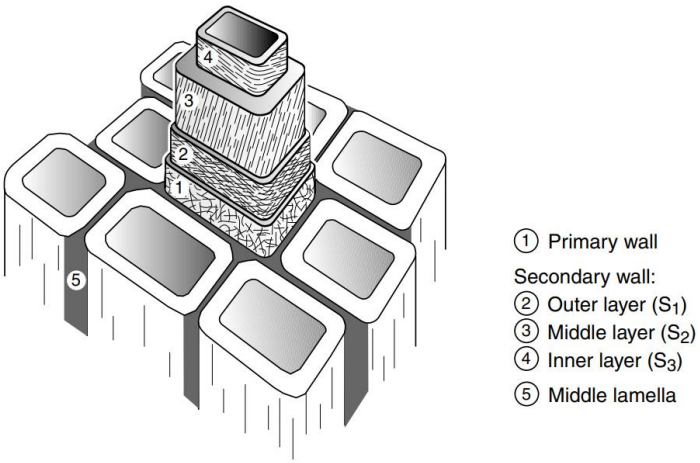

Figure 9: Schematic drawing of cell wall layers (PERSSON, 2000)

2.1.2 Knots

Knots are the weakest point of wood; the initial breaks or cracks usually happen at the knots, no matter how young or old they are. The reason is that it creates disturbances and hindrances on the continuity of the fibers in the stem, resulting in a stress concentration effect; it's when load stresses are gathered in one place instead of being spread out equally, which eventually weakens the wood and causes them to break (Sarnaghi & Kuilen, 2019).

Figure 10: Knots at the timber construction (Beam, 2023)

2.1.3 Clear wood

Clear wood is when the wood is without knots, cracks, reaction wood, resin pockets or other visual irregularities. And it appears homogenous and continuous along the longitudinal, radial and tangential directions (Dahl, 2009).

2.2 Wood physical property

Wood has several physical properties, such as density, moisture content, thermal conductivity, strength, etc. This section explains the wood's density and moisture content (Houses, 2023).

2.2.1 Density

Density is defined as the mass of a material divided by its volume.

$$\rho = \frac{m}{V} \quad \left[\frac{kg}{m^3}\right] \tag{2.1}$$

Earlywood and latewood are the important factors for determining the density of the wood. A tree with high amount of latewood compared to earlywood is higher in density because latewood has thicker cell walls and is denser than earlywood. Earlywood has a density of approximately 300 kg/m^3, and latewood can have a density of up to 1000 kg/m^3; therefore, the average is 400 kg/m^3 (Dahl, 2009). The density of dried cell walls for every wood type is around 1500 kg/m^3 (PERSSON, 2000).

2.2.2 Moisture content

Moisture content is the amount of water that exists in the wood. It's an important physical property, as the amount of it increases, the strength and stiffness of wood would decrease. (Blaß & Sandhaas, 2017).

The moisture content of wood differs between species of wood and in which environment they have grown; even with the same wood type, the moisture content is different. For example, the average moisture content of pine varied between 64-82% (Persson & Andersson, 2016). The average fiber saturation point, where the wood has reaches its maximum moisture content is at 28 percent. To use wood as a building element, the moisture content must be reduced to approximately 12%, so it would not be considered wet. In oven-dried wood, the moisture content is zero percent, and the wood shrinks when it has reached that level (Blaß & Sandhaas, 2017).

$$MC = \frac{m_u - m_d}{m_d} \cdot 100\% \tag{2.2}$$

MC = Moisture Content

m_u = Mass of the moist wood

m_d = Mass of the oven-dry wood

The figure below shows variation in the clear wood's properties with a one percent change in moisture content (Blaß & Sandhaas, 2017).

Property	Change
Compressive strength parallel to the grain	6%
Compressive strength perpendicular to the grain	5%
Bending strength	4%
Tensile strength parallel to the grain	2.5%
Tensile strength perpendicular to the grain	2%
Shear	2.5%
Modulus of elasticity (MOE) parallel to the grain	1.5%

Figure 11: Variation in the clear wood's properties with a one percent change in moisture content. The reference point is 12% moisture content (Blaß & Sandhaas, 2017).

2.3 Hooke's Law

Hooke's Law was established by Robert Hooke in 1660. It's the proportionality between the force and displacement applied in a material. So, it means higher force, higher displacement, and removing the force, the material returns to its original form. Deformation means compressing, bending, stretching, squeezing, and twisting. The formula for Hooke's Law is,

$$F = kx \tag{2.3}$$

F is force, k is constant, and x is displacement or change in length. The material's shape, length, and stiffness determine the constant value k (Britannica, Hooke's law, 2023).

In mechanics, the modulus of elasticity, shear modulus, Poisson's ratio, and orthotropy are concepts directly associated with Hooke's law, which is about the elastic behavior, deformation, and stiffness of the material.

2.3.1 Elastic modulus

Elastic modulus is called the modulus of elasticity, sometimes referred to as young's modulus. Elastic modulus measures a material's stiffness or rigidity. It's the slope line in the stress-to-strain ratio before reaching the non-elastic region. The steeper the slope line is, the stiffer is the material, and it won't deform as easily. And the lower the slope line is, the less rigid or flexible they are. As a result, they easily stretch under stress and are sloppy (CORROSIONPEDIA, 2019).

2.3.2 Shear modulus

The shear modulus is also called as modulus of rigidity. It is material's stiffness against shear force, so it won't deform easily (Britannica, shear modulus, 2023).

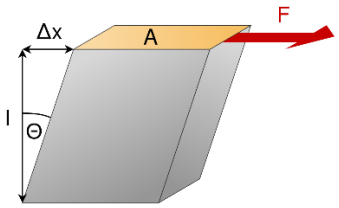

Figure 12: Shear modulus (wikipedia, 2023)

$$Shear\ modulus(G) = \frac{shear\ stress}{shear\ strain} = \frac{\frac{F}{A}}{\frac{\Delta x}{l}} \tag{2.4}$$

Shear stress = Shear force divided by its cross-sectional area

Shear strain = Change in geometry or shape in the same direction as the shear force

2.3.3 Poisson's ratio

Poisson's ratio is named after French mathematician and physicist Siméon Denis Poisson. It is indicated by the Greek letter nu, and it's the ratio of transversal strain and longitudinal strain. This means when a tensile or compressive force is applied in the axial direction of a material, simultaneously, some changes in the lateral direction will also occur, which means it will either thicken or become thinner. The ratio of these changes is called Poisson's ratio (BYJU'S, 2023). See the figure below.

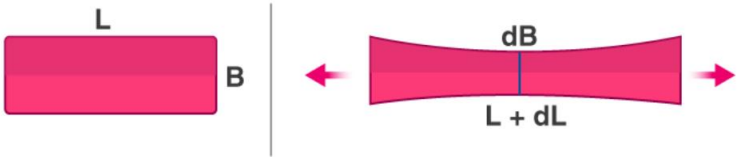

Figure 13: Poisson's ratio (BYJU'S, 2023)

$$v = Poisson's\ ratio = -\frac{\varepsilon_t}{\varepsilon_l} \tag{2.5}$$

$$\varepsilon_t = transversal\ strain = \frac{d_B}{B} \tag{2.6}$$

$$\varepsilon_l = longitudinal\ strain = \frac{d_L}{L} \tag{2.7}$$

The range for Poisson's ratio is from -1.0 to 0.5, and most materials are between 0 and 0.5. The transverse dimensions of these materials decrease when tensile force is applied, and it increases when compressive force is applied. On the other hand, materials with zero Poisson's ratio, their transversal dimension neither increases or decreases when it's applied with tensile or compressive force. The Poisson's ratio for material between 0 and -1.0 is called auxetic materials. They are engineered

materials that extend when it applies tensile force and laterally contract when it's compressed (Prawoto, 2012).

2.3.4 Orthotropy

Wood is referred to as an anisotropic material, it means that it has different mechanical properties in different directional axis. Although orthotropic material is also the same as anisotropic material, its mechanical properties differ in its three directions; the difference between the two is that in the same direction, orthotropic material is homogenous along that axis, whereas in anisotropic material, even in the same direction there are varieties. In general, wood is an anisotropic material, but with regard to engineering elastic models, its considered as orthotropic material (Madhu, 2020) and (Mascia & Lahr, 2006).

The Hooke's law for orthotropic material is the following,

$$\varepsilon = C\sigma \tag{2.8}$$

$$D = C^{-1} \tag{2.9}$$

$$\sigma = D\varepsilon \tag{2.10}$$

σ is the stress vector, ε is the elastic strain vector, and D is the material stiffness matrix (PERSSON, 2000).

$$\begin{Bmatrix} \varepsilon_{LL} \\ \varepsilon_{RR} \\ \varepsilon_{TT} \\ \gamma_{LR} \\ \gamma_{LT} \\ \gamma_{RT} \end{Bmatrix} = \begin{bmatrix} \frac{1}{E_L} & \frac{-v_{RL}}{E_R} & \frac{-v_{TL}}{E_T} & 0 & 0 & 0 \\ \frac{-v_{LR}}{E_L} & \frac{1}{E_R} & \frac{-v_{TR}}{E_T} & 0 & 0 & 0 \\ \frac{-v_{LT}}{E_L} & \frac{-v_{RT}}{E_R} & \frac{1}{E_T} & 0 & 0 & 0 \\ 0 & 0 & 0 & \frac{1}{G_{LR}} & 0 & 0 \\ 0 & 0 & 0 & 0 & \frac{1}{G_{LT}} & 0 \\ 0 & 0 & 0 & 0 & 0 & G_{RT} \end{bmatrix} \begin{Bmatrix} \sigma_{LL} \\ \sigma_{RR} \\ \sigma_{TT} \\ \tau_{LR} \\ \tau_{LT} \\ \tau_{RT} \end{Bmatrix} \tag{2.11}$$

E_L = Young's modulus in longitudinal direction

E_R = Young's modulus in radial direction

E_T = Young's modulus in tangential direction

G_{LR} = Shear modulus in the longitudinal-radial plane

G_{LT} = Shear modulus in the longitudinal-tangential plane

G_{RT} = Shear modulus in the radial-tangential plane

v_{LR} = Poisson's ratio between longitudinal and radial direction

v_{LT} = Poisson's ratio between longitudinal and tangential direction

v_{RT} = Poisson's ratio between radial and tangential direction

2.4 X-ray CT

X-ray CT “Computed Tomography” is a scanning technology used primarily in hospitals to see inside a patient’s body without doing surgery.

It sends a narrow beam of X-ray through the patient. The circular hole in the machine is called gantry, where the patient or an object is laid and moves slowly into it. While the beam tube rotates around the gantry and sends narrow X-ray beams, the digital X-ray detector is at opposite of the beam source and it picks the X-rays from the patient and transmits them into a computer. When one rotation is completed, the CT computer computes the data using complicated mathematical techniques, and produces a 2D image slice called a tomographic image. The thickness of these slices depends on the CT machine, and it usually ranges from 1-10 mm. When many slices are stacked together, it will create a 3D image. The main difference between the conventional X-ray and CT scan is that the tube source for the X-ray is fixed, where the X-ray is sent from one direction and creates a 2D image. On the other hand, CT images are more detailed and make it easier to find the exact position of a problem (NIBIB, 2022).

Figure 14: CT machine (Medicine, 2023)

Figure 15: Microtec Mito CT scanner at Luleå University

CT scanning is a non-destructive density measuring method. Objects with a higher density will be shown more explicitly and visible than objects with a lower density. For example, latewood has a higher density compared to earlywood. Therefore, it's more apparent in the figure below. The presence of the hole in the figure is caused by the nail.

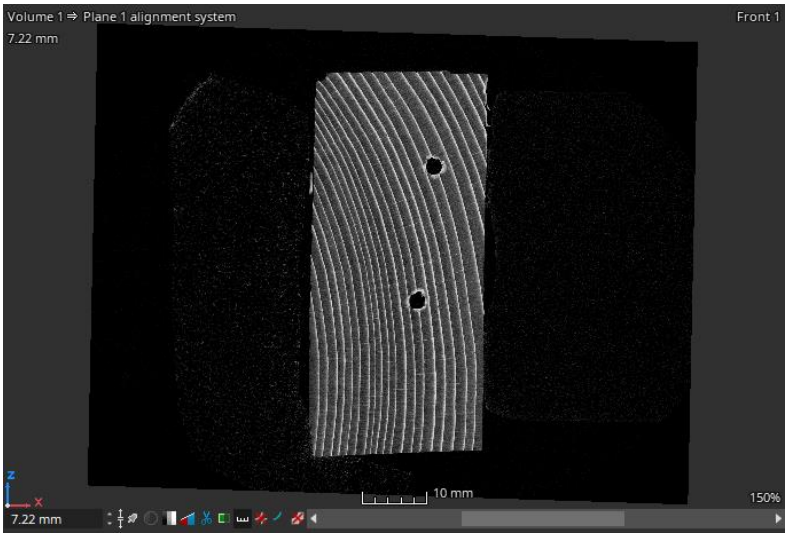

Figure 16: CT-scan image, cross section of wood piece, X and Z-axis

Besides CT scanning, there are many other non-destructive methods available for determining wood stiffness. To name a few, ultrasonic testing, resonance testing, and stress wave propagation testing.

- Ultrasonic testing is sending high-frequency sound waves through a material and analyzing the reflected waves. The defects and mechanical properties of the material will be determined by evaluating the speed of sound waves and the effects on the amplitude of frequency (Oral, Kocaman, & Ahmetli, 2022).

- Resonance testing is another non-destructive method that involves applying vibration to a material. From the resonance, the frequency of the material will be generated, which will be measured to find the material's elastic modulus, damping properties, and other characteristics (Spycher, Schwarze, & Rene´Steiger, 2007).

- Stress wave propagation testing is a non-destructive method that sends stress waves through the material, such as compression or transversal wave. Once the wave is sent, the effect on frequencies of these waves and the times it takes to pass through will be analyzed to find the material's defects, cracks, and other irregularities (Mudiyanselage, Rajeev, Gad, Sriskantharajah, & Flatley, 2019).

2.5 FEA

FEA stands for Finite Element Analysis; it is also referred to as FEM, which stands for Finite Element Method or Modeling. It is discretizing a model or geometry into smaller elements, called mesh, and it is commonly used in calculation of several engineering phenomena such as structural mechanics, heat transfer and fluid flow (Hutton, 2003). The elements consist of a set of nodes, which connects the elements together. Elements are depicted in different shapes, such as bar or beam in 1D, triangles or squares in 2D, and tetrahedral, hexahedral, etc., in 3D. See Figure 17. The shape type of the element is decided by the suitability of the geometry and the desired range of accuracy (Huber J. A., 2021).

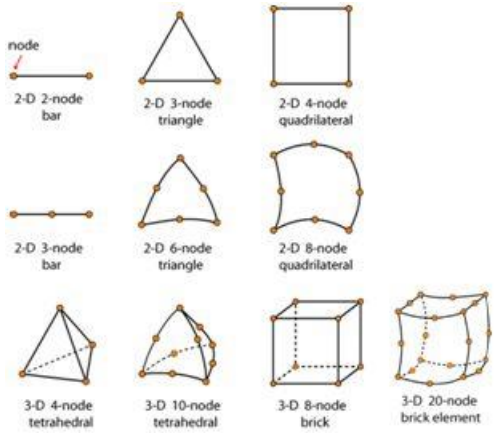

Figure 17: Different types of element shape (Cambridge, 2023)

The degree of freedom is the number of displacements and rotations in a geometry occurring at the nodes. For example, in 2D geometry, there are two degrees of freedom: displacement in the x- and y directions. In 3D, there are six degrees of freedom. Three displacements in the x-, y-, and z direction and three rotations in the x-axis, y-axis, and z-axis. The amount and the type of the degree of freedom is determined by the number of the nodes and shape of the element (Zamani, 2017).

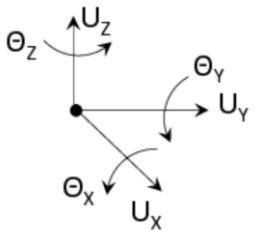

Figure 18: Degrees of freedom (Zamani, 2017)

In FEA each element possesses its own material property, stiffness matrix, and local coordinate system. For simplicity of explaining how the process of stiffness computation works, it's chosen to give an example of a bar with two elements and three nodes. All nodes have one degree of freedom.

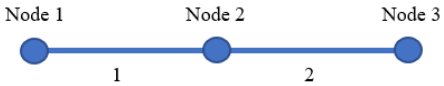

Figure 19: Bar with two element

Hooke's law used to generate the stiffness matrix of the element, and the formulation of the force and displacement.

$$\sigma = E \cdot \varepsilon \tag{2.12}$$

$$\sigma = \frac{F}{A} \ , \ \varepsilon = \frac{\Delta L}{L} \tag{2.13}$$

$$\frac{F}{A} = E \cdot \frac{\Delta L}{L} \tag{2.14}$$

$$F = \frac{E \cdot A}{L} \cdot \Delta L \tag{2.15}$$

$$F = ku \ , \ k = \frac{EA}{L} \ , \ u = \Delta L \tag{2.16}$$

F is force, u is displacement and k is the stiffness.

The following equation shows the local stiffness matrix, k, of one element with two nodes (Hutton, 2003).

$$k = \frac{E \cdot A}{L} \begin{bmatrix} 1 & -1 \\ -1 & 1 \end{bmatrix} \tag{2.17}$$

The matrices in below is the stiffness matrix of element 1 and 2.

$$k_1 = \begin{bmatrix} k_{11} & -k_{12} \\ -k_{21} & k_{22} \end{bmatrix} \tag{2.18a}$$

$$k_2 = \begin{bmatrix} k_{22} & -k_{23} \\ -k_{32} & k_{33} \end{bmatrix} \tag{2.18b}$$

After the local stiffness matrices are computed, they will assembled together to form the global stiffness matrix, which will be representative for the entire geometry of the bar.
Then the global stiffness matrix will be multiplied with displacement to find the force, or the inverse of global stiffness matrix will be multiplied with force to find the displacement (Hutton, 2003).

$$\begin{Bmatrix} F_1 \\ F_2 \\ F_3 \end{Bmatrix} = \begin{bmatrix} k_{11} & k_{12} & 0 \\ k_{21} & k_{22} + k_{22} & k_{23} \\ 0 & k_{32} & k_{33} \end{bmatrix} \begin{Bmatrix} u_1 \\ u_2 \\ u_3 \end{Bmatrix} \quad (2.19)$$

F_1, F_2, F_3 = Force at node 1, 2 and 3
u_1, u_2, u_3 = displacement at node 1, 2 and 3

$$F_1 = k_{11} * u_1 + k_{12} * u_2$$
$$F_2 = k_{21} * u_1 + (k_{22} + k_{22}) * u_2 + k_{23} * u_3$$
$$F_3 = k_{32} * u_2 + k_{33} * u_3$$

That's the process for finding force displacement in a FEA software works, this force-displacement values will be utilized later to find the stiffness. The process is the same for all types of geometries.

As explained earlier, wood is an anisotropic material, and its stiffness matrix is 6x6 with three different valus of elastic modulus, shear modulus and poisson's ratio. The process of calculating begins with discretization of the geometry into smaller elements. From there each element it will calculate its element stiffness matrix. Through node connectivity and degree of freedom, all these elements will be assembled together forming the global stiffness matrix, which will be representative for the entire geometry. Then boundary condition is applied to fix some of nodes and to apply force or displacement at some other nodes. From there global stiffness matrix will be multiplied with force or displacement.

Most software today can discretize a model into an infinite number of elements. The finer the mesh is, the better results will be, but this will increase the computational time. Therefore, a proper balance is essential, where it neither affects the accuracy nor the computational time. The figure below illustrates the stresses in a re-entrant corner, where the figure to the left shows an element size of 2 m, and the figure to the right illustrates an element size of 0.25 m. Figure right clearly demonstrates how the stress is better distributed and has better results than figure left.

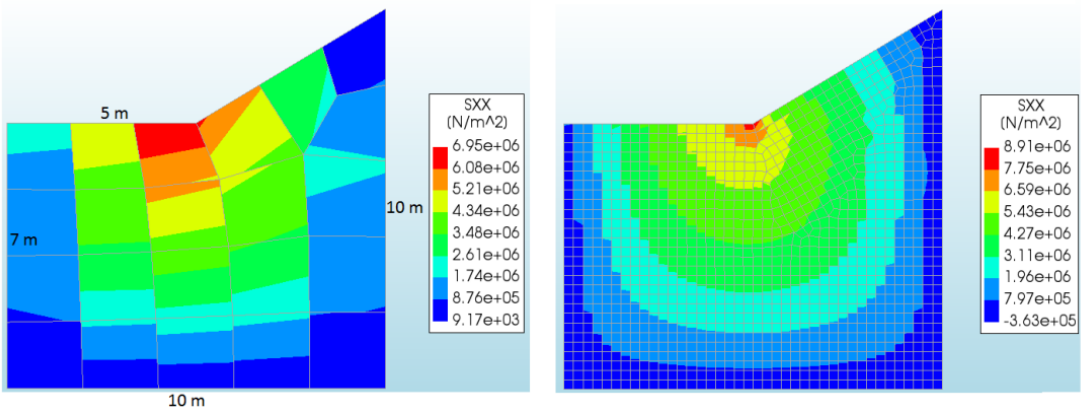

Figure 20: Stress distribution in a re-entrant corner, left figure shows element size of 2m and right figure illustrates element size of 0.25m (Skibeli, 2017).

There are several software options out there for conducting Finite Element Analysis. The popular ones are Abaqus, Solidworks simulation, ANSYS, DIANA, etc., and they offer a wide range of simulation capabilities such as structural mechanics, heat transfer, fluid mechanics, Multiphysics, etc. Moreover, these software's require a license to use. However, there are also some free and open-source FEA software, such as FEBio. Therefore, this software is employed for doing the FE analysis part of the thesis. While FEBio is mainly designed for medical purposes but also offers the capability of performing dynamic structural and mechanical analysis.

2.6 Mechanical testing

Mechanical testing is a broad term that refers to a series of tests for finding the mechanical and physical properties of a material. To mention a few, bending testing, tensile testing, torsion testing, compressive testing, fatigue testing, etc. Each test will find the mechanical property of a material, such as strength, stiffness, deformation, ductility, fatigue, etc (Direct, 2023). Various equipment and machines are used to perform these tests, such as universal testing machines, compressive testing machines, fatigue testing machines, etc. In this thesis, mechanical testing is referred to as mechanical compressive testing.

Mechanical compressive testing is putting a material under compressive force to see its behavior and determine its mechanical property. The way it's performed is a sample is placed in a compressive machine where the load or displacement is applied gradually until the material deforms or fails. Then the machine will generate data for the force-displacement or stress-strain diagram, which will say the material's strength, stiffness, and deformation characteristics (TESTRESOURCES, 2023).

In this thesis, the testing of specimens is conducted at MEGA 6-3000-300. It's a compressive and bending testing machine from a German company called FORM+TEST. The machine is in two part. The first part can have max load up to 3000 kN and the second part has a max load of 300 kN. The compressive testing of the thesis is performed in the second part. The diameter and thickness of pressure plate for upper and lower is Ø230x40mm. The results are computed on the software called PROTEUS. Based on the latest calibration test, the error percentage is at 0.1 percent, which means the testing results are quite accurate (FROM+TEST, 2023).

3. Methodology

The research method for the thesis is quantitative and involves three steps. The first step is acquiring the materials and conducting the CT scanning. The second step is to develop a 3D model based on the CT scan image for conducting the finite element analysis. Finally, the third step involves mechanical testing of the same materials. In the end, the stiffness result from the finite element analysis will be compared to the experimental result; it is to evaluate how close the stiffness prediction from FE analysis is.

The theme of the thesis was something new and interesting; a considerable amount of time has been dedicated to reading various literature and articles to understand the research problem and how to address it, including with that sufficient time has been spent on learning the different software for doing the CT segmentation and creating a 3D model from it. In addition, some time has been spent on learning the CT scanning machine and the mechanical testing machine to do the experiments and analyze the data from it. The figure below illustrates the streamline for the work process of the thesis.

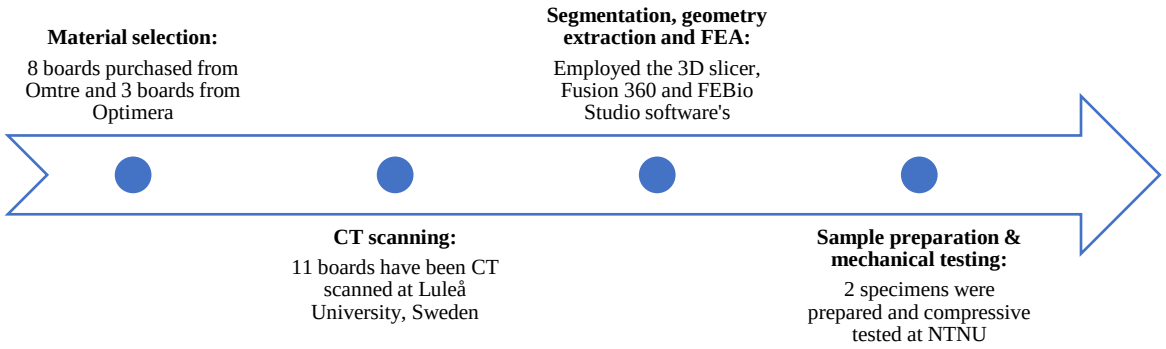

Figure 21: Streamline process

3.1 CT scanning

The author traveled to Luleå University in Sweden for one week starting on February 19th. The purpose of the trip was to gain knowledge and get practical experience in CT scanning of wood. Eleven timber boards were brought along and scanned during the trip. Three were purchased from Optimera, and the rest were from Omtre. Omtre is a wood industry that researches and develops the recycling of wood materials. Initially, the boards from Omtre were over one meter long. Therefore, each board had to be cut in half to fit easily into the baggage.

Figure 22: Purchased timber boards from Omtre

The boards from Optimera are new wood; it hasn't been used earlier. On the other hand, the boards from Omtre are reclaimed wood of various ages. Among them, the oldest one is 100 years old. Some boards even had nails in them; they weren't taken out; it was to see the effects nails in the CT images. The boards from Omtre are labeled as A, B, C, and D. Now, cut in two parts; therefore, it's named A1, A2, B1, B2, C1, C2, D1, and D2. The boards from Optimera are called X, Y, and Z. See the figure below and table 1.

Figure 23: Preparing the timber boards for CT scanning

Table 1: The material parameters of Norway spruce

Board name	Dimension	Age	Moisture content	Weight	Purchased from
A1	48x98 mm	Unknown	18,30 %	1255 g	Omtre
A2	48x98 mm	Unknown	19,30 %	1320 g	Omtre
B1	48x96 mm	50 years	29,00 %	1460 g	Omtre
B2	48x96 mm	50 years	29,30 %	1442 g	Omtre
C1	55x105 mm	70 years	22,60 %	1852 g	Omtre
C2	55x105 mm	70 years	16,50 %	1880 g	Omtre
D1	48x98 mm	100 years	18,20 %	1661 g	Omtre
D2	48x98 mm	100 years	19,70 %	1713 g	Omtre
X	20x120 mm	New	16,50 %	610 g	Optimera
Y	20x120 mm	New	16,50 %	658 g	Optimera
Z	20x120 mm	New	16,50 %	719 g	Optimera

The moisture content was measured on February 20th, and Table 1 shows relatively high moisture content in these boards; the exact reason is unclear, but it assumes that they may have been stored outside for a while. But after the measurement, it has been stored inside, and the moisture content has dropped significantly. For example, when board A1 was measured on 15th May, right before mechanical testing, the moisture content was at 12,4 %. Wood is a hygroscopic material that absorbs and releases moisture through the air. The moisture content of wood increases during wet seasons or high humidity. On the other hand, moisture content decreases during dry seasons or when the humidity is low (Glass & Zelinka, 2010). The equipment used for measuring the moisture content is a moisture meter called Delmhorst RDM-2S. The way it is measured is first to choose the wood type in the device, and for this case, is spruce, and then stick the device's nail into the wood and wait a few seconds, and then the moisture content appears on the display.

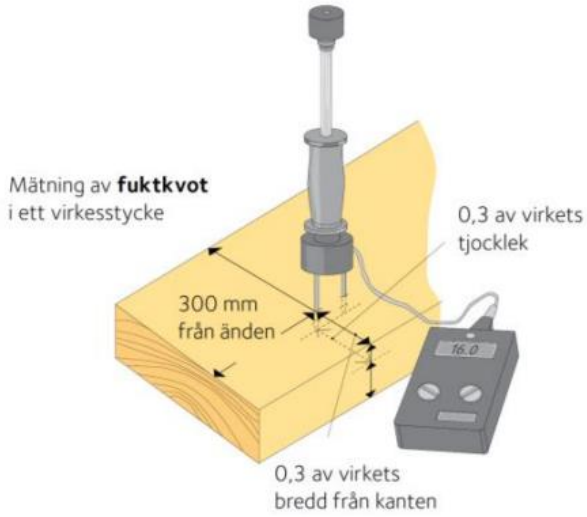

Figure 24: Moisture meter (Berggren, 2012)

However, using the measuring equipment doesn't always give an accurate result. Therefore, a sample from A2 and B1 were measured with the oven drying method, resulting in a significant difference in results. The moisture content for A2 was initially measured at 19,30 percent, but with the oven drying method, it resulted in 11,69 percent. The same was for B1. The prior moisture content was at 29,00 percent, but with the oven drying method, it resulted at 24.48 percent.

Table 2: A2 sample oven-dry method, time and mass

Oven-dry method, A2 sample		
Date	Time	Mass
23.02.2023	12:20	78.85 g
24.02.2023	09:40	70.60 g
24.02.2023	13:00	70.60 g

Figure 25: Weighing a sample from A2 board

$$MC = \frac{m_u - m_d}{m_d} \cdot 100\% \qquad (3.1)$$

m_u = 78.85 g

m_d = 70.60 g

MC = 11,69 %

Table 3: B1 sample oven-dry method, time and mass

Oven-dry method, B1 sample		
Date	Time	Mass
21.02.2023	18:00	119.23 g
22.02.2023	16:00	95.80 g
23.02.2023	08:30	95.78 g

$$MC = \frac{m_u - m_d}{m_d} \cdot 100\% \qquad (3.2)$$

m_u = 119.23 g

m_d = 95.78 g

MC = 24.48 %

Figure 26: Weighing a sample from B1 board

All the timber boards has been placed and scanned one by one at the Microtec Mito CT scanner. The object under the board is a timber as well, to better distinguish between the two, a foam has been placed in between. Foam has low density, therefore it wont appear in the CT image in figure 27, which creates a nice gap between the two board. Figure 28 illustrates the foam and the board underneath.

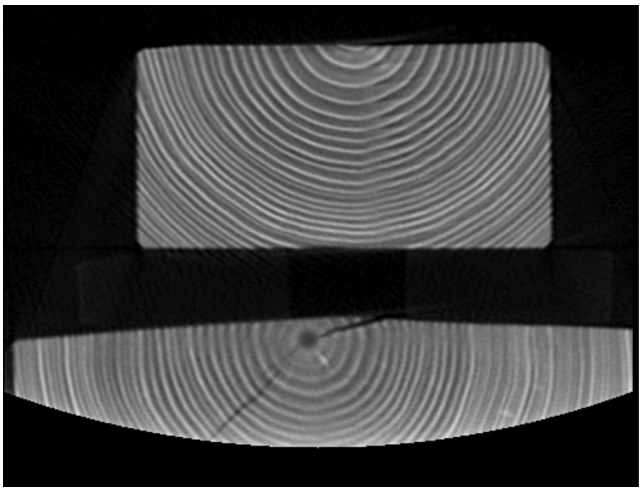

Figure 27: CT image visualize the scanned object and the board underneath

The boards were scanned with the gantry speed of 2.0 rpm (rotation per minute) and feed speed of 0.2 m/min, the rate the boards were moved towards the gantry. The scan process and file generating took approximately 5-10 minutes. Each board's file size was quite large; it ended up being around 1,2 GB (Gigabyte). At the side of each board, an arrow was drawn pointing to the right, which means the scanning starts from the left and ends towards the right. In addition to that, it also means that on that

side, the board was initially cut earlier. For example, in A1, you will see the arrow is on the right side, and in A2, the arrow is on the left. It means it is where these two boards were separated. All this makes analyzing and identifying the start and end of the CT images easier.

Figure 28: Preparing and placing the A1 and A2 board in the CT scanner

3.2 Geometry extraction

To conduct the FE analysis, three software were used. First, 3D Slicer was utilized to convert the Scan data into a 3D model. Then Fusion 360 was used to make a 2D sketch out of the 3D model from Slicer, which was subsequently converted to a simpler 3D model. Finally, the finite element modeling is conducted at FEBio Studio. In this chapter, it describes the first two steps where geometry is prepared for the finite element modeling.

Figure 29: Software workflow for FEM development

3.2.1 3D Slicer

The file from CT scanning machine is first imported into 3D slicer for doing the segmentation. Segmentation is creating a 3D model out of the CT scan images. The scan images consist of various shades of gray. The human eye can distinguish only a few shades of them, and segmenting CT images into different colors will make identifying different X-ray attenuation in the board easier.

The CT scan of the A1 timber board produced a density range from 0 up to 1623 kg/m^3; each number represents a shade of grey color which defines the value of x-ray attenuation or the x-ray amount that penetrated through the object. The lighter the grey color is, the denser that area is, which means that the x-ray penetration has been low. Conversely, the darker the gray color, the lower the density and the higher the X-ray penetration.

For the thesis, three segmentation models have been created. First is earlywood, whose threshold range is from 300 to 500. The reason for selecting 300 not at 0 is because the range less than 300 visualizes noise and air around the board. The density range from 500 to 730 is used for capturing latewood, and the rest is from 730 up to 1623; the knots are located in this range. So according to the CT images, knots are denser than earlywood and latewood.

Figure 30: The earlywood segmentation of A1 timber board

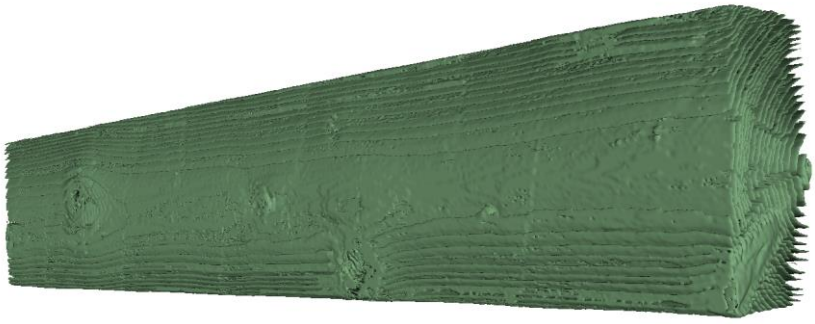

Figure 31: The latewood segmentation of A1 timber board

Figure 32: The knots segmentation of A1 timber board

Figure 33:The combined segmentation of earlywood, latewood, and knots of A1 board

Since the voxel size of the CT scan images is at 0,3 mm, the file size of the segmented model became quite large. The size of each model was approximately 3-4 GB. Since it was so large, it would make the process slow and time-consuming for the next software. Therefore, it had to be decimated before being imported to Fusion 360. A certain decimation percentage was applied so the file won't lose so much of the data; after some experiments, the 95% decimation was a fair number. So, the file size reduced to approximately 168 MB or 0,16 GB, the file is still large, but it’s feasible for Fusion 360. See the figure below; the segmented model to the left shows the original size and the right figure illustrates the decimated one. You don't notice any change even though the left figure is only 5% of the right figure.

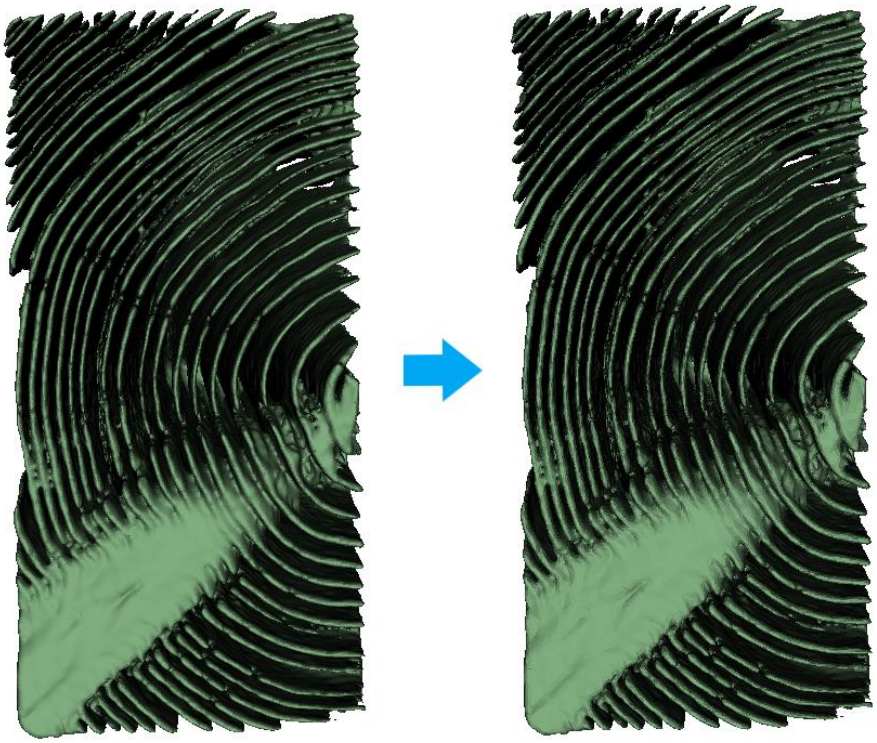

Figure 34: The decimation of earlywood segmentation

3.2.2 Fusion 360

Fusion 360 is a software from the Autodesk family. From the segmentation models above, the latewood model is chosen for creating the 2D sketch. The reason is that latewood model has thinner rings with bigger gaps in between the rings, which makes it easier to sketch. Two sketches will be made, called specimen 1 and specimen 2. The sketch for specimen 1 is 150 mm away from the center of the board, and the sketch for specimen 2 is 215 mm away from center of the board. See figure 35, orange color indicates the sketches.

Specimen 1 is a more straightforward sketch with no knots or significant deformation. On the other hand, specimen 2 is a bit complex because it has a knot. Fusion 360 was chosen over many other software options because it was easy to learn, and there were many available online tutorials. Also, it made creating the sketch more straightforward and quicker than the other software.

The process of creating the sketch is straightforward. It begins with clicking the sketch button, then choosing the sketch's direction and entering the dimension where the sketch should be placed. Since the model is placed in the center, choosing the value zero will create the sketch in the middle. Therefore, if the number is higher than zero, the sketch will be placed to the right of the model, and if the number is below zero, then the sketch will be created to the left. Refer to Figure 35, which indicates the sketch of specimen 1 and specimen 2; both are placed on the right side of the model.

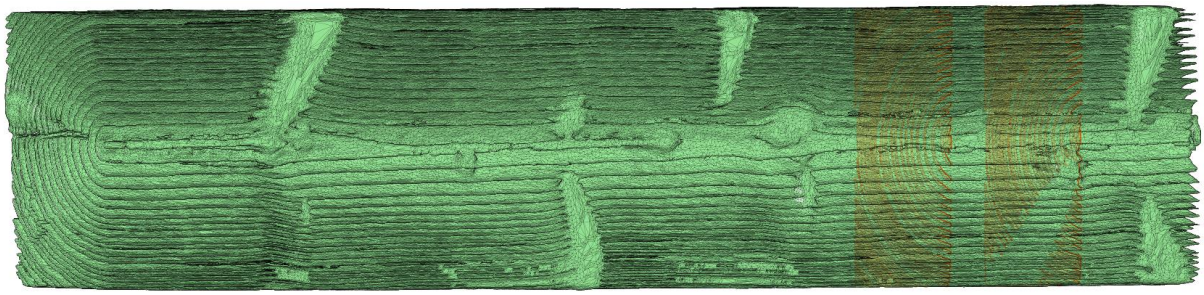

Figure 35: Latewood segmented model visualizing the sketch slice of specimen 1 and specimen 2

After the sketch is made, the next step is to draw and edit the lines. Editing and drawing is a semi-automatic process, by selecting the sketch, the lines are drawn automatically without manually drawing them. But some areas had to be fixed manually, especially at the edges. Therefore, the dots in the figure below illustrate these minor changes.

Sketch with minor details makes the 3D model heavy and complex, making the FE analysis tedious and time-consuming. As shown, most of the dots are located at the edges because the segmentation created the edges curved and round; while in the actual timber boards, the edges are straight and clean-cut. Later in FEBio, it makes the process of selecting the surfaces of growth rings would much easier.

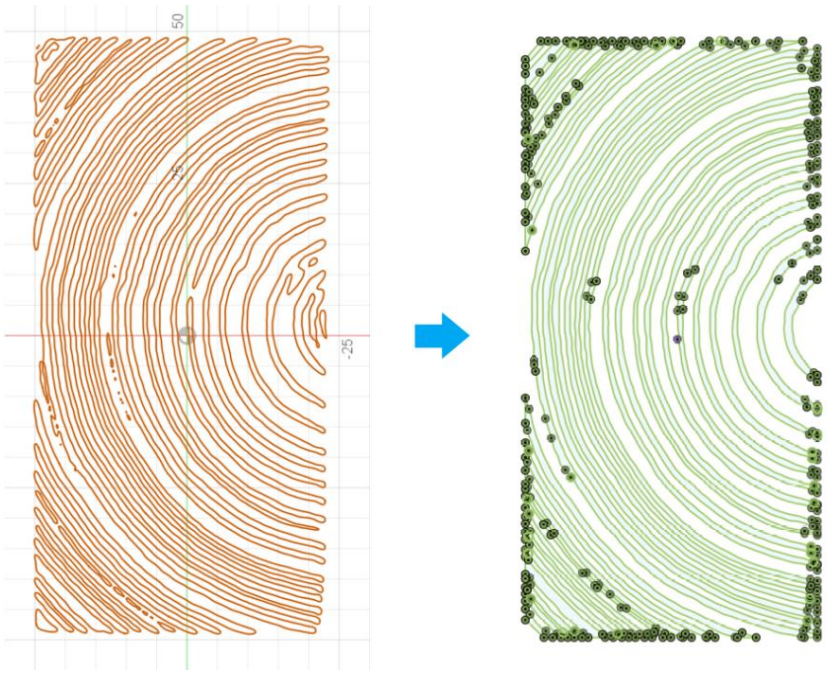

Figure 36: Sketching process of specimen 1

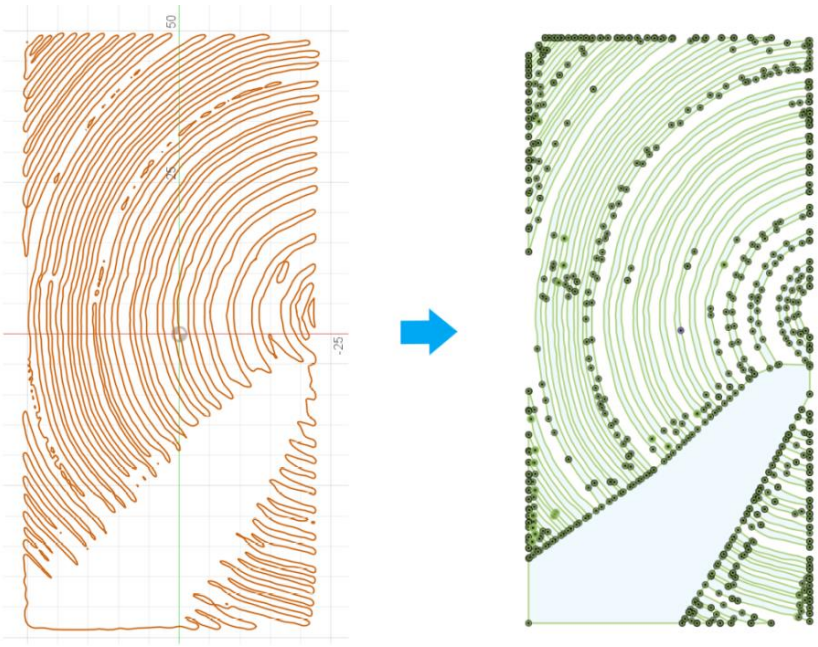

Figure 37: Sketching process of specimen 2

After the editing is complete, the sketch is transformed into a 3D model. This will happen through an extrusion tool with an extrusion length of 40 mm. When the latewood model is created, instead of doing the whole process again for earlywood, a model of a box with the same height, width, and length as latewood will be utilized as a cutting function, where the latewood cuts through the box, and creates the earlywood model. See the figures below.

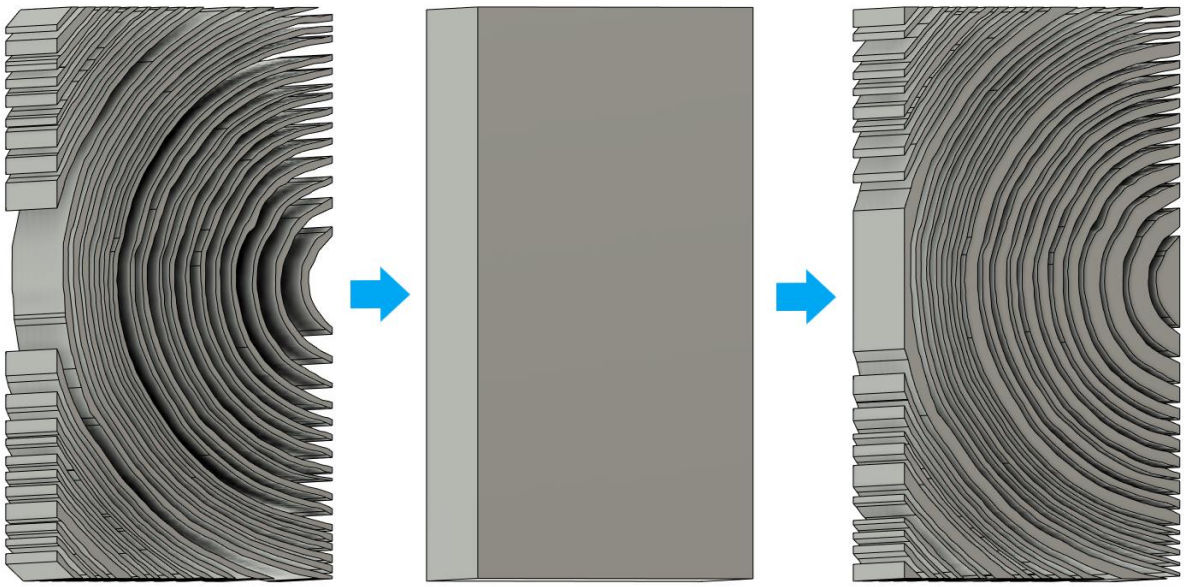

Figure 38: The extrusion and cutting process of earlywood of specimen 1

The process for specimen 2 is similar to specimen 1. But the cutting process starts with knot and the the latewood. After that, the earlywood will be cut through a rectangular box with the same height, weight and length value.

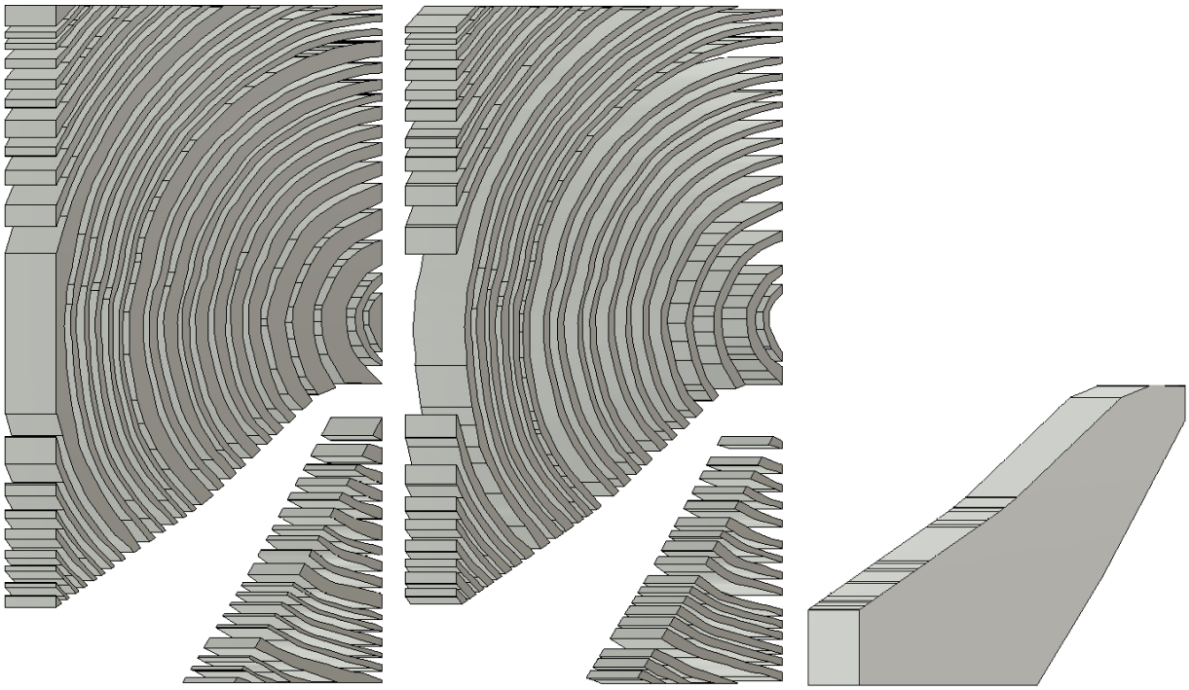

Figure 39: The sketch model of earlywood, latewood, and the knot

3.3 Finite Element Modeling

After the model of specimen 1 and specimen 2 is created, it will be inserted to the FEBio Studio. It's six steps process for performing the FE analysis of the specimens. In the paragraphs below, all these steps and how they are executed will be explained in detail.

Figure 40: The six-step process of conducting the FE analysis on FEBio

Specimen 1 and Specimen 2 is inserted in FEBio, different color is applied for distinguishing the earlywood, latewood, and the knot.

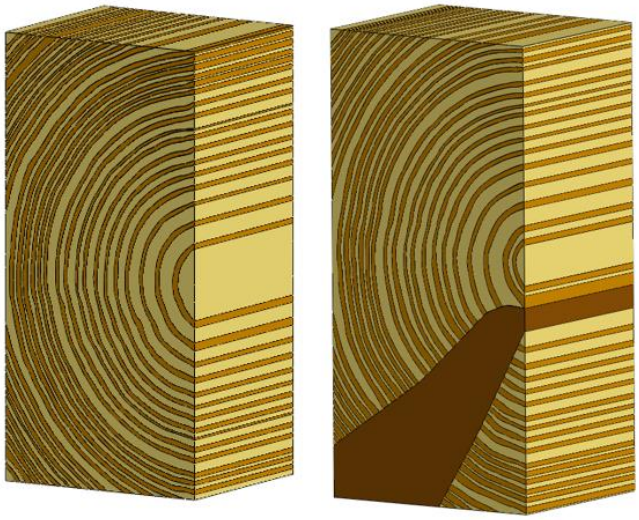

Figure 41: The 3D model of specimen 1 and 2 at FEBio Studio

1. Mesh

After the model from Fusion 360 is imported into FEBio, the software automatically creates a surface mesh for it. However, as shown in the left Figure 42, the mesh is non-uniform. The Mesh Inspector tool shows that some elements have an element edge length of 50 mm, some have an edge length of less than zero, and the average is between 5-10 mm. To make the mesh more uniform, the model will remesh with an element size of 5 and a minimum size of 3 mm. Figure 42 illustrates the transformation from a non-uniform to a more uniform mesh. The reason for changing the mesh size is to make the FE results more accurate. Now that the surface mesh is transformed, the model is converted into a solid mesh; in this case, it will be a tetrahedral mesh.

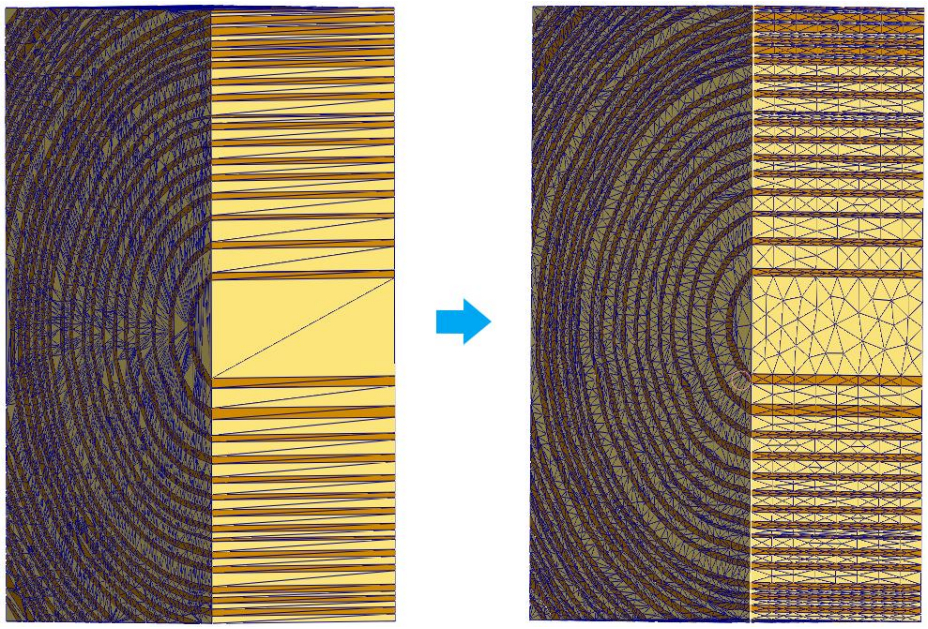

Figure 42: Transformation of specimen 1 surface mesh from non-uniform to uniform mesh

2. Local coordinate system

After the meshing step is completed, the next step is to set the material's local coordinate system. Since the annual rings of earlywood and latewood are more like a curve shape, the local coordinate of each element differs, which means the Cartesian coordinate system won't be applicable. Instead, the cylindrical coordinate system is applied because it best suits cylindrical geometries. To make the cylindrical coordinate system applicable, the center of the cylindrical geometry must be placed at the center of the cartesian coordinate system. The center of the specimens model is its pith. To locate the pith, several rings of the annual were drawn in Fusion 360 to find the center of the specimen, as shown in Figure 43. After that, the specimen was positioned 5 mm in the X-direction and 51 mm in the Y-direction away from the origin. With a cylindrical coordinate system come vectors A and D. Vector A is along the longitudinal direction, and vector D is the radial direction displayed in red; green is the tangential direction perpendicular to the radial direction. The value input for A is {0,0,1}, and for D is {1,0,0}. Figure 45 illustrates the cartesian coordinate system's transformation into the latewood's cylindrical coordinate system.

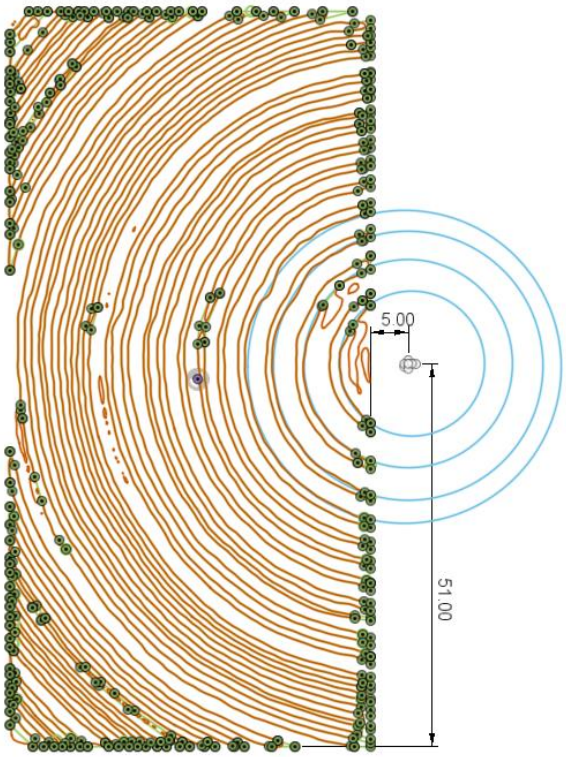

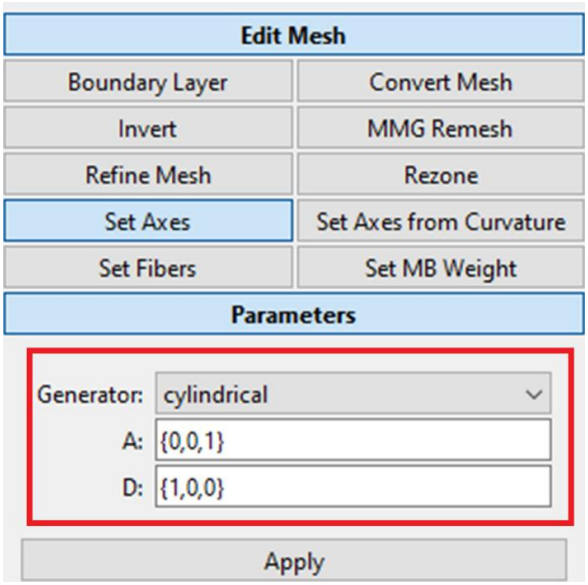

Figure 43: Calculating the position of the pith

Figure 44: Inserting the input value for vectors A and D

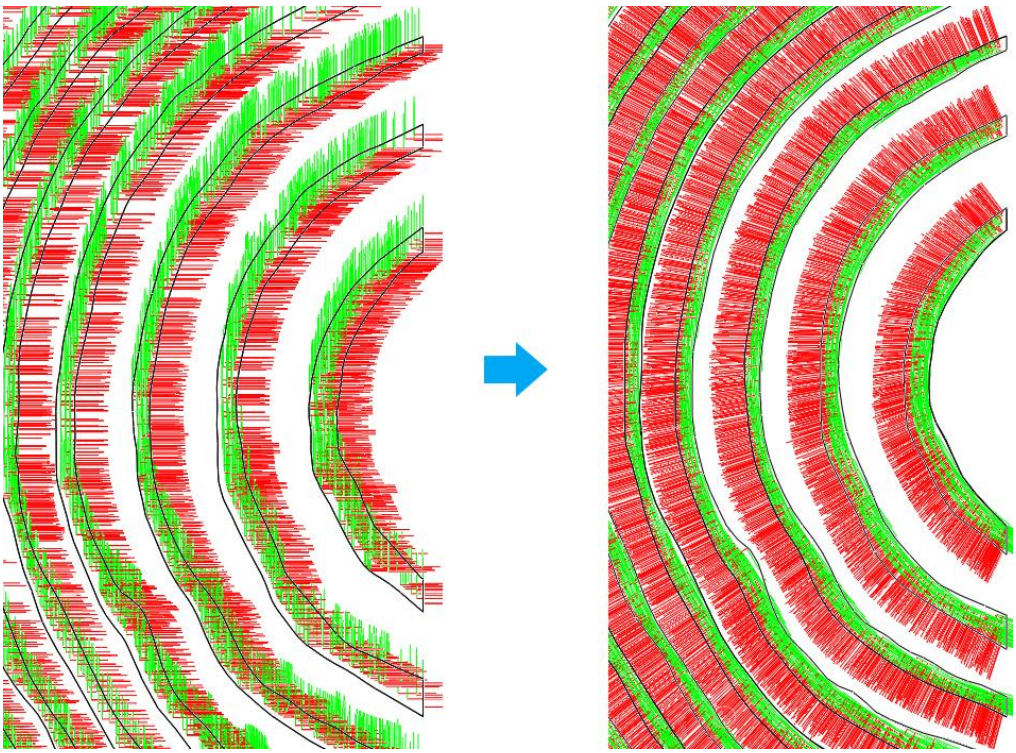

Figure 45: Transforming the local cartesian coordinate system to cylindrical coordinate system

3. Material

The third step is to add the material parameter. Since wood is an anisometric material, therefore Orthotropic Elastic has been chosen as the material type. This material type allows the insertion of Young's modulus, shear modulus, and Poisson's ratio across all three directions. So, in total, it will be inserted nine values for each model. Nine for the earlywoods, nine for the latewoods, and nine for the knots. However, there is no literature out there that can give the material parameters of earlywood, latewood, and knot separately, but they provide an overall value. Therefore to calculate the material parameters separately, the density from the CT model of the specimens is used. The way it's calculated is that the average density of each CT model is divided by reference density and then multiplied by the material parameters from the literature. It's essential to choose the correct value because the average density of each specimen differs. This multiplication will be only applied to the parameter values of elastic and shear modulus; for Poisson's ratio, it won't be any multiplication. See the formula.

$$\frac{\rho}{\rho_0} \cdot \begin{Bmatrix} E_{RR} \\ E_{TT} \\ E_{LL} \\ G_{RT} \\ G_{LT} \\ G_{LR} \end{Bmatrix} \tag{3.3a}$$

$\rho = Density\ from\ CT\ images$

$\rho_0 = Reference\ value$

	A	B	C	D	E	F
1	**Specimen 1**	**Number of voxels**	**Volume [mm3]**	**Mean**	**Median**	**Standard Deviation**
2	Earlywood	4520163	4.52016e+06	396.934	393	55.473
3	Latewood	2391316	2.39132e+06	588.734	582	57.1905

Figure 46: The average density value of earlywood and latewood for specimen 1

	A	B	C	D	E	F
1	**Specimen 2**	**Number of voxels**	**Volume [mm3]**	**Mean**	**Median**	**Standard Deviation**
2	Earlywood	3626307	3.62631e+06	404.653	401	55.4091
3	Latewood	2649494	2.64949e+06	600.553	598	68.2276
4	Knot	453907	453907	892.293	847	136.326

Figure 47: The average density value of earlywood, latewood and knot for specimen 2

The reference value for Norway spruce ρ_0 is 390 kg/m^3 (Huber, Broman, Ekevad, Oja, & Hansson, 2022).

Table 4: Components of stiffness matrix for Norway spruce (Huber, Broman, Ekevad, Oja, & Hansson, 2022)

Type	E_{LL}	E_{RR}	E_{TT}	G_{LR}	G_{LT}	G_{RT}	V_{TR}	V_{TL}	V_{LR}
Norway spruce	10700	710	430	500	620	23	0.31	0.025	0.38

The only value that changes in the formula below is the average density obtained from Figures 46 and 47.

$$\frac{\rho}{390} \cdot \begin{Bmatrix} 710 \\ 430 \\ 10700 \\ 23 \\ 620 \\ 500 \end{Bmatrix} \tag{3.3b}$$

Figures 48 and 49 illustrate how material parameters for earlywood and latewood of specimen 1 look after the multiplication, as the figures show that the values are not similar without the value of Poisson's ratio.

Property	Value
E1 modulus	724
E2 modulus	437
E3 modulus	10914
G12 shear modulus	23
G23 shear modulus	632
G31 shear modulus	510
V12	0.31
V23	0.025
V31	0.38

Figure 48: Material parameters of earlywood specimen 1

Property	Value
E1 modulus	1065
E2 modulus	645
E3 modulus	16050
G12 shear modulus	35
G23 shear modulus	930
G31 shear modulus	750
V12	0.31
V23	0.025
V31	0.38

Figure 49: Material parameters for latewood specimen 1

4. Contact

The fourth step is to tie the models together to function as one model. The initial reason for the creation of two models was to be able to put different mechanical properties in other models. If it were just one model, FEBio couldn't insert two values in one geometry.

FEBio ties the two models by taking the surface of one model and connecting them with the surface of another model that shares contact with it. Figure 50 illustrates the tying system of specimen 1; in Primary, the surfaces of earlywood are inserted, and in Secondary, the surfaces of latewood are inserted. Only surfaces that share contact with each other will be inserted..

For specimen 2, there will be implemented two elastic tie systems. The first is between the surfaces of earlywood and latewood, and the second is between the surfaces of knot and the surfaces of earlywood and latewood together.

The penalty factor is set as one, and the auto penalty is turned on so that the software can estimate the correct penalty factor based on the stiffness and element size of the material. The importance of the penalty factor is that it prevents gaps and collisions between the surfaces. The other values will be set as default.

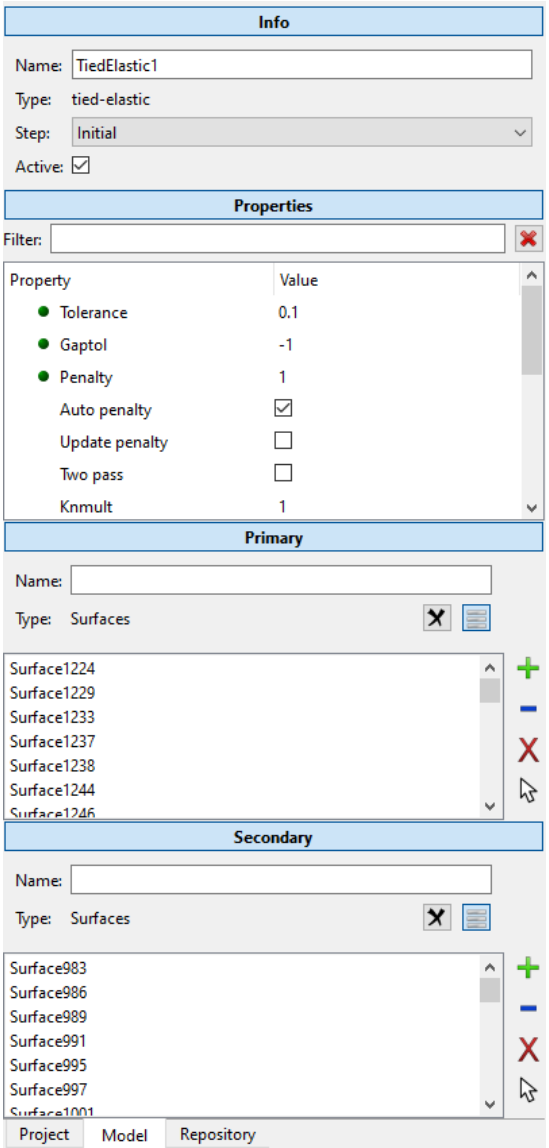

Figure 50: The tie elastic system

5. Boundary condition

The fifth step is applying the boundary condition. The specimens in the thesis are compression tested at its two sides. The following paragraph explains how the boundary condition is used on one side of the specimen. The process is also similar for the other sides.

First, the bottom of the board will be fixed, and there will be no displacement. As figure 51 illustrates the boundary condition of specimen 2, the bottom of the specimen is fixed in the Y-direction, and all the bottom surfaces are selected and inserted in the selection tab. Then the prescribed displacement will be set on the opposite side of the board; at the top, all the surfaces at the top are selected and inserted at the selection tab. The displacement value is -0.59 in the Y-direction, pushing the specimen downwards.

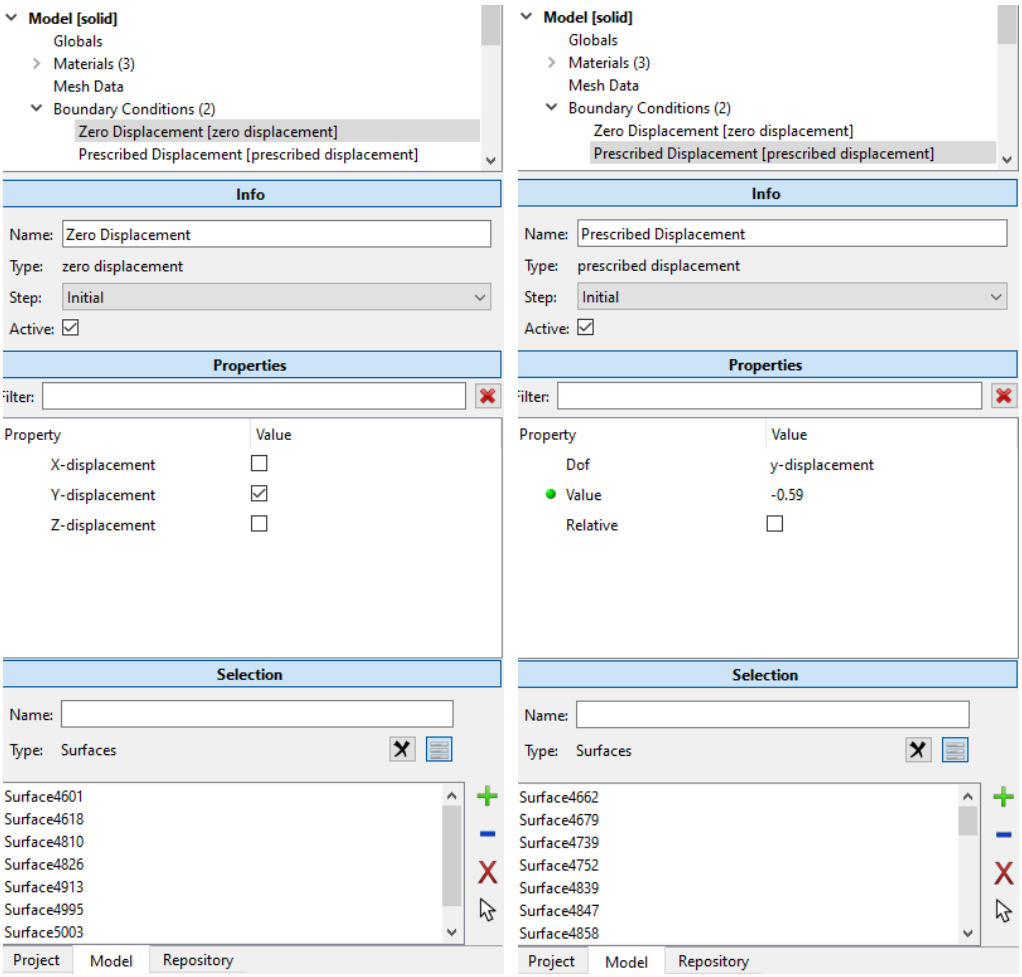

Figure 51: Boundary condition at bottom of the specimen 2

Figure 52: Boundary condition at top of the specimen 2

6. Analysis step

The sixth and the final step is to add an analysis step, defining the duration and type of the simulation process. The step values are left as default and the time steps is ten with step size of 0.1, which means it will take 1 second to complete the analysis. Before running the simulation, the model will be saved first, and once the simulation is executed, a new window will be opened called Postview, which displays the analysis results, colormap, displacement map, and the graph. See figure 54.

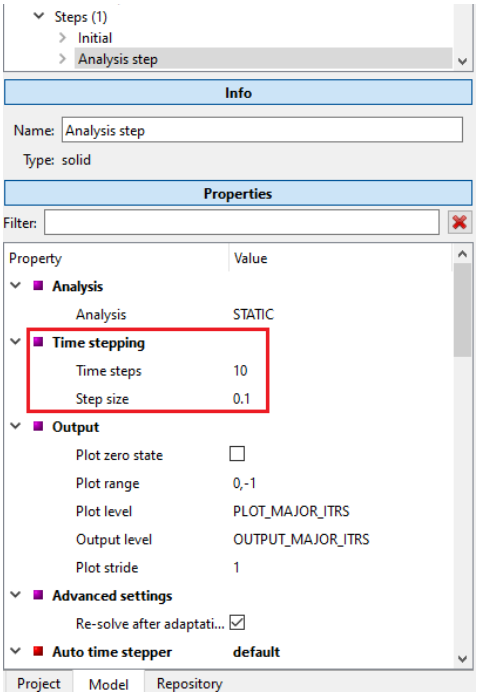

Figure 53: The analysis step

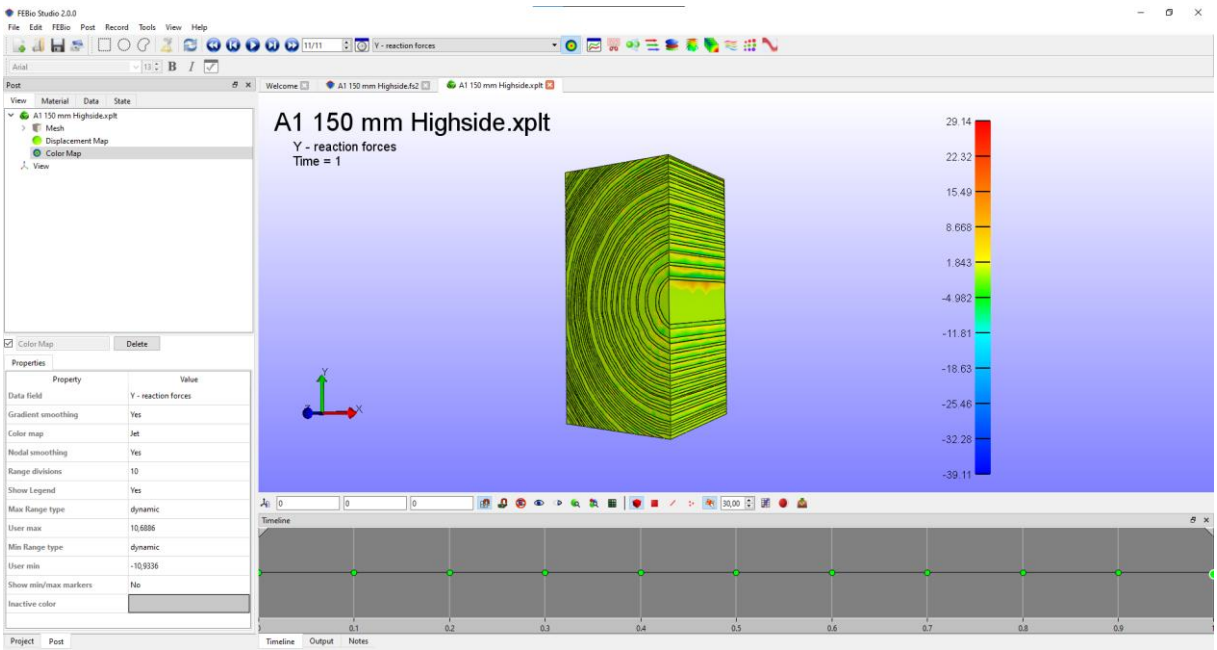

Figure 54: Postview window

3.4 Mechanical Testing

To perform the mechanical testing, the first step is to calculate the elastic region of the material by finding the maximum load and displacement that can be applied so that the material won't break. Then the next step is the preparation of the specimens before conducting the test.

3.4.1 Analytical calculation and preparation

The calculation is done by using Hooke's law. Due to the anisometric nature of the wood, the estimation might not be a hundred percent accurate, but it provides a reasonable assumption of where the elastic region is.

The specimen is calculated to find the maximum force and displacement in two directions: highside and lowside. The highside is, as its name explains, it's the tallest side of the specimen with a height of 98 mm. The lowside is the lowest side of the specimen, with a dimension of 48 mm. The thickness is 40 mm. Both specimens has similar dimensions.

Highside

$$\sigma = E \cdot \varepsilon \tag{3.4}$$

$$\sigma = \frac{F}{A} \ , \ \varepsilon = \frac{\Delta L}{L} \tag{3.5}$$

$$\frac{F}{A} = E \cdot \frac{\Delta L}{L} \tag{3.6}$$

Assume the strength class C24

$f_{c,90,k} = 2{,}5 \frac{N}{mm^2}$ (Table1, NS-EN 338 2016)

$E_{90,mean} = 370 \frac{N}{mm^2}$ (Table1, NS-EN 338 2016)

$$2{,}5 \frac{N}{mm^2} = 370 \frac{N}{mm^2} \cdot \frac{\Delta L}{98\ mm}$$

$$\Delta L = \frac{2{,}5 \frac{N}{mm^2} \cdot 98\ mm}{370 \frac{N}{mm^2}} = 0{,}66\ mm$$

$$F = 2{,}5 \frac{N}{mm^2} \cdot 48\ mm \cdot 40\ mm = 4800\ N$$

Lowside

$$\frac{F}{A} = E \cdot \frac{\Delta L}{L} \tag{3.7}$$

$$f_{c,90,k} = 2{,}5\,\frac{N}{mm^2}$$

$$E_{90,mean} = 370\,\frac{N}{mm^2}$$

$$2{,}5\,\frac{N}{mm^2} = 370\,\frac{N}{mm^2} \cdot \frac{\Delta L}{48\,mm}$$

$$\Delta L = \frac{2{,}5\,\frac{N}{mm^2} \cdot 48\,mm}{370\,\frac{N}{mm^2}} = 0{,}32\,mm$$

$$F = 2{,}5\,\frac{N}{mm^2} \cdot 40\,mm \cdot 98\,mm = 9800\,N$$

Later, two specimens are cut from the A1 board. The first specimen is cut within the range of 110-150 mm from the center of the board, which gives a longitudinal thickness of 40 mm. The specimen 2 is cut within the 200-240 mm range, and it contains a knot within.

3.4.2 Compressive testing

The specimens were put in the compression testing machine with a speed force of 50 newtons per second. To be on the safer side and not break the specimens. Only half of the value from the calculation is applied. This means in the highside direction, it used 2400 newtons, and on the lowside applied 4900 newtons.

A sensor was attached to the machine for better and more accurate results. See figures 55 and 56, the metal stick on the right side of the machine. It's called HBM LVDT 20 mm transducer, a sensor with a 15 decimals precision.

Figure 55: Lowside compressive testing

Figure 56: Highside compressive testing

3.5 Evaluation

To assess the credibility and applicability of this procedure, it is important to examine its reliability, validity, and generalizability.

3.5.1 Reliability and Validity

Reliability is the measurement of consistency and stability of an outcome when it's repeatedly measured. And validity is about the accuracy of the results; it's to what extent a measuring device or instrument can measure what it is intended to measure (Carmines & Zeller, 1979).

The procedure is made with high accuracy, and every detail is taken care of, so its results will be reliable and valid. The CT images of the samples are scanned with high precision, and the geometry extraction is made with high accuracy. All the guidelines for creating an excellent finite element model for the wood specimen are considered, such as choosing the right mesh size, applying the material parameters, setting the cylindrical coordinate system, and boundary condition.

To measure the consistency of the results, it is tested with only two samples, and each sample is tested on two sides. Based on the results, it's reliable. However, two samples are insufficient to draw a reasonable conclusion on how reliable this procedure is. Therefore, conducting more measurements and analyses on additional samples is necessary.

To assess the procedure's validity, its results are compared with those from the mechanical testing. The results are not entirely aligned, but they are reasonably close. This indicates that the procedure has high validity. However, to draw a better conclusion, more samples must be tested.

3.5.2 Generalizability

Generalizability is making a general representation from smaller and specific cases or samples (Carminati, 2018).

This procedure involves CT scanning and finite element modeling of the Norway spruce samples. The common thing between every wood type is its physical characteristics, such as its growth rings. Every wood type's growth ring is built similarly, with earlywood and latewood. Therefore, this procedure is applicable for every wood type, whether reclaimed wood or new wood, with different dimensions and density. Because the development of FEM started from the growth ring.

4. Results

4.1 CT model

The figure below illustrates the CT model of A1, and specimen 1 and specimen 2. The CT model of the other boards are shown at appendices.

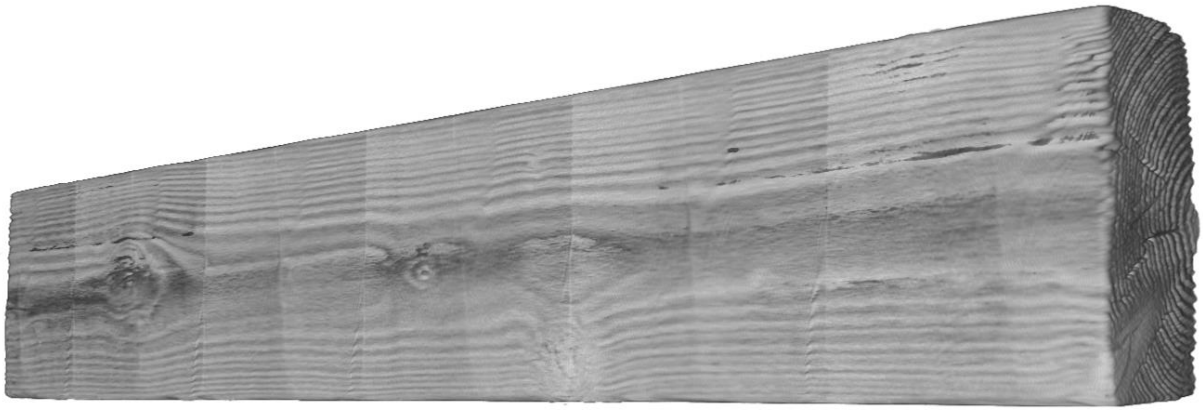

Figure 57: CT model of A1

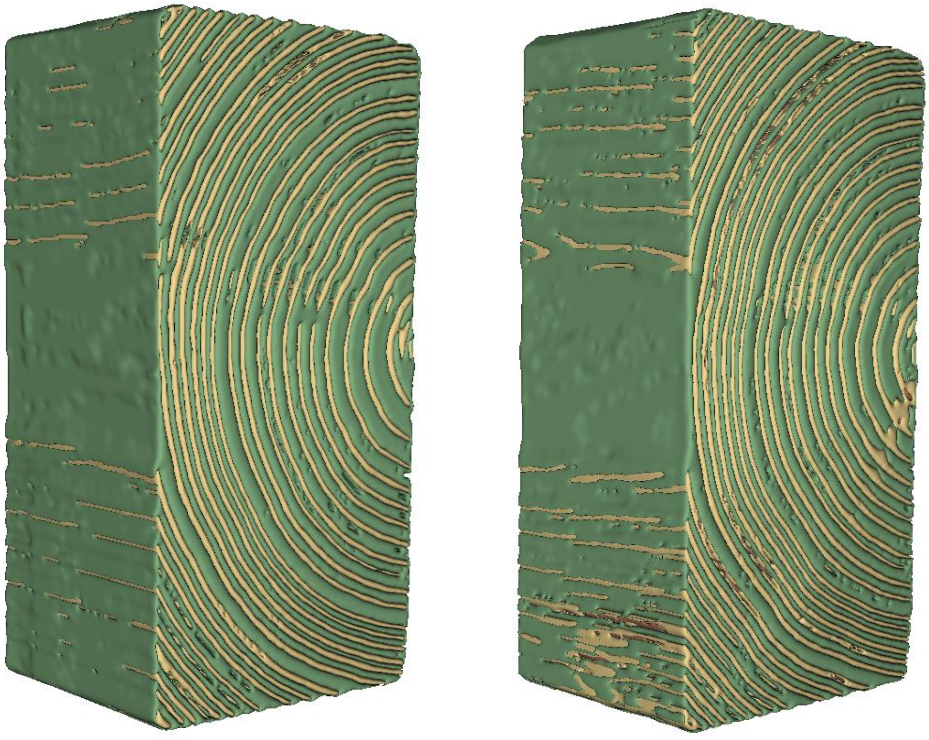

Figure 58: Segmented model of specimen 1 and 2

4.2 FEA

This section presents the FEA results of specimens 1 and 2. In FEBio Studio, the displacement value was used as the input, and the result here will display the reaction force. The value of displacement for both FEA and mechanical testing are the same.

4.2.1 Specimen 1

Highside

As input for prescribed displacement, the value of 1.06 mm was used. After execution of the analysis, the postview appeared with the color map of the reaction force in the Y-direction. The color map illustrates how the reaction force is distributed across different areas of the specimen. The total reaction force at the top of the surface is 3029.03 N. The following Hooke's formula, calculates the Young's modulus, resulting in a value of 145.86 N/mm^2.

$$E = \frac{\sigma}{\varepsilon} \tag{4.1}$$

$$\sigma = \frac{F}{A} = \frac{3029.03\ N}{48 \times 40\ mm^2}$$

$$\varepsilon = \frac{\Delta l}{L} = \frac{1.06\ mm}{98\ mm}$$

$$E = 145.86\ {}^{N}/_{mm^2}$$

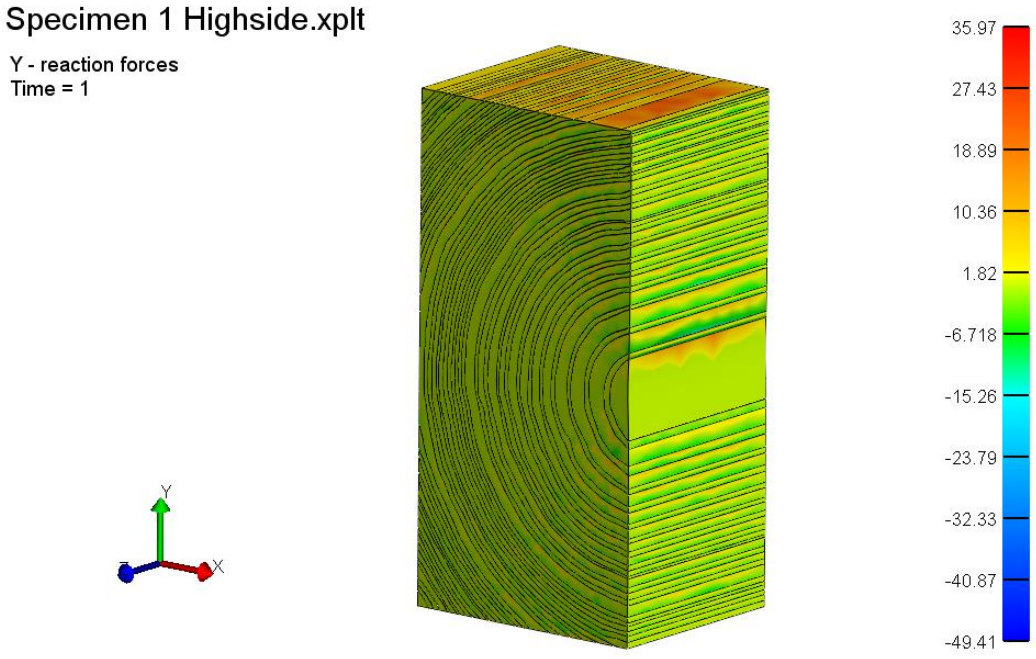

Figure 59: The color map of the reaction force of specimen 1 highside

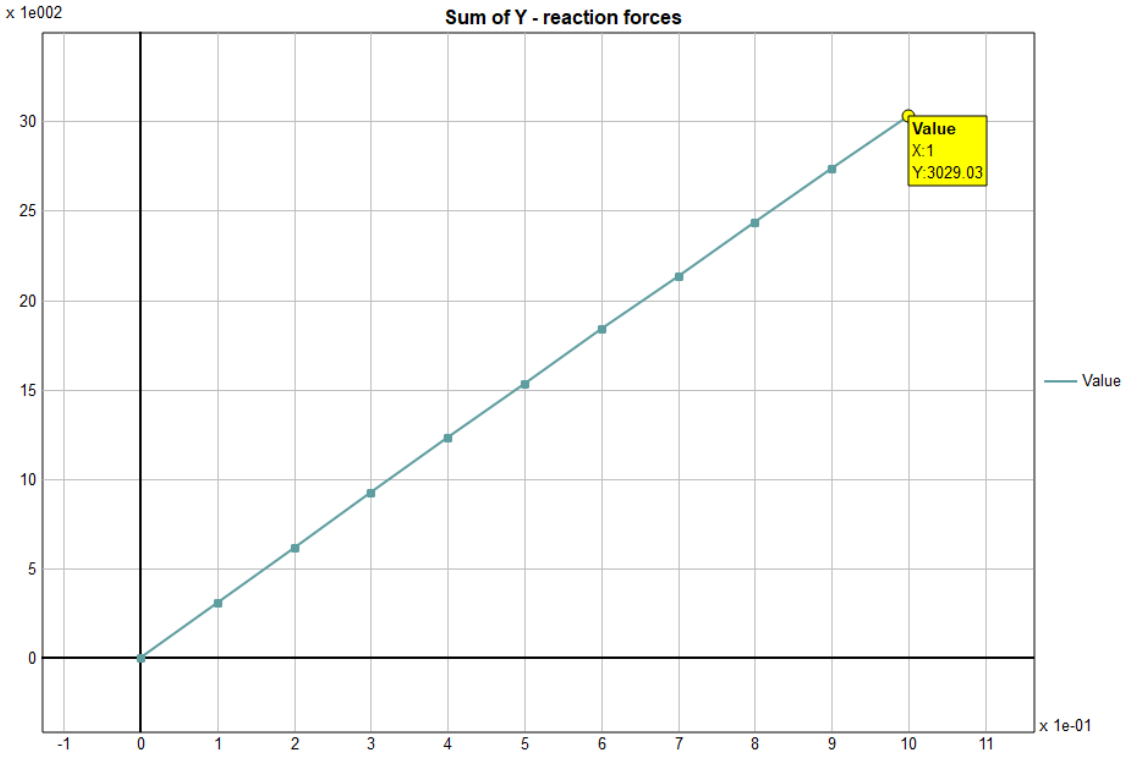

Figure 60: The total reaction force of specimen 1 highside

Lowside

The prescribed displacement value is set at 0.6 mm. The postview illustrates the color map of the reaction force of the lowside in the X-direction. The total reaction force at the top surface of the lowside is computed at 7987.72 N. Using the following formula, young's modulus is determined to be 163.01 N/mm^2.

$$E = \frac{\sigma}{\varepsilon} \tag{4.2}$$

$$\sigma = \frac{F}{A} = \frac{7987.72\ N}{98 \times 40\ mm^2}$$

$$\varepsilon = \frac{\Delta l}{L} = \frac{0.6\ mm}{48\ mm}$$

$$E = 163.01\ {}^{N}/_{mm^2}$$

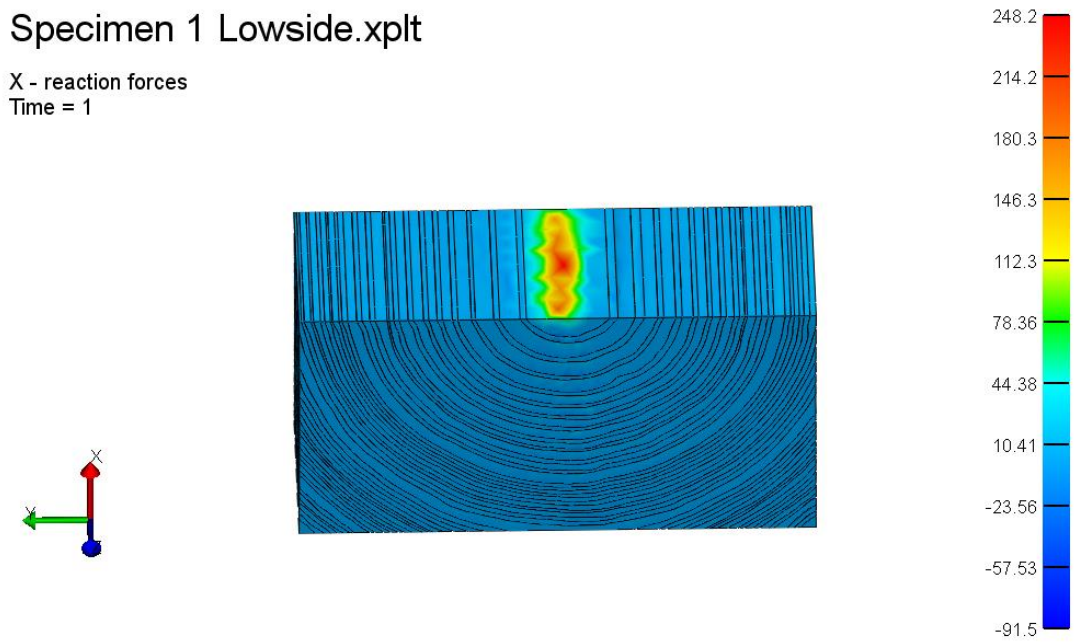

Figure 61: The color map of the reaction force of specimen 1 lowside

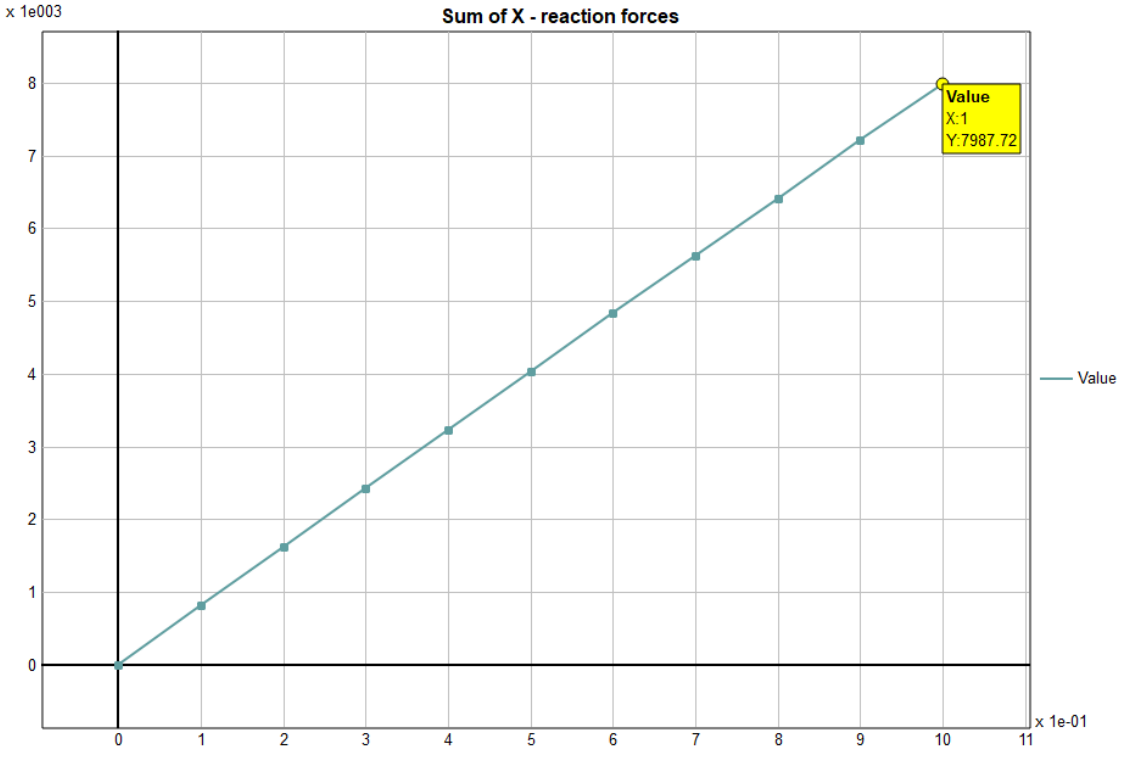

Figure 62: The total reaction force of specimen 1 lowside

4.2.2 Specimen 2

Highside

The input for the prescribed displacement value is set at 0.59 mm. The color map illustrates the reaction force of the highside in the Y-direction. The total reaction force at the top of the surface is computed to be 2446.86 N, and the young's modulus is calculated to be 211.68 N/mm^2.

$$E = \frac{\sigma}{\varepsilon} \tag{4.3}$$

$$\sigma = \frac{F}{A} = \frac{2446.86\ N}{48 \times 40\ mm^2}$$

$$\varepsilon = \frac{\Delta l}{L} = \frac{0.59\ mm}{98\ mm}$$

$$E = 211.68\ {}^{N}/_{mm^2}$$

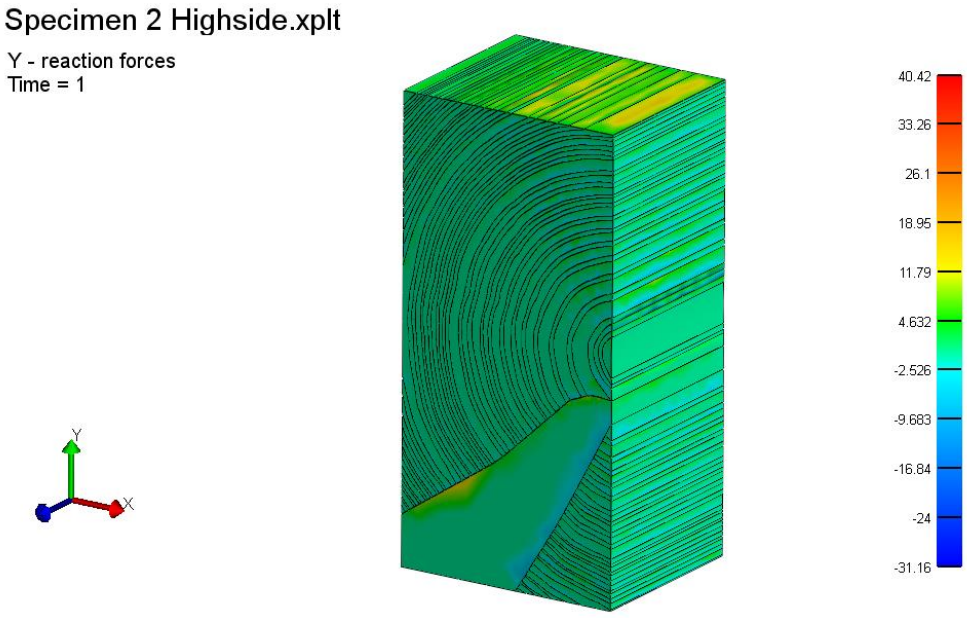

Figure 63: The color map of the reaction force of specimen 2 highside

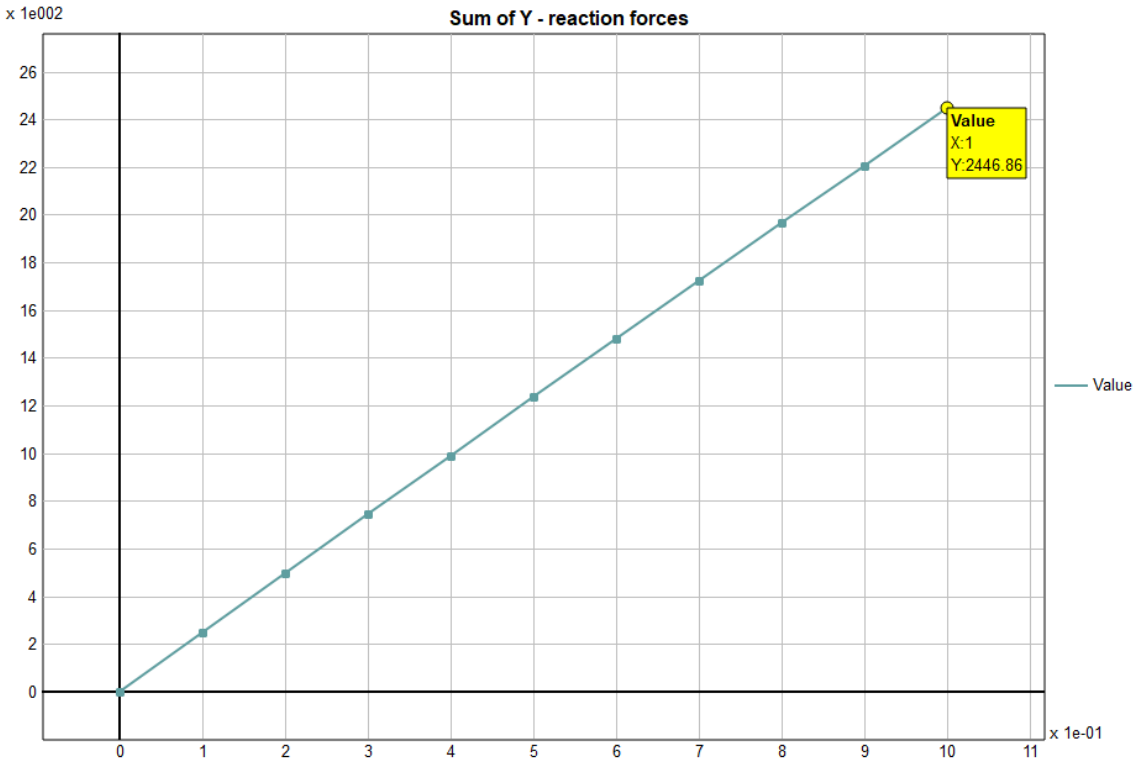

Figure 64: The total reaction force of specimen 2 highside

Lowside

The input for the prescribed displacement is set at 0.6 mm. The postview visualizes the color map of the reaction force in the X-direction. The total reaction force at the top surface of the lowside is 9845.33 N, and Young's modulus is computed to be 200.93 N/mm^2.

$$E = \frac{\sigma}{\varepsilon} \tag{4.4}$$

$$\sigma = \frac{F}{A} = \frac{9845.33\ N}{98 \times 40\ mm^2}$$

$$\varepsilon = \frac{\Delta l}{L} = \frac{0.6\ mm}{48\ mm}$$

$$E = 200.93\ {}^{N}/_{mm^2}$$

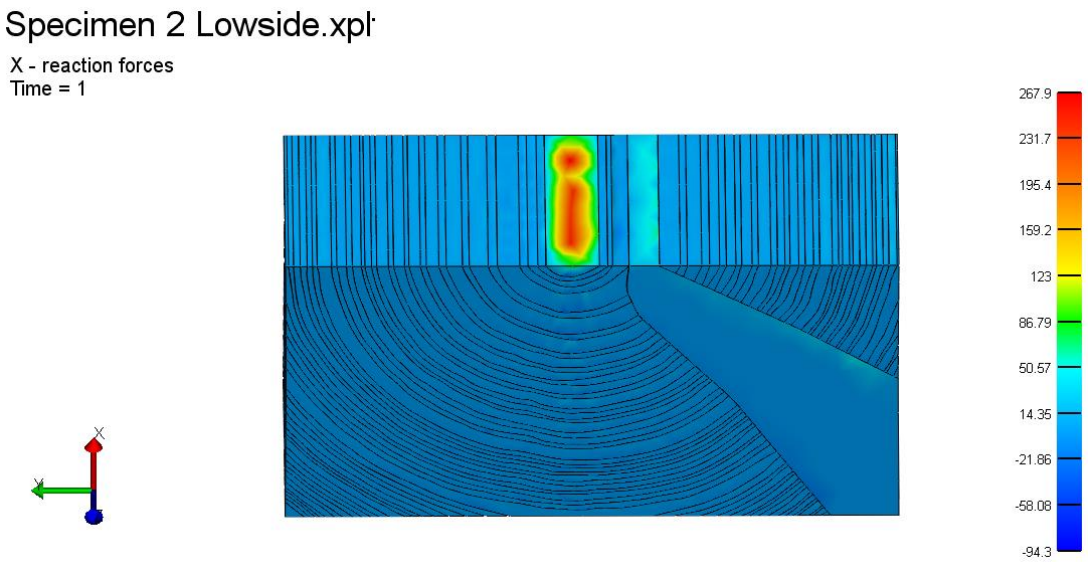

Figure 65: The color map of the reaction force of specimen 2 lowside

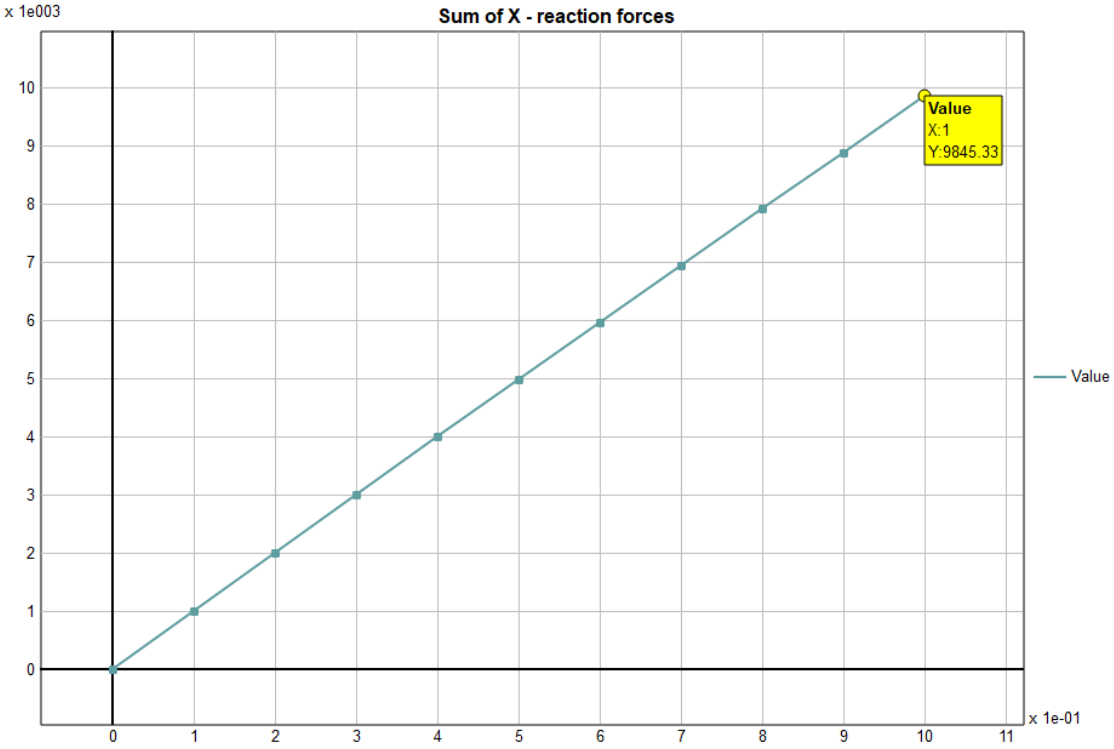

Figure 66: The total reaction force of specimen 2 lowside

4.3 Mechanical testing

After conducting the mechanical test, the machine provides the force and displacement values. To find young's modulus, the value of force and displacement is transformed into a stress and strain diagram, and from there, the elastic region is determined by calculating the slope, which represents Young's modulus. To create the slope, a regression line is drawn close to the points of the elastic region. The proximity of the regression line for most of the diagrams is relatively close to the curve, with a value of 0.99.

The figure below illustrates the force-displacement curves of the highside and lowside of the both specimens. The specimen 1 highside curve starts at point 160 N and 0.00 and continues to 2420 N and 1.06 mm. The specimen 1 lowside begins at 150 N and 0 mm and continues until 5040 N and 0.6 mm. The specimen 2 highside starts at 160 N and 0.04 and extends to 2430 N and 0.59 mm. The specimen 2 lowside commences at 150 N and 0.02 mm and goes on until 4930 N and 0.6 mm.

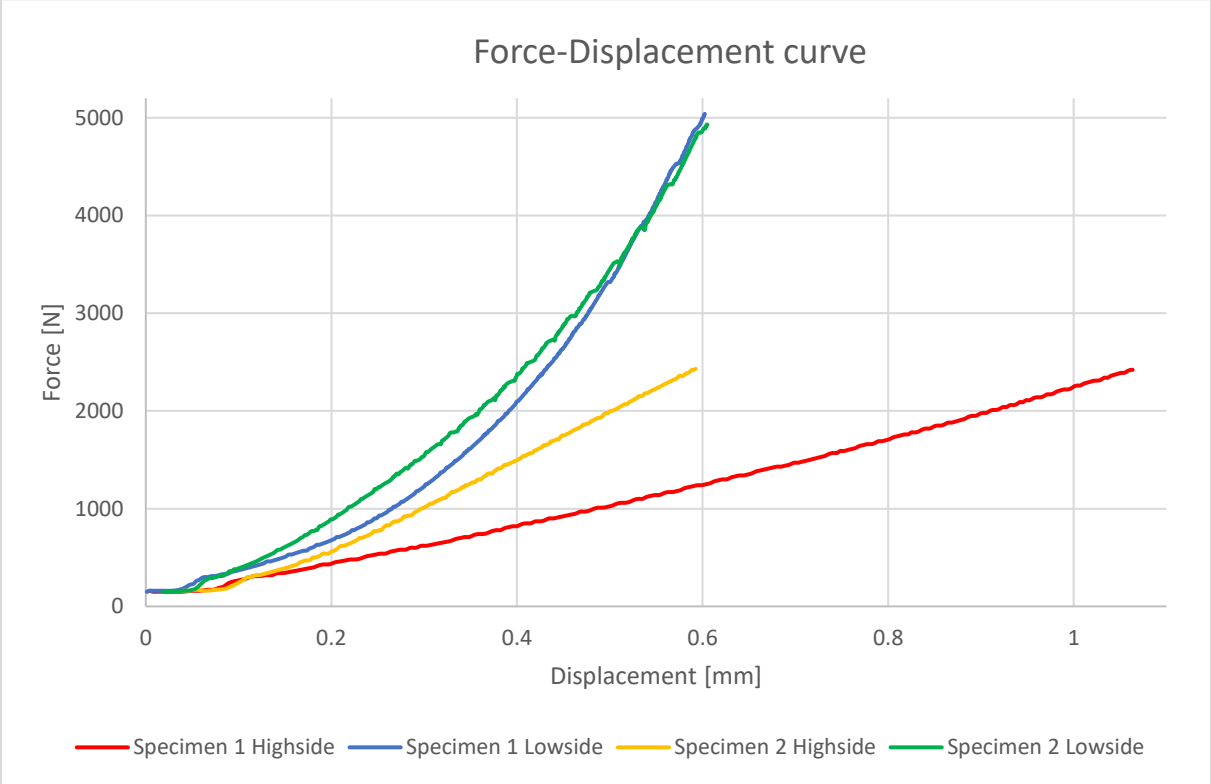

Figure 67: Force-Displacement curves of specimens 1 and 2

To calculate the stress and strain of the highside, all its forces are divided to the section area of 48x40 mm; for strain, all the displacement values are divided to a height of 98 mm. As a result, for the highside of specimen 1, the force of 2420 N and the displacement value of 1.06 mm is transformed to a stress of 1.26 N/mm^2 and a strain of 0.011. Similarly, for the highside of specimen 2, a force of 2430 N and a displacement value of 0.59 mm is converted to a stress value of 1.27 N/mm^2 and a strain value of 0.006.

To compute the stress and strain of the lowside, the forces are divided into the cross-sectional area of 98x40 mm, and the displacement is divided by a height of 48 mm. Hence, the force value of 5040 N with a displacement value of 0.6 mm is transformed to a stress of 1.29 N/mm^2 and a strain of 0.013. The same applies for the lowside at specimen 2; a force of 4930 N and a displacement value of 0.61 mm is converted to the stress value of 1.26 N/mm^2 and a strain value of 0.013.

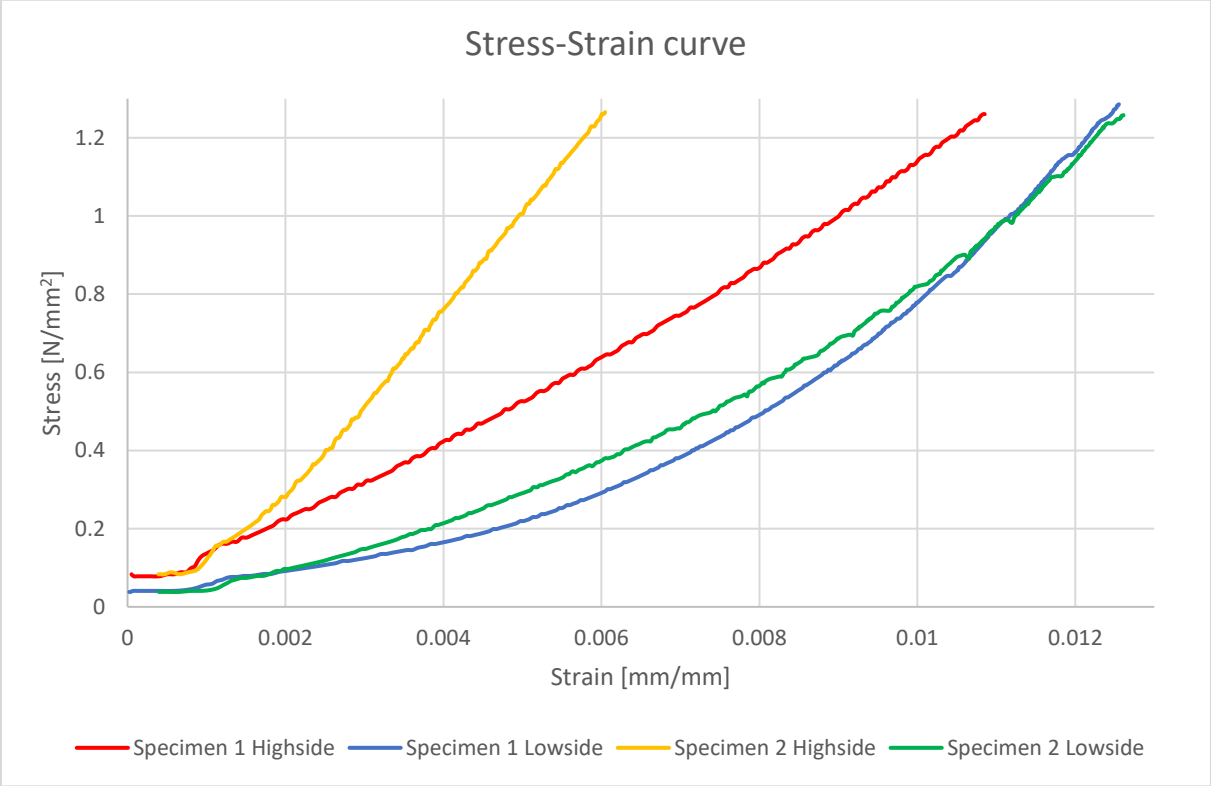

Figure 68: Stress-Strain curves of specimens 1 and 2

The mechanical testing for specimens is not conducted until failure of the material, and this makes it challenging to locate where the elastic region is and where it begins and where it ends. To define young's modulus, defining the elastic region is essential. Based on the calculation before the compressive testing, the half-point of the elastic region has been calculated, but its start point is still uncertain.

To reasonably assume the elastic region, the starting point statrs from 0.8 N/mm^2 and continues until the half-point, and this will be used for calculating the slope or young's modulus. In addition, the starting point is relatively close to the half-point, which increases the likelihood for the value of the slope to be within the elastic region.

The starting point for specimen 1 highside is at 0.8 N/mm^2 and 0.0075 and continues till 1.26 N/mm^2 till 0.0109. Young's modulus results at 135.87 N/mm^2, and the regression line is 0.99, which indicates that line is pretty close to the curve. The intercept value is not used because it's not important for calculating the young's modulus.

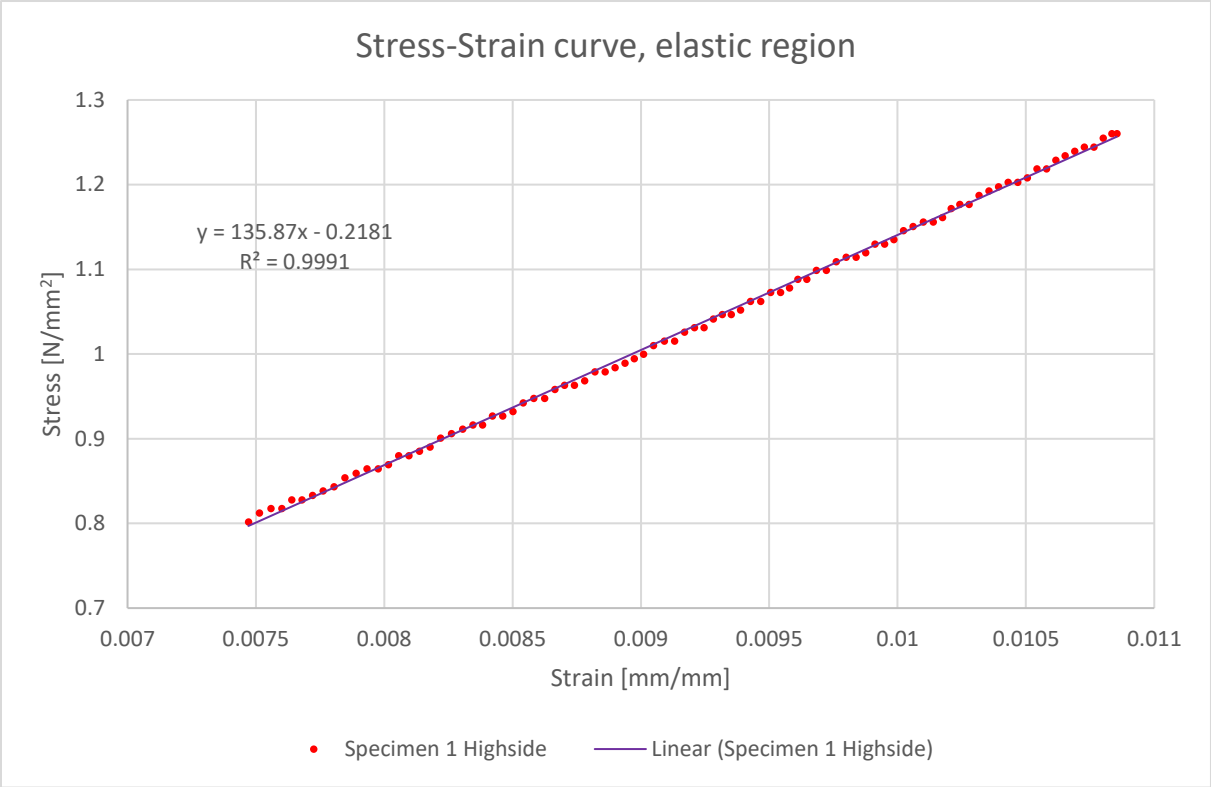

Figure 69: Stress-strain curve of specimen 1 highside

The starting point for specimen 1 lowside is at 0.8 N/mm^2 and 0.0101 and end at 1.29 N/mm^2 and 0.0126. Young's modulus is calculated at 202.72 N/mm^2, and the regression line is 0.99.

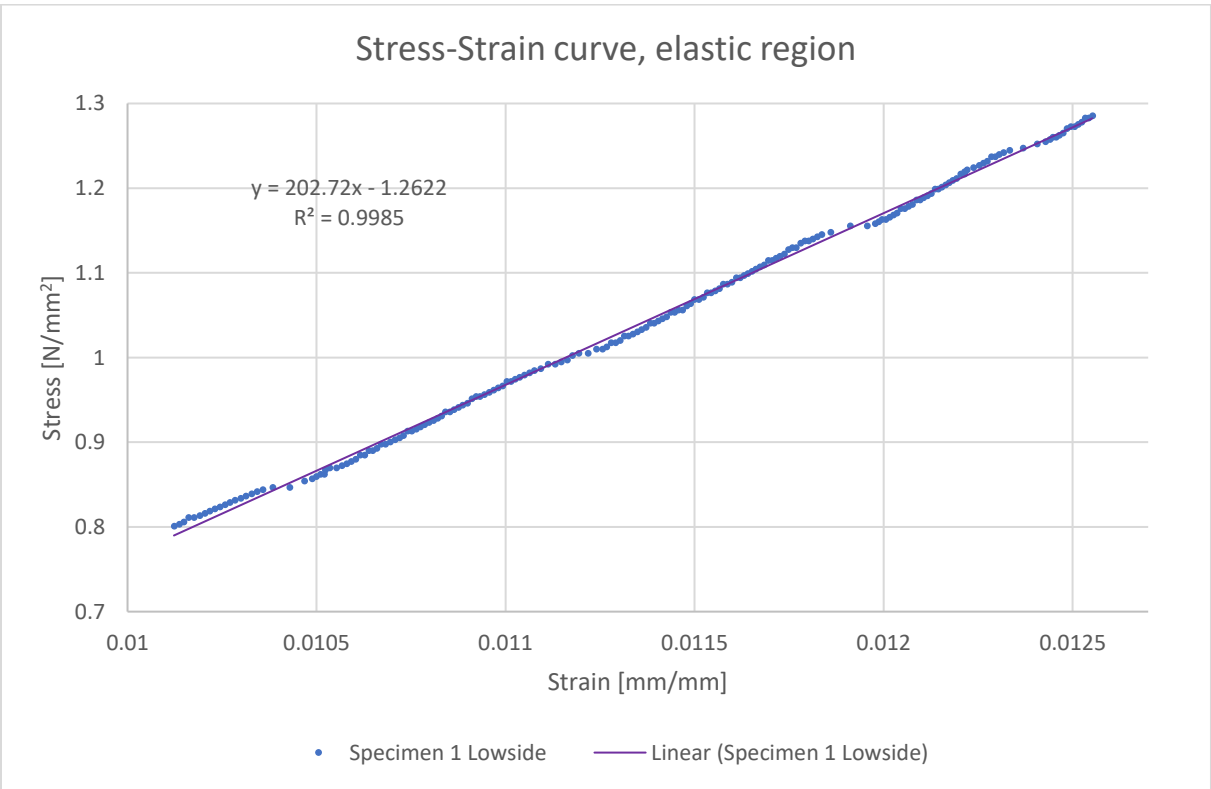

Figure 70: Stress-strain curve of specimen 1 lowside

The starting point for highside specimen 2 commences at 0.8 N/mm^2 and 0.0042, and it extends to 1.27 N/mm^2 and 0.006. Young's modulus is computed at 247.27 N/mm^2, and the regression line at 0.99.

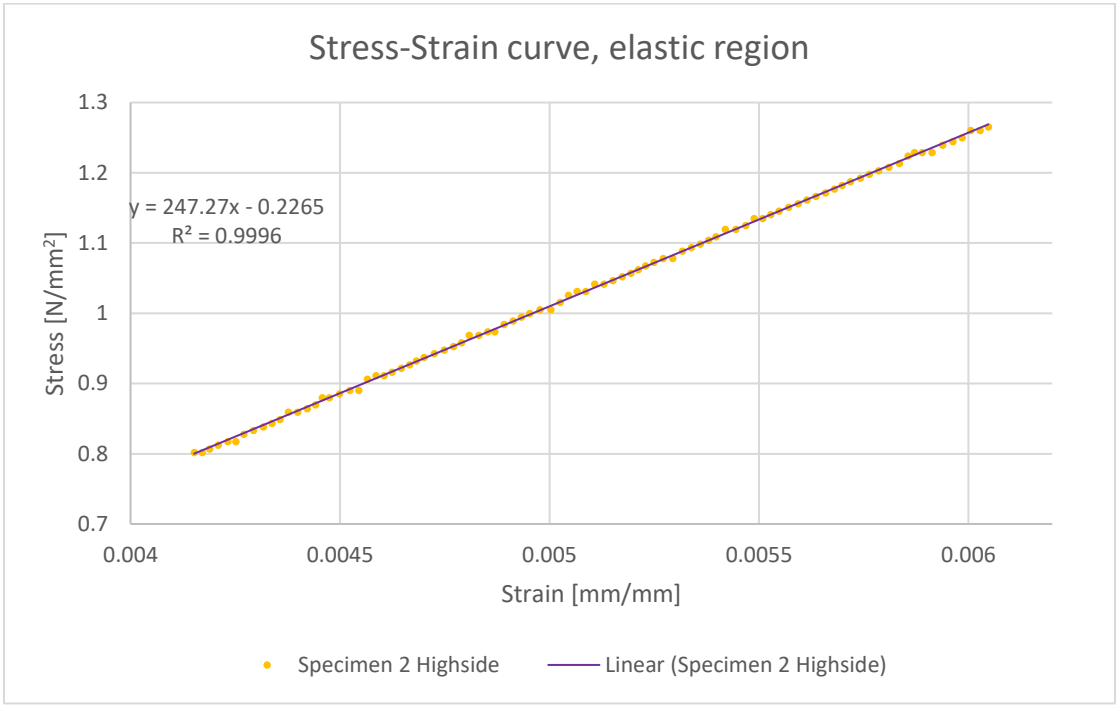

Figure 71: Stress-strain curve of specimen 2 highside

The starting point for specimen 2 lowside initiates at point 0.8 N/mm^2 and 0.0099, and it goes on until point 1.26 N/mm^2 and 0.0126. The regression line is 0.99, and Young's modulus is computed at 172.62 N/mm^2.

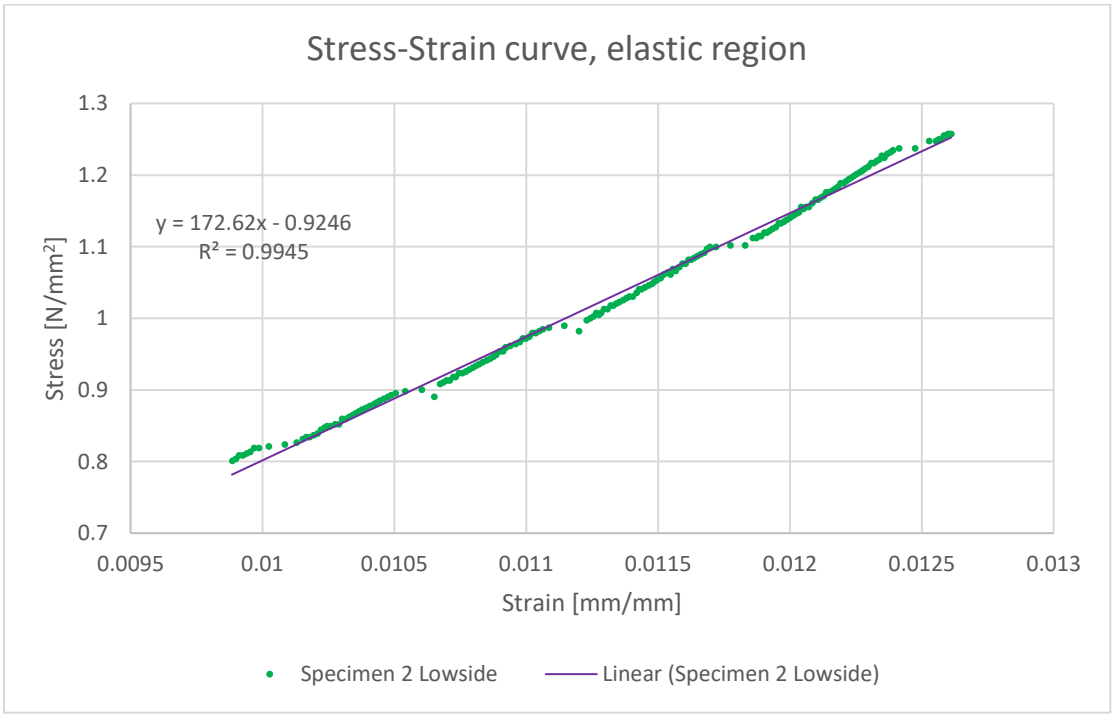

Figure 72: Stress-strain curve of specimen 2 lowside

5. Discussion

Three topics will be discussed in this chapter. Firstly, it will discuss creating the 3D modeling of the specimens and its challenges. Secondly, it will review comparing the FE results with the experimental results. Lastly, it will explore the benefits of using CT scanning to predict timber boards.

5.1 3D model

This section discusses some difficulties, advantages, and disadvantages of simulating and creating CAD and segmented models.

5.1.1 CAD model

CAD stands for "Computer-Aided Design," representing the 3D model of a 2D image or sketch. The advantage of using a CAD model is that there will be fewer chances for computational error at FEBio. The reason is that there are fewer surfaces, less complex details, and well-defined edges. And the surfaces are smooth, which makes it easier to pick and apply the displacement and the boundary condition.

The CAD model of the specimen is based on a slice from the entire sample; it is the worst-case scenario. Therefore, it makes the result to be more conservative. But the disadvantage is that the whole sample would have the same stiffness value, making its result less accurate than the experimental result. It's because the stiffness of a sample varies along its position.

Another drawback with the CAD modeling is that the process for creating the model and doing the simulation involves many steps, which makes the whole process time-consuming. The first step is to create the model, which takes some considerable time. Additionally, manual editing is often required, especially when there are errors in the segmented model, which must be fixed manually.

To tie the earlywood and latewood models, their surfaces need to be manually selected and attached together. For instance, specimen 1 has around 150 surfaces, and specimen 2 has even more. Picking these surfaces one by one takes time, and it becomes harder to pick when the gaps between some of the rings are smaller. Furthermore, selecting the surfaces one by one and adding the boundary condition is another tedious process.

Furthermore, creating a CAD model requires a different software of its own, and utilizing additional software prolongs the complexity of the software chain; it means that it will take a significant number of software to perform a relatively small task, which is predicting the stiffness of a small sample. Including this, all these software had to be learned, and learning them takes time and effort.

For instance, if an error appears in the model, let's say in FEBio, it has to go back in Fusion 360 to fix that error and start over all the process of meshing, tying, coordinating system, and boundary condition in FEBio again. And this cycle can occur multiple times because minor errors often appear later, especially during the simulation phase.

5.1.2 Segmented model

The segmented model refers to the models that are created at the 3D slicer. One advantage of using the segmented model is that it represents the entire specimen. Therefore, it won't be necessary to create CAD models at different positions on the board. As a result, the process is less tedious, and the simulation results are more accurate.

However, the drawback with the segmented model is that it contains a significant amount of details, which makes its file size extremely large and later makes the simulation on FEBio slow. After 95 percent decimation of A1 board, the model was still heavy, but it was a bit more manageable.

Segmented models usually have lots of noise, and extra software for cleaning these noises are needed, such as Meshlab. And for some reason, some lines got intersected with each other, and it gave the error of "self-intersection," which halted the progress. It became quite challenging to fix this error. Even other software, such as Meshmixer and Blender, couldn't able to resolve it. Therefore, this was one of the main motivations for transitioning toward creating CAD models.

Another disadvantage of the segmented model is that the edges of the latewood didn't extend to the board's edge entirely, making it challenging to apply boundary condition at the latewood. This issue was resolved in CAD modeling by manually editing and prolonging the ring, as shown in figures 36 and 37. However, it isn't easy to accomplish such editing in a segmented model.

Doing the tying system and selecting the surfaces is complex and time-consuming in a segmented model than in a CAD model. Because in the CAD model, on one side of the ring, the surface is smooth, and it's just one single surface that can easily be selected. But in the segmented model, there are hundreds of small surfaces on just one side of the ring and selecting all of them will take some considerable amount of time, and if a small error happens, the whole process has to be started over again. And, the same applies to selecting the surfaces for adding the boundary condition.

In future attempts, one of the different approaches that can be experienced is to try some other FE software, especially those with the paying license; they may offer better capabilities when dealing with the problem of applying material property to a single model. The main reason at the first place for creating separate models for earlywood and latewood was the limitation in FEBio; the software didn't allow the application of two material properties in one single model. Therefore, separate models of the specimen were created to apply the different material properties. Maybe some other finite element software can resolve this issue, where different material properties can be applied in one model. And, this will lead to eliminate the difficulties of tying, selecting the surfaces, meshing, and boundary conditions. The whole process will be less time-consuming, and the simulation will be quick and effortless.

Another approach to consider is developing a program code that automates all the manual steps so that the whole process is executed quickly and easily.

5.2 Comparison

The stiffness results from the FE analysis and the experimental results show a high correlation. To compare them percentagewise, they are 80-95 percent close to each other. But before jumping on the reasons for congruity and deviation, this procedure is tested with only at two samples. To draw a comprehensive and conclusive analysis, further tests are necessary. Nevertheless, based on the findings from these two samples, this chapter explores and discusses some potential reasons for congruity and deviation between the FEA and experimental results.

5.2.1 Congruity

There are several reasons why the finite element result is quite close to the experimental findings. First, the model of earlywood and latewood is accurately made. Even though it represents one slice of a specimen, its precision is relatively high. The choice of the slice is determined on the worst-case scenario so that the results would be accurate and representative for the entire specimen. For example, in specimen 2, the slice illustrates the knot at its maximum height. The knot changes through the specimen, but in slice 215 mm, it's at its ultimate peak. Therefore, the slice of that area is made as a model for the entire specimen.

Also, some extra editing is performed on the edges and surfaces of the annual rings to enhance their sharpness and flatness. So that they would be more visible on the surface and facilitate the application of the displacement on the surface of each growth ring and the knot. Doing this makes it easier to distribute the force and displacement across the whole surface and consider the minor and major details so that the stiffness prediction becomes as accurate as possible.

Moreover, determining the right mesh size is crucial for the accuracy of the FEA results. Therefore, it is aimed to have a relatively uniform mesh size through the entire model, so that the accuracy of the model and the results will be accurate. On the other hand, the mesh size is not that small either, so that prolongs the simulation duration. The earlywood and latewood are two separate models, having uniform mesh sizes will also help the tying system between the models so that they would get a good grip on each other and function as one cohesive model.

Similarly, applying different material properties on different models improves the reliability and precision of the analysis. For instance, the material property of latewood is different than the material property of earlywood. It's because the latewood is stiffer; therefore, it applies higher young's modulus and shear modulus. Furthermore, the material property for the knots is even higher than both earlywood and latewood. The overall material property is obtained from the literature, but to transform them into different stiffness values, the densities of specimens from the scan model are utilized for giving a fair estimation for determining these material properties.

Additionally, transitioning the local coordinate system of the material from a cartesian to a cylindrical coordinate system is another essential factor for achieving better results. It's because timber boards are cut from tree logs, which looks like a cylindrical object. Changing its material axis to a cylindrical coordinate system will allow its radial and tangential direction to vary depending on the model's position, which immensely affects the overall outcomes of the analysis.

To conclude, many factors are considered so that the FEA findings will be proximate to the experimental results. However, there are still some deviations in the results, and this will be discussed in the next section.

5.2.2 Deviation

To perform the FE analysis, two models are created for depicting the earlywood and latewood, and with an additional model for the knot. The reasons for making these models are to put different material properties so that results would become more precise. As mentioned earlier, the derived density from the CT scan is used to estimate the material properties of earlywood, latewood, and the knot. However, the annual rings have a transition phase between earlywood and latewood, called transitionwood. See figures 73 and 74. The peaks in the graph show the latewood, and the low points show earlywood; whatever is in between is transitionwood, and it possesses its own density property. So, this detail is not considered in the modeling of the specimens because it would increase the level of complexity. Also, it's time consuming to create an extra layer between each ring. It's uncertain how much of a big difference this model would make if it was created. But it will be interesting to see whether this would decrease or increase some of the deviations.

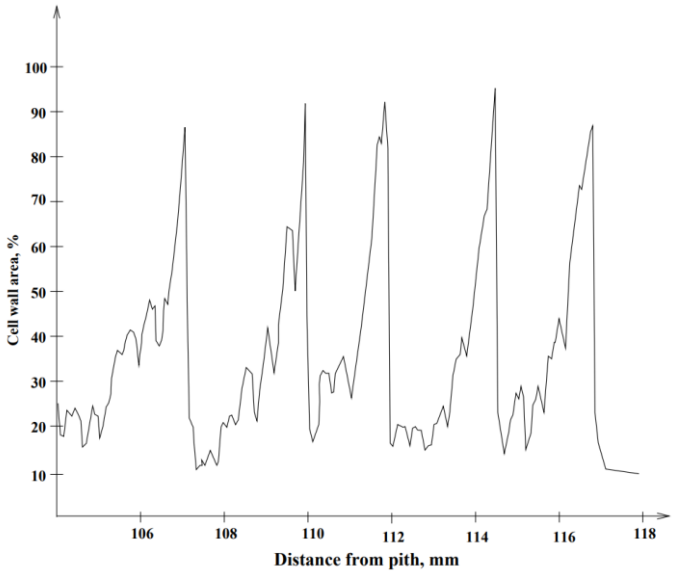

Figure 73: Variation in density over a few growth rings in the radial direction

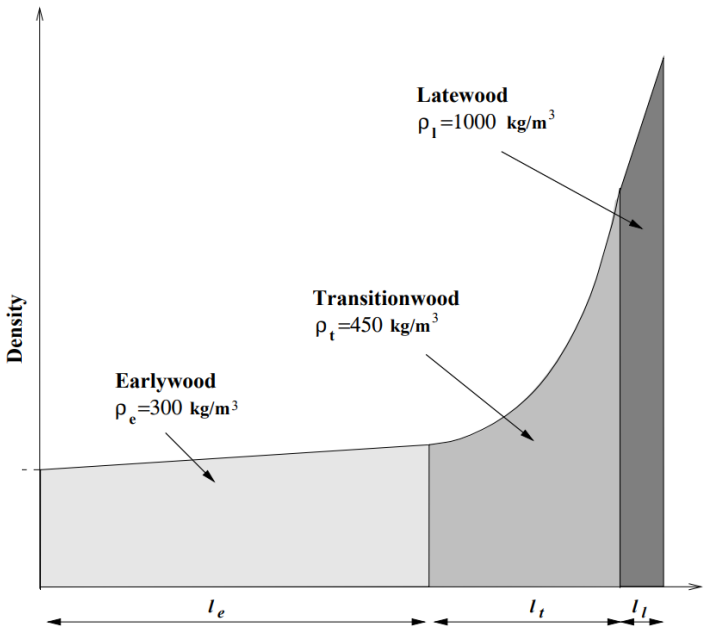

Figure 74: Density over a growth ring divided into three regions

Another significant factor for deviation in the FEA results is the presence of gaps and overlaps in the segmentations. By overlap means, for instance, when earlywood covers some of the density of the latewood, or vice versa, and when latewood covers some of the density of the knot. And creating the segmented model is a repetitive visual process where various input is tried until the rings appear correctly defined. Even though the segmentation for specimen 2 was made carefully, some gaps still occurred. For example, see igure 75; it shows some overlaps between the latewood and the knot and some tiny holes inside and at the edges of the green ring. The green ring represents earlywood. As the specimen's density decides the material property, these inconsistencies in the segmented model will directly affect the material property, and thereafter influence the FEA results.

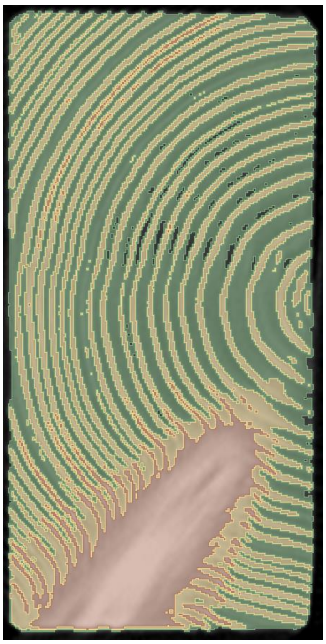

Figure 75: Segmented slice of specimen 2

Furthermore, another reason that potentially influences the deviations is that the specimens are taken from reclaimed wood. And there is some uncertainty with its age, previous usage, and specific type and class. Based on visual assessment, it is believed to be Norway spruce. Therefore, the reference value for its density and material property is obtained from the literature. The density values from the CT scan and the literature values contributed to defining the material property of earlywood, latewood, and the knot. Since there is some uncertainty with the Norway spruce and its class, this might create some minor deviations. This is because the reference value from the literature represents the average value of Norway spruce, not the specific wood class. However, it's doubtful that the deviation would be massive since the average value is quite close to the different classes of Norway spruce.

The other potential cause for deviation is that the sketch has been manually edited several times. Some rings had some disruptions and holes, and they were edited and linked together. And there were some smaller rings in the sketch, which were removed to reduce the complexity of the model and the computational time in FEBio. Some minor adjustments were made at the edge of the specimen to make them appear clean and straight. So, this kind of minor edit indirectly affects the FEA results. First, the model is now changed compared to the real specimen, and second, the material property assignment is messed, because in some areas the material property of latewood is assigned with the material property of earlywood, and some material property of earlywood is assigned with latewood.

Lastly, as explained in the moisture content chapter and Figure 11. A slight change in moisture content can impact the stiffness and strength of wood. The moisture content for the A1 board in February was 18.3 percent, and in May, right before the mechanical testing, it was 12.4 percent. So this means that the moisture content before CT scanning was higher than during the mechanical testing. But, measuring the moisture content through a moisture meter is less reliable than the oven-dry method. For example, the moisture content of A2 was estimated at 19.3 percent, and when the oven-dried method was applied, the moisture content resulted in 11.69 percent. This is a huge difference. However, both results of A1 were measured similarly through a moisture meter. This means no matter how unreliable the equipment is when both measurements have occurred under similar equipment and the value has changed. It means that the moisture content has changed. It’s not that clear to say how much due to the unreliability of the measuring equipment, but it can be confirmed that moisture content has changed during this period. So, this might have affected some of the deviations between the FEA results and the mechanical results.

5.3 CT scanning

There are several benefits of using CT scanning on timber boards. To begin with, it is a non-destructive method, where there is no need to destroy the material or prepare a specific specimen, thereby reducing unnecessary waste. Many non-destructive methods exist, but CT scanning is the most effective because it visualizes the defects, which the other non-destructive method can't do. The other non-destructive method only produces a graph of a material but not a 3D model of it. CT scanning can quickly and accurately identify the defects, where the defect starts and where it ends, which direction it goes, how it impacts its surroundings, etc.

Secondly, CT scanning produces high-resolution images, which makes it easier to understand the internal structure of the wood, such as annual rings, the complexity of knots, how its density is spread out, etc. This valuable information can be used to optimize the timber's stiffness quality. Furthermore, CT scanning is highly effective at examining the internal structure of reclaimed timber, for instance, the effect of cracks, decay, and nails. This analysis determines whether the wood is still reusable or should be destroyed. Figure 76 illustrates a CT image of the C1 board, which shows the presence of cracks and nail in the middle with the brightest color. Nail is a metal, and it's a highly dense material. In CT scanning, metal interferes with the CT images, but in this case, the interference was minimal and didn't impact the quality of the image that much.

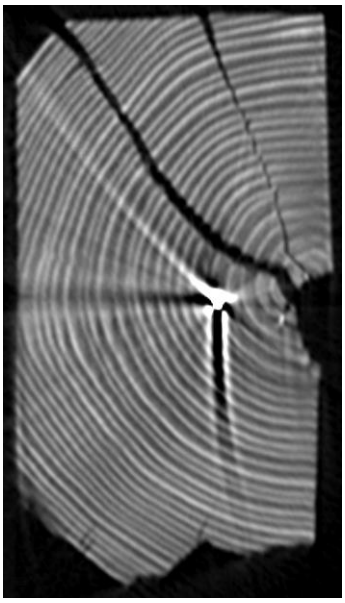

Figure 76: CT image of C1 board

Furthermore, CT scanning is a wonderful method for measuring density. It can quickly identify and measure the density of the entire model or just a specific section of it. Density is an important parameter for calculating the wood's material properties and stiffness.

Finally, CT scanning is beneficial for accurately extracting a detailed 3D model of an object or timber board, including size, shape, and internal structure. It can extract the entire model or just a small part, which can then be used to perform the finite element analysis.

Even though there are numerous benefits to CT scanning, one of the challenges of it is that it produces a lot of data; in one aspect, this is one of the advantages of CT scanning. But on the other hand, this makes the process slower compared to the other non-destructive methods, where they generate some diagrams, which is a quick read. But with the CT scanning, some time had to be spent on reading and analyzing the CT images, extracting the model in software, etc.

6. Conclusion

This thesis studies developing a Finite element Model based on CT images of timber boards to predict the local stiffness. Eleven boards were CT scanned, and only two samples were used for geometry extraction and Finite element modeling. In addition, a mechanical test of the same sample was also conducted to compare the FEA results with the mechanical results. The dimensions for the specimens are 98 mm in height, 48 mm in weight, and 40 mm in length. The samples were tested at two sides, called highside and lowside, and both sides were perpendicular to the grain. Highside is the height side of the specimen, and the lowside is the weight side of the specimen.

The stiffness value for specimen 1 highside from FEA resulted in 145.86 N/mm^2, compared to 135.87 N/mm^2 from mechanical testing. The FEA stiffness value is slightly higher than the mechanical stiffness value, but they are close. For specimen 1 lowside, the FEA stiffness value calculated in 163.01 N/mm^2, while the mechanical testing measured 202.72 N/mm^2. The FEA value is lower than the mechanical stiffness value, with a difference of 80 percent.

Moving forward to specimen 2, the FEA stiffness value for the highside is computed at 211.68 N/mm^2, compared to 247.27 N/mm^2 from mechanical testing. The FEA value is lower than the mechanical testing result, but they are close to each other. Lastly, the young's modulus of specimen 2 lowside is calculated at 200.93 N/mm^2, while the mechanical testing is computed as 172.62 N/mm^2. The FEA stiffness value is higher than the mechanical value, with a difference of 86 percent.

This procedure is only applied on two samples, and more tests are needed to draw a better conclusion on the reasons for congruity and deviations between the results. However, to make an assumptions based on these few samples. The reasons for congruity are that the earlywood, latewood, and knot models are accurately made. The mesh size is approximately uniform, the material parameters are estimated correctly, and the cylindrical coordinate system was employed for the local coordinate system of the elements. The reasons for deviations are transitionwood between earlywood and latewood is not included in the model; the segmentation model had some minor gaps which affected density which later influenced the material parameter; and manual editing has also affected some of the density values and the material parameters.

CT scanning is a non-destructive measuring method, and it's highly used in the wood industry. The main contribution of this study is to provide a procedure that would predict the stiffness of wood without doing mechanical testing, and this would help to reach the stiffness potential of wood to a higher level and give a new life to reclaimed wood, ultimately reducing waste.

A limitation of this procedure is that it's tested on a few samples, which doesn't give a proper conclusion on this method's reliability and validity. Nevertheless, the primary objective of this thesis is to create a process that utilizes CT scanning and building finite element modeling. The development of this procedure required the use and learning of various software, and significant time was dedicated to creating it. Performing additional tests on this procedure can be pursued in the future work.

7. Future work

The future work of this procedure is to first conduct more tests with many different samples. It can be tested with samples with different dimensions, wood types such as pine, new wood, reclaimed wood, and samples with two or more knots, etc. These tests will help to provide a comprehensive understanding of how reliable and valid this procedure is, and it would make the reasons for the deviations more apparent; once the causes are identified, it would be easier to address them.

The next step is to improve this procedure for predicting the board's entire stiffness. This would make the performance of finite element analysis much easier and quicker. The overall results would become more accurate. And it will not be necessary to create models based on slice sketches representing a small section. Also, this results in reducing the use of multiple software.

This procedure can be tried and experienced with other FE software, such as Abaqus, Ansys, Solidworks, etc. It's to find out if the other software offers some better solutions than FEBio Studio when it comes to skipping some of the tedious steps, such as manual selecting of the surfaces one by one, doing the tying operation, or able to add more material on one model instead of being restricted to add one material in one model.

If the other FE software offers the same features as FEBio Studio, the next step is to develop a programming code to automate those tiresome steps. Many FE software can take programming code as input, such as Abaqus. Also, make sure to choose the programming language which that software supports. For example, Abaqus supports Python.

Lastly, this procedure can be experienced in predicting the other physical properties of the wood, such as strength. Prediction of strength is much more complex than stiffness, and it would be nice to investigate how CT scanning can predict strength. Find out the challenges and limitations and how they could be overcome.

Bibliography

Abundance, Z. (2023, May 10). THE HORYUJI: WORLD'S OLDEST SURVIVING WOODEN ARCHITECTURE. Retrieved from https://www.interactiongreen.com/5034-2/

Arkitekter, V. (2023, May 10). OM PROSJEKTET. Retrieved from https://vollark.no/portfolio_page/mjostarnet/

Beam, B. P. (2023, June 2). What Species of Wood to Use in a Timber Frame? Retrieved from https://www.brookspostandbeam.com/blog/what-species-of-wood-to-use-in-a-timber-frame/

Berggren, G. (2012, September 20). Instruktioner för fuktkvotsmätning i fält och rekommendation av mätinstrument. *SP Sveriges Tekniska Forskningsinstitut*. Retrieved from https://www.maleriforetagen.se/globalassets/dokumentbank-oppna/sp-ytfuktkvotsrapport-20120920.pdf

Blaß, H. J., & Sandhaas, C. (2017). Timber Engineering - Principles for Design. Retrieved from https://publikationen.bibliothek.kit.edu/1000069616

Britannica. (2023, May 26). Hooke's law. Retrieved from https://www.britannica.com/science/Hookes-law

Britannica. (2023, June 1). shear modulus. Retrieved from https://www.britannica.com/science/shear-modulus

Buildings, K. (2019, July 2). A brief history of Wooden Buildings. Retrieved from https://kirtonbuildings.co.uk/2019/07/02/a-brief-history-of-wooden-buildings/

BYJU'S. (2023, April 24). Poisson's Ratio - Longitudinal Strain and Lateral Strain. Retrieved from https://byjus.com/physics/poissons-ratio/

Cambridge, U. o. (2023, June 1). Nodes, elements, degrees of freedom and boundary conditions. Retrieved from https://www.doitpoms.ac.uk/tlplib/fem/node.php

Carminati, L. (2018). Generalizability in Qualitative Research: A Tale of Two Traditions. Retrieved from https://journals.sagepub.com/doi/pdf/10.1177/1049732318788379

Carmines, E. G., & Zeller, R. A. (1979). *Reliability and Validity Assessment.*

Cool, I. J. (2023, May 10). Buddhist art of Horyu-ji Temple. Retrieved from https://www.ana-cooljapan.com/destinations/nara/buddhistartofhoryu-jitemple

CORROSIONPEDIA. (2019, May 4). Elastic Modulus. Retrieved from https://www.corrosionpedia.com/definition/429/elastic-modulus

Dahl, K. B. (2009, December). Mechanical properties of clear wood from Norway spruce. Retrieved from https://ntnuopen.ntnu.no/ntnu-xmlui/bitstream/handle/11250/236422/280301_FULLTEXT04.pdf?sequence=1

Deng, Q., Li, S., & Chen, Y. (2012, June 20). Mechanical properties and failure mechanism of wood cell wall layers. Retrieved from https://www.sciencedirect.com/science/article/pii/S0927025612003291

Direct, R. (2023, June 2). What Is Mechanical Testing: Different Types of Mechanical Testing of Materials. Retrieved from https://www.rapiddirect.com/blog/what-is-mechanical-testing/

Folkebladet. (2023, June 5). Flisa bru må forsterkes før gjenåpning. Retrieved from https://www.folkebladet.no/norgeogverden/i/76dRq4/flisa-bru-maa-forsterkes-foer-gjenaapning

FROM+TEST. (2023, May 20). Compression and Bending/Flexure Testing Machine MEGA 6. Retrieved from https://www.formtest.de/en/Products/Machine-Series/MEGA-6-Series.php

Glass, S. V., & Zelinka, S. L. (2010). Moisture relations and physical properties of wood. Retrieved from https://www.fpl.fs.usda.gov/documnts/fplgtr/fplgtr190/chapter_04.pdf

Houses, A. W. (2023, May 22). Wood main physical properties. Retrieved from https://ownwoodenhouse.com/index.pl?act=NEWSSHOW&id=2011062001

Huber, J. A. (2021, October). Numerical Modelling of Timber Building Components to Prevent Disproportionate Collapse. Retrieved from https://ltu.diva-portal.org/smash/get/diva2:1562953/FULLTEXT01.pdf

Huber, J. A., Broman, O., Ekevad, M., Oja, J., & Hansson, L. (2022, February). A method for generating finite element models of wood boards from X-ray computed tomography scans. Retrieved from https://www.sciencedirect.com/science/article/pii/S0045794921002248#t0005

HUBER, J. A., EKEVAD, M., & BROMAN, O. (2021, April 5). USING COMPUTED TOMOGRAPHY DATA FOR FINITE ELEMENT MODELS OF WOOD BOARDS. Retrieved from https://www.researchgate.net/publication/350239036_Using_Computed_Tomography_Data_for_Finite_Element_Models_of_Wood_Boards

Hutton, D. V. (2003). *Fundamentals of Finite Element Analysis.* Retrieved from https://wp.kntu.ac.ir/fz_kalantary/Source/Finite%20element%20method/Books-Numerical/Fundamentals%20of%20Finite%20Element%20Analysis,%20Hutton%20(2004).pdf

KLEPPE, O. (2023). Trebruer i Norge i dag og tidligere. Retrieved from https://dms-cf-10.dimu.org/file/0136KRRRo7au

Laver, A. (2022, October 19). Hardwood Vs softwood whats the difference? Retrieved from https://www.laver.co.uk/blog/hardwood-vs-softwood-whats-the-difference.html

Madhu. (2020, August 10). Difference Between Orthotropic and Anisotropic. Retrieved from https://www.differencebetween.com/difference-between-orthotropic-and-anisotropic/

Mascia, N. T., & Lahr, F. A. (2006, May 12). Remarks on orthotropic elastic models applied to wood. Retrieved from https://www.researchgate.net/publication/250029609_Remarks_on_orthotropic_elastic_models_applied_to_wood

Medicine, J. H. (2023, May 10). Computed Tomography (CT) Scan. Retrieved from https://www.hopkinsmedicine.org/health/treatment-tests-and-therapies/computed-tomography-ct-scan

Mudiyanselage, S., Rajeev, P., Gad, E., Sriskantharajah, B., & Flatley, I. (2019, May 11). Application of stress wave propagation technique for condition assessment of timber poles. Retrieved from https://www.tandfonline.com/doi/full/10.1080/15732479.2019.1610463

Nations, U. (2023, June 2). Goal 11. *Make cities and human settlements inclusive, safe, resilient and sustainable*. Retrieved from https://sdgs.un.org/goals/goal11

Nations, U. (2023, June 2). Goal 12. *Ensure sustainable consumption and production patterns*. Retrieved from https://sdgs.un.org/goals/goal12

Nations, U. (2023, June 2). Goal 13. *Take urgent action to combat climate change and its impacts*. Retrieved from https://sdgs.un.org/goals/goal13

Nations, U. (2023, June 2). Goal 15. *Protect, restore and promote sustainable use of terrestrial ecosystems, sustainably manage forests, combat desertification, and halt and reverse land degradation and halt biodiversity loss*. Retrieved from https://sdgs.un.org/goals/goal15

Nations, U. (2023, June 3). Goal 17. *Strengthen the means of implementation and revitalize the Global Partnership for Sustainable Development*. Retrieved from https://sdgs.un.org/goals/goal17

Nations, U. (2023, June 2). Goal 8. *Promote sustained, inclusive and sustainable economic growth, full and productive employment and decent work for all*. Retrieved from https://sdgs.un.org/goals/goal8

Nations, U. (2023, June 2). Goal 9. *Build resilient infrastructure, promote inclusive and sustainable industrialization and foster innovation*. Retrieved from https://sdgs.un.org/goals/goal9

Nations, U. (2023, June 2). The 17 Sustainable Development Goals. Retrieved from https://sdgs.un.org/goals

NIBIB, N. I. (2022, June). Computed Tomography (CT). Retrieved from https://www.nibib.nih.gov/science-education/science-topics/computed-tomography-ct

Norway, V. (2023, May 9). STÅLEKLEIVLOFTET - ONE OF THE OLDEST WOODEN BUILDINGS IN THE WORLD. Retrieved from https://www.visitnorway.com/listings/st%C3%A5lekleivloftet-one-of-the-oldest-wooden-buildings-in-the-world/207516/

Oral, I., Kocaman, S., & Ahmetli, G. (2022, June 30). Characterization of unmodified and modified apricot kernel shell/epoxy resin biocomposites by ultrasonic wave velocities. Retrieved from https://link.springer.com/article/10.1007/s00289-022-04328-6

Persson, F., & Andersson, J.-E. (2016). Automatisk övervakning och uppföljning i torkprocessen. *SP Sveriges Tekniska Forskningsinstitut*. Retrieved from https://www.diva-portal.org/smash/get/diva2:1073496/FULLTEXT01.pdf

PERSSON, K. (2000, October). MICROMECHANICAL MODELLING OF WOOD AND FIBRE PROPERTIES. Retrieved from https://www.byggmek.lth.se/fileadmin/byggnadsmekanik/publications/tvsm1000/web1013.pdf

Prawoto, Y. (2012, June). Seeing auxetic materials from the mechanics point of view: A structural review on the negative Poisson's ratio. Retrieved from https://www.sciencedirect.com/science/article/pii/S092702561200078X

Sarnaghi, A. K., & Kuilen, J. v. (2019, January 16). Strength prediction of timber boards using 3D FE-analysis. Retrieved from https://www.sciencedirect.com/science/article/pii/S0950061819300327

Skibeli, M. (2017, June). Concrete Plates Designed with FEM. Retrieved from https://ntnuopen.ntnu.no/ntnu-xmlui/bitstream/handle/11250/2454104/16980_FULLTEXT.pdf?sequence=1&isAllowed=y

Spycher, M., Schwarze, F. W., & Rene´Steiger. (2007, November 14). Assessment of resonance wood quality by comparingits physical and histological properties. Retrieved from

https://www.researchgate.net/publication/226807771_Assessment_of_resonance_wood_quality_by_comparing_its_physical_and_histological_properties

Table1. (NS-EN 338 2016).

Telemarkshistorier. (2023, May 12). Åse Stålekleiv – «Dronninga i Eidsborg». Retrieved from https://telemarkshistorier.no/kultur-og-tradisjon/ase-stalekleiv-dronninga-i-eidsborg/

TESTRESOURCES. (2023, May 28). What is Compression Testing? Retrieved from https://www.testresources.net/applications/test-types/compression-test/

wikipedia. (2023, June 1). Shear modulus. Retrieved from https://en.wikipedia.org/wiki/Shear_modulus

Zamani, N. G. (2017, September 12). The Challenges of Teaching Finite Element Analysis in the Undergraduate Curriculum. Retrieved from https://www.researchgate.net/publication/307090373_The_Challenges_of_Teaching_Finite_Element_Analysis_in_the_Undergraduate_Curriculum

Appendices

Appendix A

- CT models of the other boards

Appendix B

- Mechanical compressive testing data

Appendix C

The following appendices will be sent digitally to NTNU in a separate file.

- CT Scan
    - CT scan A1
    - CT scan A2
    - CT scan B1
    - CT scan B2
    - CT scan C1
    - CT scan C2
    - CT scan D1
    - CT scan D2
    - CT scan X
    - CT scan Y
    - CT scan Z
- 3D slicer
    - Earlywood segmentation model – Specimen 1
    - Latewood segmentation model – Specimen 1
    - Earlywood segmentation model – Specimen 2
    - Latewood segmentation model – Specimen 2
    - Knot segmentation model – Specimen 2
- Fusion 360
    - Earlywood and Latewood sketch model – Specimen 1
    - Earlywood, Latewood and knot sketch model – Specimen 2
- FEBio Studio
    - Specimen 1 Highside
    - Specimen 1 Lowside
    - Specimen 2 Highside
    - Specimen 2 Lowside

Appendix A

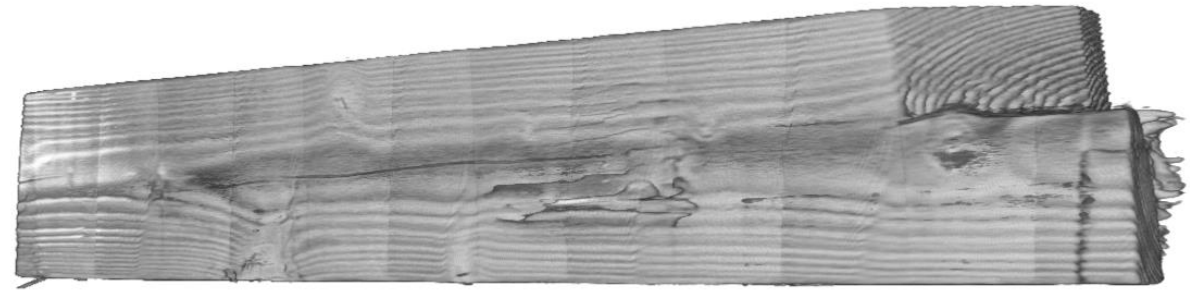

Figure 77: CT model of A2

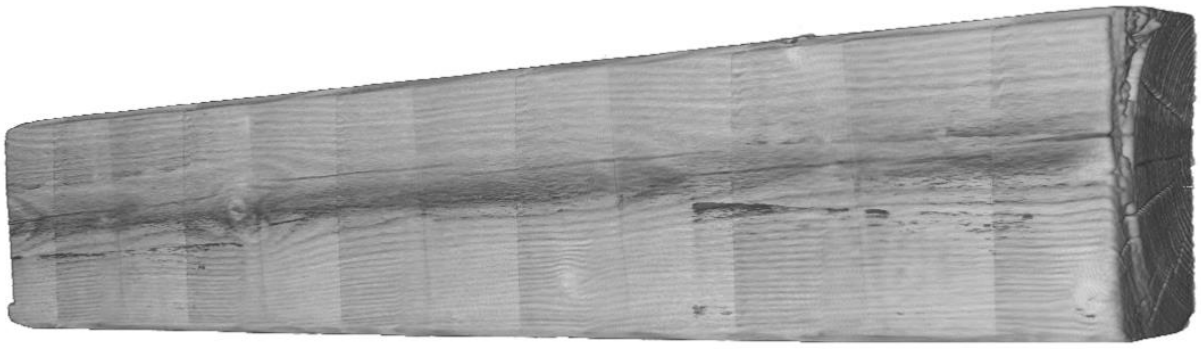

Figure 78: CT model of B1

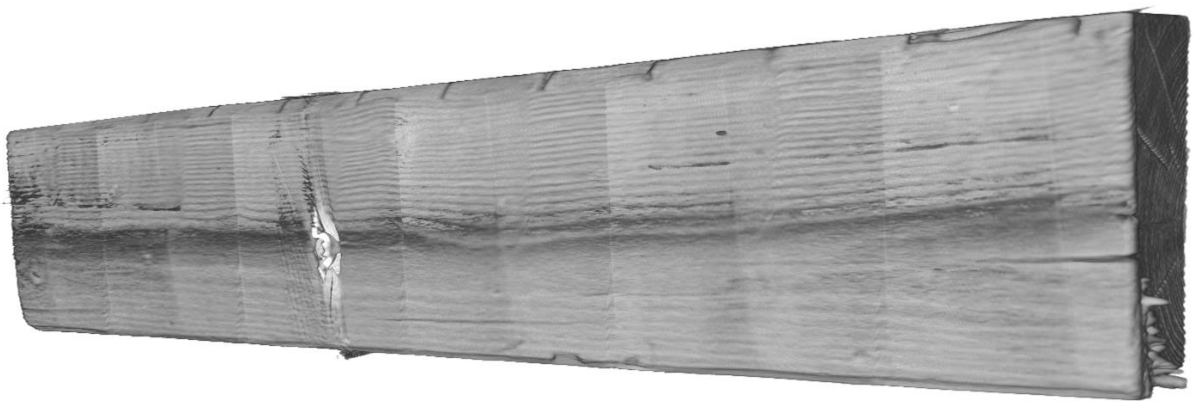

Figure 79: CT model of B2

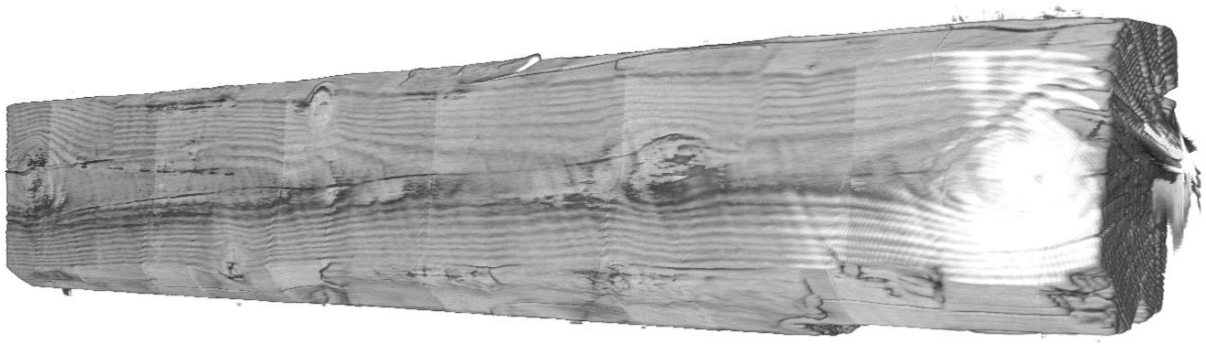

Figure 80: CT model of C1

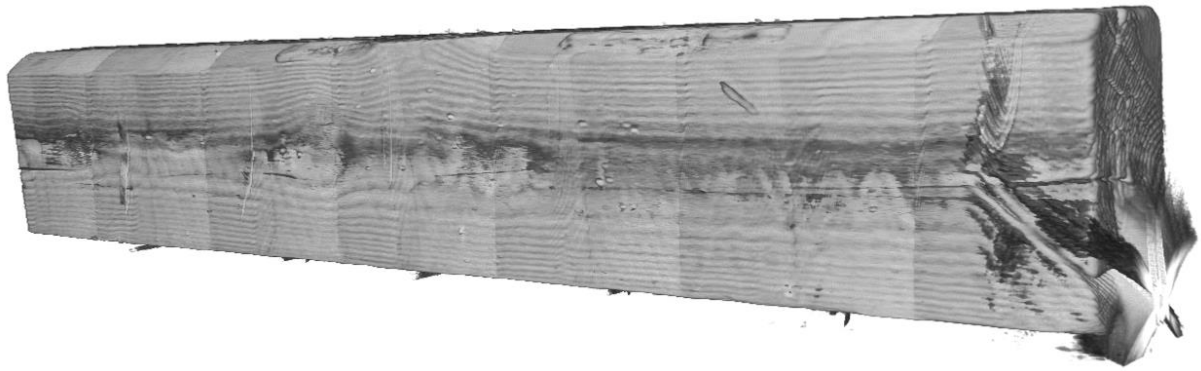

Figure 81: CT model of C2

Figure 82: CT model of D1

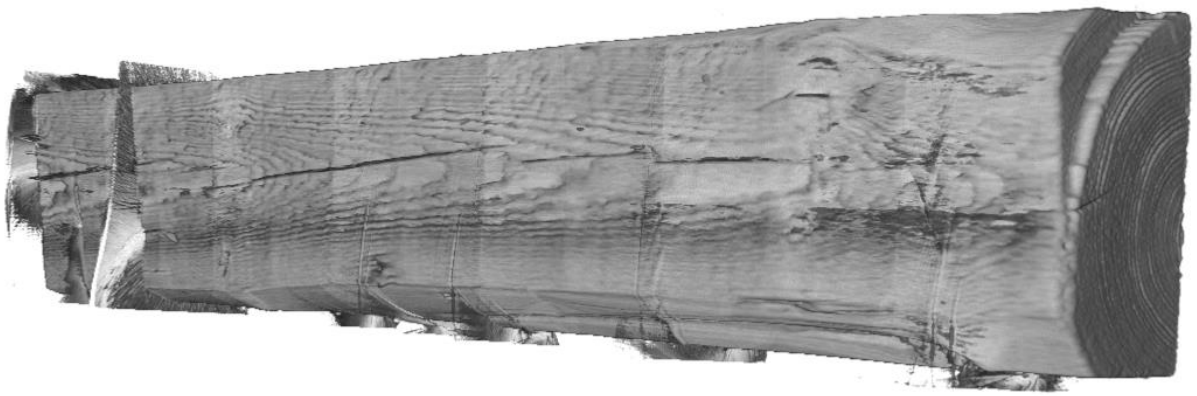

Figure 83: CT model of D2

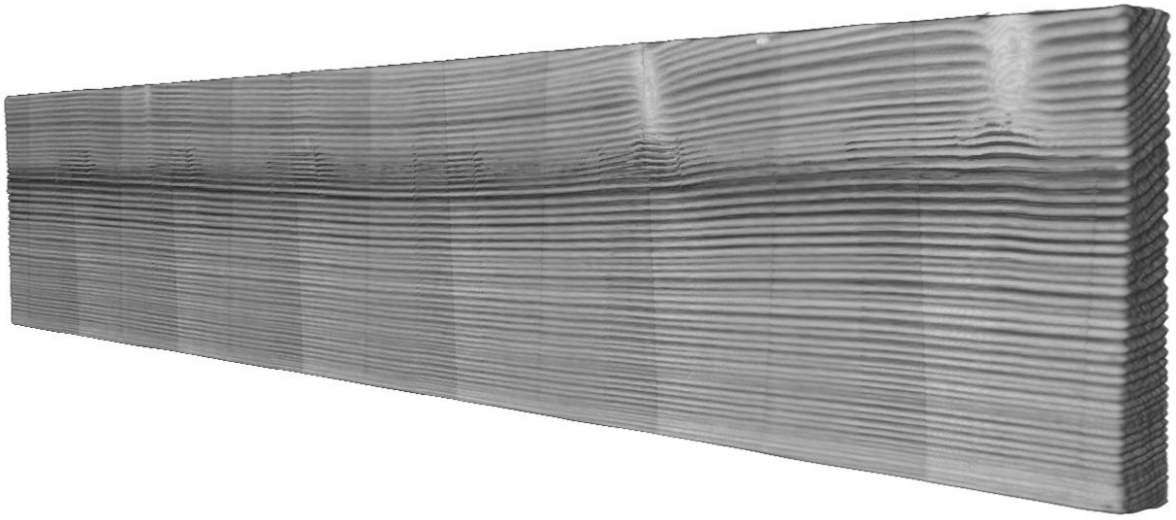

Figure 84: CT model of X

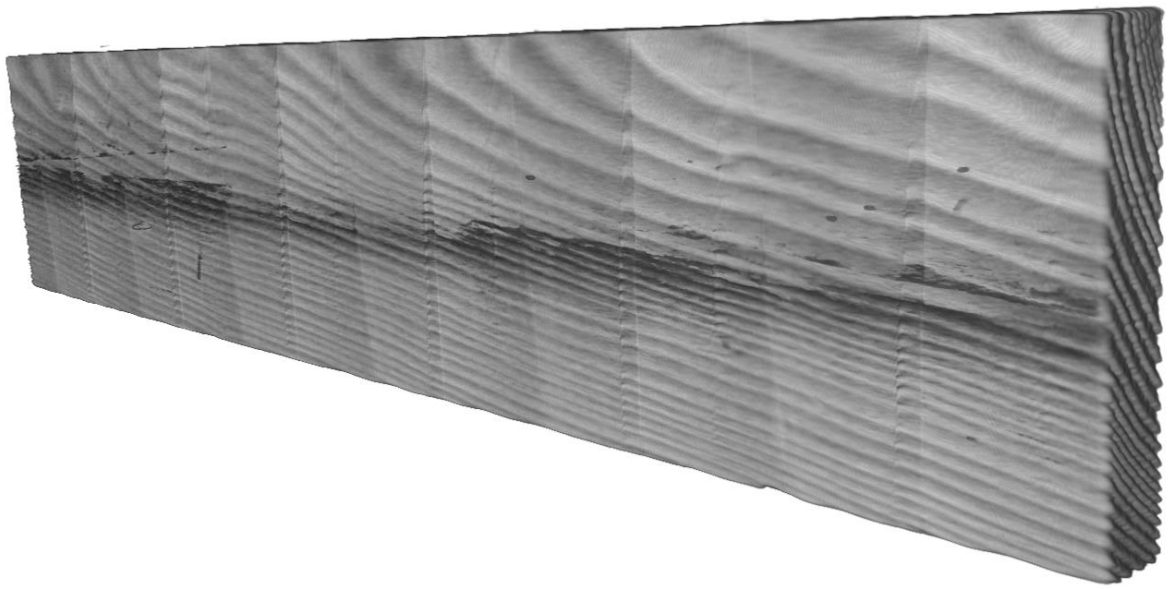

Figure 85: CT model of Y

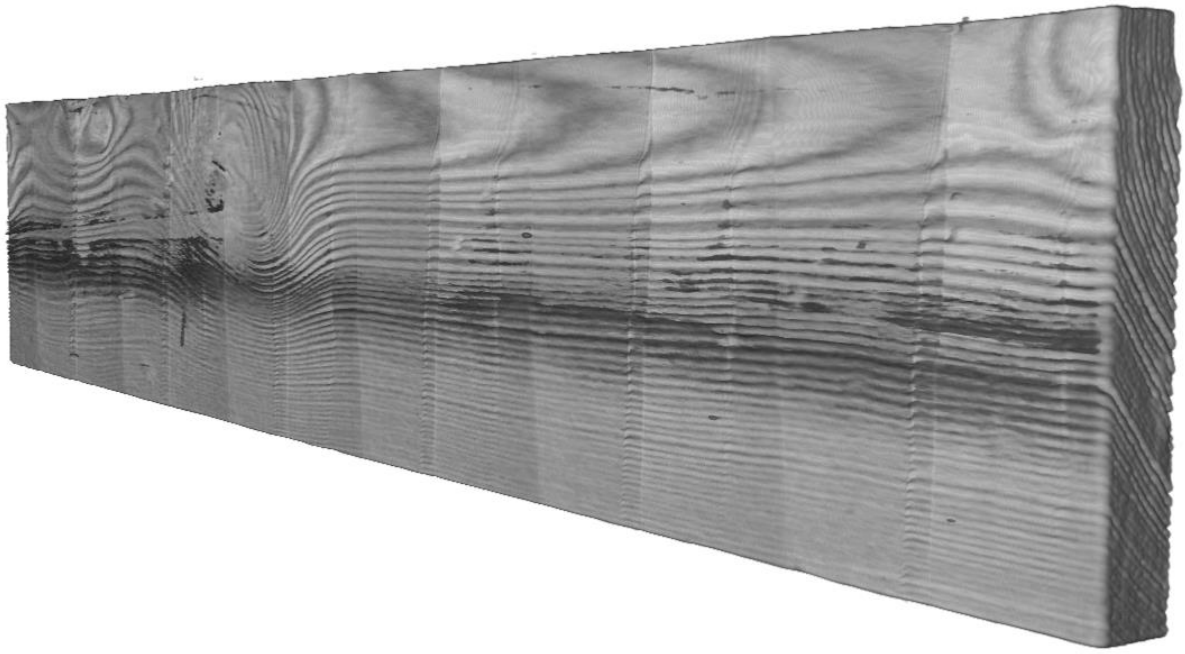

Figure 86: CT model of Z

Appendix B

Specimen 1

Specimen 1				Specimen 1			
Highside		Lowside		Highside		Lowside	
Displacement	Force	Displacement	Force	Strain	Stress	Strain	Stress
mm	N	mm	N	mm/mm	N/mm2	mm/mm	N/mm2
0.004934905	160	0.001086997	150	5.03562E-05	0.083333	2.26458E-05	0.038265
0.00780838	150	0.001944687	150	7.96773E-05	0.078125	4.05143E-05	0.038265
0.012388743	150	0.003391509	160	0.000126416	0.078125	7.06564E-05	0.040816
0.019466812	150	0.006419963	160	0.000198641	0.078125	0.000133749	0.040816
0.028906714	150	0.01205864	160	0.000294966	0.078125	0.000251222	0.040816
0.039316826	150	0.019855343	160	0.000401192	0.078125	0.000413653	0.040816
0.049251385	160	0.028219948	160	0.000502565	0.083333	0.000587916	0.040816
0.058159478	160	0.035797983	170	0.000593464	0.083333	0.000745791	0.043367
0.066070817	170	0.042015176	190	0.000674192	0.088542	0.000875316	0.048469
0.072963126	170	0.047103997	220	0.000744522	0.088542	0.000981333	0.056122
0.078719631	190	0.051191825	230	0.000803262	0.098958	0.001066496	0.058673
0.083519727	200	0.054489899	260	0.000852242	0.104167	0.001135206	0.066327
0.087912202	230	0.057366561	270	0.000897063	0.119792	0.001195137	0.068878
0.092378989	250	0.060185898	290	0.000942643	0.130208	0.001253873	0.07398
0.097025163	260	0.063286535	300	0.000990053	0.135417	0.001318469	0.076531
0.101877272	270	0.066778861	300	0.001039564	0.140625	0.001391226	0.076531
0.106862068	280	0.070617236	310	0.001090429	0.145833	0.001471192	0.079082
0.112123914	300	0.074779376	310	0.001144122	0.15625	0.001557904	0.079082
0.117737114	310	0.079020061	320	0.001201399	0.161458	0.001646251	0.081633
0.123646475	310	0.083043136	330	0.001261699	0.161458	0.001730065	0.084184
0.129689574	320	0.087465338	330	0.001323363	0.166667	0.001822195	0.084184
0.135812297	320	0.091865242	350	0.00138584	0.166667	0.001913859	0.089286
0.141902119	340	0.096099563	360	0.001447981	0.177083	0.002002074	0.091837
0.147800863	340	0.100241527	370	0.001508172	0.177083	0.002088365	0.094388
0.153460771	350	0.104298569	380	0.001565926	0.182292	0.002172887	0.096939
0.159111127	360	0.108313158	390	0.001623583	0.1875	0.002256524	0.09949
0.164849579	370	0.112299085	400	0.001682139	0.192708	0.002339564	0.102041
0.170364067	380	0.116199024	410	0.001738409	0.197917	0.002420813	0.104592
0.17568323	390	0.119975835	420	0.001792686	0.203125	0.002499497	0.107143
0.181110665	400	0.12357007	430	0.001848068	0.208333	0.002574376	0.109694
0.1866294	420	0.127077252	440	0.001904382	0.21875	0.002647443	0.112245
0.192162991	430	0.130588695	460	0.001960847	0.223958	0.002720598	0.117347
0.197766632	430	0.134125605	460	0.002018027	0.223958	0.002794283	0.117347
0.20354861	450	0.13770391	470	0.002077027	0.234375	0.002868831	0.119898
0.209374115	460	0.14133954	480	0.002136471	0.239583	0.002944574	0.122449
0.215079665	470	0.144843549	490	0.00219469	0.244792	0.003017574	0.125
0.220567614	480	0.147968605	500	0.00225069	0.25	0.003082679	0.127551

0.225978062	480	0.150902584	510	0.002305899	0.25	0.003143804	0.130102
0.231407627	490	0.153909802	530	0.002361302	0.255208	0.003206454	0.135204
0.236807466	510	0.15699558	530	0.002416403	0.265625	0.003270741	0.135204
0.242142558	520	0.160073921	540	0.002470842	0.270833	0.003334873	0.137755
0.247557253	530	0.163235068	550	0.002526094	0.276042	0.003400731	0.140306
0.253035635	540	0.166608498	560	0.002581996	0.28125	0.00347101	0.142857
0.258407891	540	0.170055181	570	0.002636815	0.28125	0.003542816	0.145408
0.263645321	560	0.173221633	570	0.002690258	0.291667	0.003608784	0.145408
0.268951744	570	0.176007003	590	0.002744406	0.296875	0.003666813	0.15051
0.274374932	580	0.17872338	600	0.002799744	0.302083	0.003723404	0.153061
0.279867142	580	0.181505561	610	0.002855787	0.302083	0.003781366	0.155612
0.285430431	600	0.18422088	630	0.002912555	0.3125	0.003837935	0.160714
0.291137069	600	0.186926633	630	0.002970786	0.3125	0.003894305	0.160714
0.296805471	620	0.189807549	640	0.003028627	0.322917	0.003954324	0.163265
0.302225471	620	0.192758501	650	0.003083933	0.322917	0.004015802	0.165816
0.307465017	630	0.195538566	660	0.003137398	0.328125	0.00407372	0.168367
0.312775701	640	0.198080853	670	0.003191589	0.333333	0.004126684	0.170918
0.318214804	650	0.200594485	680	0.00324709	0.338542	0.004179052	0.173469
0.323548853	660	0.203224882	690	0.003301519	0.34375	0.004233852	0.17602
0.328754425	670	0.205831915	710	0.003354637	0.348958	0.004288165	0.181122
0.333995044	690	0.208322197	710	0.003408113	0.359375	0.004340046	0.181122
0.339222908	700	0.210851744	720	0.003461458	0.364583	0.004392745	0.183673
0.344190717	710	0.213478953	730	0.00351215	0.369792	0.004447478	0.186224
0.348872989	710	0.215908721	740	0.003559928	0.369792	0.004498098	0.188776
0.353517056	730	0.218059316	750	0.003607317	0.380208	0.004542902	0.191327
0.358305454	740	0.220134541	760	0.003656178	0.385417	0.004586136	0.193878
0.363187283	740	0.222193852	780	0.003705993	0.385417	0.004629039	0.19898
0.368116885	750	0.224219188	780	0.003756295	0.390625	0.004671233	0.19898
0.373052865	770	0.226245582	790	0.003806662	0.401042	0.00471345	0.201531
0.377844453	780	0.228373885	800	0.003855556	0.40625	0.004757789	0.204082
0.382263482	780	0.230638057	810	0.003900648	0.40625	0.00480496	0.206633
0.386523277	800	0.232838556	820	0.003944115	0.416667	0.004850803	0.209184
0.390886039	810	0.234783217	830	0.003988633	0.421875	0.004891317	0.211735
0.395403773	820	0.236659944	840	0.004034732	0.427083	0.004930416	0.214286
0.399994731	820	0.238678917	860	0.004081579	0.427083	0.004972477	0.219388
0.404662162	840	0.240678772	860	0.004129206	0.4375	0.005014141	0.219388
0.409601301	850	0.242514104	870	0.004179605	0.442708	0.005052377	0.221939
0.414778233	850	0.244326085	880	0.004232431	0.442708	0.005090127	0.22449
0.419940293	870	0.246247396	900	0.004285105	0.453125	0.005130154	0.229592
0.424896419	870	0.248120934	900	0.004335678	0.453125	0.005169186	0.229592
0.429693341	880	0.249834195	910	0.004384626	0.458333	0.005204879	0.232143
0.434410632	900	0.251567632	930	0.004432762	0.46875	0.005240992	0.237245
0.439122617	900	0.253451765	930	0.004480843	0.46875	0.005280245	0.237245
0.443895102	910	0.25534761	940	0.004529542	0.473958	0.005319742	0.239796
0.448821515	920	0.257196754	950	0.004579811	0.479167	0.005358266	0.242347
0.453832865	930	0.259018272	960	0.004630948	0.484375	0.005396214	0.244898

0.458758205	940	0.260729402	970	0.004681206	0.489583	0.005431863	0.247449
0.46352008	950	0.26229617	990	0.004729797	0.494792	0.005464504	0.252551
0.468344599	970	0.263784409	990	0.004779027	0.505208	0.005495509	0.252551
0.473311335	970	0.26531297	1000	0.004829707	0.505208	0.005527354	0.255102
0.478222907	980	0.267004997	1020	0.004879826	0.510417	0.005562604	0.260204
0.483072877	1000	0.26867792	1020	0.004929315	0.520833	0.005597457	0.260204
0.488049179	1010	0.270240426	1030	0.004980094	0.526042	0.005630009	0.262755
0.493077487	1010	0.271844357	1040	0.005031403	0.526042	0.005663424	0.265306
0.497930676	1020	0.273598999	1050	0.005080925	0.53125	0.005699979	0.267857
0.502597034	1030	0.275327116	1070	0.005128541	0.536458	0.005735982	0.272959
0.507282495	1050	0.276925743	1070	0.005176352	0.546875	0.005769286	0.272959
0.51203692	1060	0.278490394	1080	0.005224867	0.552083	0.005801883	0.27551
0.516827464	1060	0.280047625	1090	0.00527375	0.552083	0.005834326	0.278061
0.521553218	1070	0.281581461	1100	0.005321972	0.557292	0.00586628	0.280612
0.526198387	1090	0.283090919	1110	0.005369371	0.567708	0.005897727	0.283163
0.530804217	1100	0.284623742	1120	0.00541637	0.572917	0.005929661	0.285714
0.535257161	1100	0.286186248	1130	0.005461808	0.572917	0.005962214	0.288265
0.539613545	1120	0.287679791	1140	0.005506261	0.583333	0.005993329	0.290816
0.544131339	1130	0.289044857	1150	0.005552361	0.588542	0.006021768	0.293367
0.548959017	1140	0.290392965	1160	0.005601623	0.59375	0.006049853	0.295918
0.553890705	1140	0.291790962	1180	0.005651946	0.59375	0.006078978	0.30102
0.558626056	1160	0.293202758	1180	0.005700266	0.604167	0.006108391	0.30102
0.563223422	1170	0.294646382	1190	0.005747178	0.609375	0.006138466	0.303571
0.567819715	1170	0.296191931	1200	0.005794079	0.609375	0.006170665	0.306122
0.572292864	1180	0.297736406	1210	0.005839723	0.614583	0.006202842	0.308673
0.576475143	1190	0.299120605	1220	0.005882399	0.619792	0.006231679	0.311224
0.580634117	1210	0.300382733	1230	0.005924838	0.630208	0.006257974	0.313776
0.585127413	1220	0.301655471	1250	0.005970688	0.635417	0.006284489	0.318878
0.589799106	1230	0.303054512	1250	0.006018358	0.640625	0.006313636	0.318878
0.594435692	1240	0.304493904	1260	0.00606567	0.645833	0.006343623	0.321429
0.599101007	1240	0.305898279	1270	0.006113276	0.645833	0.006372881	0.32398
0.603803396	1250	0.307293087	1280	0.006161259	0.651042	0.006401939	0.326531
0.608373165	1260	0.308704883	1290	0.006207889	0.65625	0.006431352	0.329082
0.612785816	1280	0.310041308	1300	0.006252916	0.666667	0.006459194	0.331633
0.617211223	1290	0.311280072	1310	0.006298074	0.671875	0.006485001	0.334184
0.621778846	1300	0.312540054	1320	0.006344682	0.677083	0.006511251	0.336735
0.62635386	1300	0.313867986	1330	0.006391366	0.677083	0.006538916	0.339286
0.630835533	1320	0.315159857	1340	0.006437097	0.6875	0.00656583	0.341837
0.635294855	1330	0.316418767	1350	0.006482601	0.692708	0.006592058	0.344388
0.639848709	1340	0.317707449	1370	0.006529068	0.697917	0.006618905	0.34949
0.644419491	1340	0.31906721	1370	0.006575709	0.697917	0.006647234	0.34949
0.648844898	1350	0.320434421	1380	0.006620866	0.703125	0.006675717	0.352041
0.653067529	1360	0.321686983	1390	0.006663954	0.708333	0.006701812	0.354592
0.657341123	1380	0.322851449	1400	0.006707562	0.71875	0.006726072	0.357143
0.661778212	1390	0.324062616	1420	0.006752839	0.723958	0.006751304	0.362245
0.666267276	1400	0.325315207	1420	0.006798646	0.729167	0.0067774	0.362245

0.67079246	1410	0.326578379	1430	0.006844821	0.734375	0.006803716	0.364796
0.675423741	1420	0.327858537	1440	0.006892079	0.739583	0.006830386	0.367347
0.680042326	1430	0.329249114	1450	0.006939207	0.744792	0.006859357	0.369898
0.684550524	1430	0.330649227	1460	0.006985209	0.744792	0.006888526	0.372449
0.689092636	1440	0.33193469	1470	0.007031558	0.75	0.006915306	0.375
0.693806767	1450	0.333209544	1490	0.007079661	0.755208	0.006941866	0.380102
0.698476315	1470	0.334555537	1490	0.007127309	0.765625	0.006969907	0.380102
0.702853918	1470	0.335922748	1500	0.007171979	0.765625	0.006998391	0.382653
0.707081854	1480	0.337253869	1510	0.007215121	0.770833	0.007026122	0.385204
0.71144253	1490	0.338504314	1520	0.007259618	0.776042	0.007052173	0.387755
0.715790391	1500	0.33971867	1530	0.007303984	0.78125	0.007077472	0.390306
0.719918549	1510	0.340923458	1540	0.007346108	0.786458	0.007102572	0.392857
0.723938465	1520	0.342086852	1550	0.007387127	0.791667	0.007126809	0.395408
0.728028417	1530	0.343185514	1570	0.007428861	0.796875	0.007149698	0.40051
0.732157648	1540	0.344326615	1570	0.007470996	0.802083	0.007173471	0.40051
0.736308098	1560	0.345514446	1590	0.007513348	0.8125	0.007198218	0.405612
0.740601838	1570	0.346689522	1590	0.007557162	0.817708	0.007222698	0.405612
0.744830847	1570	0.347870976	1610	0.007600315	0.817708	0.007247312	0.410714
0.748551428	1590	0.349124581	1610	0.00763828	0.828125	0.007273429	0.410714
0.752473652	1590	0.350364417	1620	0.007678303	0.828125	0.007299259	0.413265
0.756494582	1600	0.351471573	1630	0.007719332	0.833333	0.007322324	0.415816
0.760549545	1610	0.352524579	1640	0.00776071	0.838542	0.007344262	0.418367
0.764683008	1620	0.353650808	1650	0.007802888	0.84375	0.007367725	0.420918
0.768899262	1640	0.354851365	1660	0.007845911	0.854167	0.007392737	0.423469
0.773115516	1650	0.356007338	1670	0.007888934	0.859375	0.00741682	0.42602
0.777358353	1660	0.357132524	1680	0.007932228	0.864583	0.007440261	0.428571
0.781538546	1660	0.35832566	1690	0.007974883	0.864583	0.007465118	0.431122
0.785534024	1670	0.359549552	1700	0.008015653	0.869792	0.007490616	0.433673
0.789376616	1690	0.360704482	1710	0.008054863	0.880208	0.007514677	0.436224
0.793285072	1690	0.36177659	1720	0.008094746	0.880208	0.007537012	0.438776
0.797342122	1700	0.362895399	1730	0.008136144	0.885417	0.007560321	0.441327
0.801424623	1710	0.364080042	1750	0.008177802	0.890625	0.007585001	0.446429
0.805461526	1730	0.365230709	1750	0.008218995	0.901042	0.007608973	0.446429
0.8096385	1740	0.366359085	1770	0.008261617	0.90625	0.007632481	0.451531
0.8138569	1750	0.367536277	1770	0.008304662	0.911458	0.007657006	0.451531
0.817765355	1760	0.368634939	1780	0.008344544	0.916667	0.007679895	0.454082
0.821451902	1760	0.369612575	1800	0.008382162	0.916667	0.007700262	0.459184
0.825236142	1780	0.370607197	1800	0.008420777	0.927083	0.007720983	0.459184
0.829153061	1780	0.371696293	1810	0.008460746	0.927083	0.007743673	0.461735
0.833044529	1790	0.372824669	1820	0.008500454	0.932292	0.007767181	0.464286
0.836949766	1810	0.373886168	1830	0.008540304	0.942708	0.007789295	0.466837
0.841032326	1820	0.374900937	1840	0.008581963	0.947917	0.007810436	0.469388
0.845181704	1820	0.376002789	1850	0.008624303	0.947917	0.007833391	0.471939
0.849084854	1840	0.377095073	1860	0.008664131	0.958333	0.007856147	0.47449
0.852782011	1850	0.378102422	1870	0.008701857	0.963542	0.007877134	0.477041
0.856521666	1850	0.379093856	1890	0.008740017	0.963542	0.007897789	0.482143

0.860414207	1860	0.38013202	1900	0.008779737	0.96875	0.007919417	0.484694
0.864344895	1880	0.381220043	1900	0.008819846	0.979167	0.007942084	0.484694
0.868200302	1880	0.382343113	1910	0.008859187	0.979167	0.007965482	0.487245
0.872023821	1890	0.38343963	1920	0.008898202	0.984375	0.007988326	0.489796
0.875795305	1900	0.384541482	1930	0.008936687	0.989583	0.008011281	0.492347
0.879379988	1910	0.385660291	1940	0.008973265	0.994792	0.008034589	0.494898
0.882912636	1920	0.386688888	1950	0.009009313	1	0.008056019	0.497449
0.886726618	1940	0.387635738	1970	0.009048231	1.010417	0.008075745	0.502551
0.890821874	1950	0.388639927	1970	0.009090019	1.015625	0.008096665	0.502551
0.894825816	1950	0.389764041	1980	0.009130876	1.015625	0.008120084	0.505102
0.898593068	1970	0.390673757	1990	0.009169317	1.026042	0.008139037	0.507653
0.90230304	1980	0.391141862	2000	0.009207174	1.03125	0.008148789	0.510204
0.905995965	1980	0.392187446	2010	0.009244857	1.03125	0.008170572	0.512755
0.90955627	2000	0.393473983	2020	0.009281186	1.041667	0.008197375	0.515306
0.913010359	2010	0.39454928	2030	0.009316432	1.046875	0.008219777	0.517857
0.916445374	2010	0.395499319	2040	0.009351483	1.046875	0.008239569	0.520408
0.919991851	2020	0.39649713	2050	0.009387672	1.052083	0.008260357	0.522959
0.923762262	2040	0.397506624	2060	0.009426146	1.0625	0.008281388	0.52551
0.927626133	2040	0.398432225	2070	0.009465573	1.0625	0.008300671	0.528061
0.931491017	2060	0.399356812	2090	0.00950501	1.072917	0.008319934	0.533163
0.935271025	2060	0.400332332	2100	0.009543582	1.072917	0.008340257	0.535714
0.938664615	2070	0.401301473	2100	0.00957821	1.078125	0.008360447	0.535714
0.941828966	2090	0.402221799	2110	0.0096105	1.088542	0.008379621	0.538265
0.945216179	2090	0.403104961	2120	0.009645063	1.088542	0.00839802	0.540816
0.948911309	2110	0.404028445	2130	0.009682768	1.098958	0.008417259	0.543367
0.952706158	2110	0.404981673	2140	0.009721491	1.098958	0.008437118	0.545918
0.956507385	2130	0.405874401	2150	0.009760279	1.109375	0.008455717	0.548469
0.960305393	2140	0.406722546	2160	0.009799035	1.114583	0.008473386	0.55102
0.964070559	2140	0.407630116	2170	0.009837455	1.114583	0.008492294	0.553571
0.967739046	2150	0.408632159	2180	0.009874888	1.119792	0.00851317	0.556122
0.971313119	2170	0.409605563	2190	0.009911358	1.130208	0.008533449	0.558673
0.974886119	2170	0.410469621	2200	0.009947818	1.130208	0.00855145	0.561224
0.978519619	2180	0.411334753	2220	0.009984894	1.135417	0.008569474	0.566327
0.982121289	2200	0.412265688	2220	0.010021646	1.145833	0.008588869	0.566327
0.985818505	2210	0.413218915	2230	0.010059373	1.151042	0.008608727	0.568878
0.989697218	2220	0.414155155	2240	0.010098951	1.15625	0.008628232	0.571429
0.993538797	2220	0.415077597	2250	0.010138151	1.15625	0.00864745	0.57398
0.997085273	2230	0.415991545	2260	0.01017434	1.161458	0.008666491	0.576531
1.00032711	2250	0.416838616	2270	0.010207419	1.171875	0.008684138	0.579082
1.003607035	2260	0.417683572	2280	0.010240888	1.177083	0.008701741	0.581633
1.007169485	2260	0.418603897	2290	0.01027724	1.177083	0.008720915	0.584184
1.010943055	2280	0.419581532	2300	0.010315745	1.1875	0.008741282	0.586735
1.01471889	2290	0.420520961	2310	0.010354274	1.192708	0.008760853	0.589286
1.018398046	2300	0.421379715	2320	0.010391817	1.197917	0.008778744	0.591837
1.022100568	2310	0.42224589	2330	0.010429598	1.203125	0.008796789	0.594388
1.025833845	2310	0.423205465	2350	0.010467692	1.203125	0.008816781	0.59949

1.029489636	2320	0.424201161	2350	0.010504996	1.208333	0.008837524	0.59949
1.033103943	2340	0.425135285	2360	0.010541877	1.21875	0.008856985	0.602041
1.036738515	2340	0.426056653	2380	0.010578964	1.21875	0.00887618	0.607143
1.040328503	2360	0.427028984	2370	0.010615597	1.229167	0.008896437	0.604592
1.043879271	2370	0.427993894	2390	0.010651829	1.234375	0.008916539	0.609694
1.047509551	2380	0.428886622	2400	0.010688873	1.239583	0.008935138	0.612245
1.051210999	2390	0.429795265	2420	0.010726643	1.244792	0.008954068	0.617347
1.054889083	2390	0.430739999	2420	0.010764174	1.244792	0.00897375	0.617347
1.058389902	2410	0.431632698	2430	0.010799897	1.255208	0.008992348	0.619898
1.06176126	2420	0.432446867	2450	0.010834299	1.260417	0.00900931	0.625
1.063644409	2420	0.433248311	2450	0.010853514	1.260417	0.009026006	0.625
		0.434100688	2470			0.009043764	0.630102
		0.43503058	2470			0.009063137	0.630102
		0.435980618	2480			0.00908293	0.632653
		0.436884999	2490			0.009101771	0.635204
		0.437819123	2500			0.009121232	0.637755
		0.438740492	2510			0.009140427	0.640306
		0.439569533	2520			0.009157699	0.642857
		0.440393269	2540			0.00917486	0.647959
		0.441282779	2540			0.009193391	0.647959
		0.442207366	2550			0.009212653	0.65051
		0.44313404	2560			0.009231959	0.653061
		0.444052249	2580			0.009251089	0.658163
		0.444969386	2590			0.009270196	0.660714
		0.445823878	2590			0.009287997	0.660714
		0.446600884	2610			0.009304185	0.665816
		0.447384268	2620			0.009320506	0.668367
		0.448212236	2630			0.009337755	0.670918
		0.448997766	2630			0.00935412	0.670918
		0.449711084	2640			0.009368981	0.673469
		0.450485975	2650			0.009385124	0.67602
		0.451353222	2660			0.009403192	0.678571
		0.452149332	2670			0.009419778	0.681122
		0.452829778	2690			0.009433954	0.686224
		0.453460306	2690			0.00944709	0.686224
		0.45413965	2700			0.009461243	0.688776
		0.454928339	2710			0.009477674	0.691327
		0.455719173	2720			0.009494149	0.693878
		0.456440985	2740			0.009509187	0.69898
		0.457173407	2740			0.009524446	0.69898
		0.457912207	2750			0.009539838	0.701531
		0.458563983	2760			0.009553416	0.704082
		0.459186018	2780			0.009566375	0.709184
		0.459885538	2780			0.009580949	0.709184
		0.4606148	2800			0.009596142	0.714286
		0.461286724	2810			0.00961014	0.716837

	0.461962909	2810		0.009624227	0.716837
	0.462708056	2820		0.009639751	0.719388
	0.463449001	2830		0.009655188	0.721939
	0.464161247	2850		0.009670026	0.727041
	0.464929789	2850		0.009686037	0.727041
	0.465776861	2860		0.009703685	0.729592
	0.466662139	2870		0.009722128	0.732143
	0.467614323	2890		0.009741965	0.737245
	0.468706578	2890		0.00976472	0.737245
	0.469849825	2900		0.009788538	0.739796
	0.470801979	2920		0.009808375	0.744898
	0.471513182	2930		0.009823191	0.747449
	0.472129911	2940		0.00983604	0.75
	0.472811401	2940		0.009850238	0.75
	0.473510921	2950		0.009864811	0.752551
	0.474176496	2970		0.009878677	0.757653
	0.474844158	2970		0.009892587	0.757653
	0.475511849	2980		0.009906497	0.760204
	0.476192266	2990		0.009920672	0.762755
	0.476831287	3000		0.009933985	0.765306
	0.477417231	3020		0.009946192	0.770408
	0.478040338	3020		0.009959174	0.770408
	0.478734553	3030		0.009973637	0.772959
	0.479419231	3050		0.009987901	0.778061
	0.480051875	3050		0.010001081	0.778061
	0.480721682	3060		0.010015035	0.780612
	0.481396794	3070		0.0100291	0.783163
	0.482011408	3080		0.010041904	0.785714
	0.482604772	3090		0.010054266	0.788265
	0.48325336	3100		0.010067778	0.790816
	0.483919978	3110		0.010081666	0.793367
	0.484561116	3120		0.010095023	0.795918
	0.485221386	3130		0.010108779	0.798469
	0.485893309	3140		0.010122777	0.80102
	0.486533374	3150		0.010136112	0.803571
	0.487132072	3160		0.010148585	0.806122
	0.487750918	3180		0.010161477	0.811224
	0.488432407	3180		0.010175675	0.811224
	0.489136189	3190		0.010190337	0.813776
	0.48979643	3200		0.010204092	0.816327
	0.490406781	3210		0.010216808	0.818878
	0.491046876	3220		0.010230143	0.821429
	0.491727293	3230		0.010244319	0.82398
	0.492349327	3240		0.010257278	0.826531
	0.492968202	3250		0.010270171	0.829082
	0.493640125	3260		0.010284169	0.831633

	0.494339645	3270		0.010298743	0.834184
	0.495020062	3280		0.010312918	0.836735
	0.495718539	3290		0.01032747	0.839286
	0.496436089	3300		0.010342419	0.841837
	0.497179151	3310		0.010357899	0.844388
	0.498407304	3320		0.010383486	0.846939
	0.500574887	3320		0.010428643	0.846939
	0.502432525	3350		0.010467344	0.854592
	0.503412247	3360		0.010487755	0.857143
	0.503955781	3370		0.010499079	0.859694
	0.504474819	3380		0.010509892	0.862245
	0.504984319	3380		0.010520507	0.862245
	0.505091548	3400		0.010522741	0.867347
	0.505642474	3410		0.010534218	0.869898
	0.506499112	3410		0.010552065	0.869898
	0.507200778	3420		0.010566683	0.872449
	0.507794142	3430		0.010579045	0.875
	0.508374751	3440		0.010591141	0.877551
	0.508935213	3450		0.010602817	0.880102
	0.509497821	3470		0.010614538	0.885204
	0.51006788	3470		0.010626414	0.885204
	0.510610282	3490		0.010637714	0.890306
	0.511115551	3490		0.010648241	0.890306
	0.511637807	3500		0.010659121	0.892857
	0.512174904	3520		0.010670311	0.897959
	0.512729049	3520		0.010681855	0.897959
	0.513333023	3530		0.010694438	0.90051
	0.513938069	3540		0.010707043	0.903061
	0.51450491	3550		0.010718852	0.905612
	0.515018702	3560		0.010729556	0.908163
	0.515515447	3580		0.010739905	0.913265
	0.51604408	3580		0.010750918	0.913265
	0.516614139	3590		0.010762795	0.915816
	0.5171597	3600		0.01077416	0.918367
	0.517686248	3610		0.01078513	0.920918
	0.518242478	3620		0.010796718	0.923469
	0.518815637	3630		0.010808659	0.92602
	0.51934427	3640		0.010819672	0.928571
	0.519837916	3650		0.010829957	0.931122
	0.520344198	3670		0.010840504	0.936224
	0.520883441	3670		0.010851738	0.936224
	0.521436512	3680		0.010863261	0.938776
	0.521981061	3690		0.010874605	0.941327
	0.522536218	3700		0.010886171	0.943878
	0.523133814	3710		0.010898621	0.946429
	0.523710251	3730		0.01091063	0.951531

	0.524218678	3740		0.010921222	0.954082
	0.524721861	3740		0.010931705	0.954082
	0.525304615	3750		0.010943846	0.956633
	0.52588737	3760		0.010955987	0.959184
	0.526450992	3770		0.010967729	0.961735
	0.527022123	3780		0.010979628	0.964286
	0.527603805	3790		0.010991746	0.966837
	0.528144121	3810		0.011003003	0.971939
	0.528651536	3810		0.011013574	0.971939
	0.529175878	3820		0.011024497	0.97449
	0.52976501	3830		0.011036771	0.977041
	0.530388117	3840		0.011049752	0.979592
	0.531001687	3850		0.011062535	0.982143
	0.53164494	3860		0.011075936	0.984694
	0.532447398	3870		0.011092654	0.987245
	0.533379436	3890		0.011112072	0.992347
	0.534261525	3890		0.011130448	0.992347
	0.535061896	3900		0.011147123	0.994898
	0.53579855	3910		0.01116247	0.997449
	0.536475837	3930		0.01117658	1.002551
	0.537288904	3940		0.011193519	1.005102
	0.538443804	3940		0.011217579	1.005102
	0.539519131	3960		0.011239982	1.010204
	0.540269613	3960		0.011255617	1.010204
	0.540835381	3970		0.011267404	1.012755
	0.541368246	3990		0.011278505	1.017857
	0.541956306	3990		0.011290756	1.017857
	0.542535901	4000		0.011302831	1.020408
	0.543060303	4020		0.011313756	1.02551
	0.543591022	4020		0.011324813	1.02551
	0.544157863	4030		0.011336622	1.028061
	0.544703484	4040		0.011347989	1.030612
	0.545255482	4050		0.011359489	1.033163
	0.545803189	4060		0.0113709	1.035714
	0.546332896	4080		0.011381935	1.040816
	0.54685086	4080		0.011392726	1.040816
	0.547374189	4090		0.011403629	1.043367
	0.547889054	4100		0.011414355	1.045918
	0.548418701	4110		0.01142539	1.048469
	0.548952639	4130		0.011436513	1.053571
	0.549435616	4130		0.011446575	1.053571
	0.549909055	4140		0.011456439	1.056122
	0.550438762	4140		0.011467474	1.056122
	0.550969481	4160		0.011478531	1.061224
	0.551468432	4170		0.011488926	1.063776
	0.551971555	4190		0.011499407	1.068878

	0.552532017	4190		0.011511084	1.068878
	0.553079784	4200		0.011522495	1.071429
	0.55357337	4220		0.011532779	1.076531
	0.554059505	4220		0.011542906	1.076531
	0.554582834	4230		0.011553809	1.079082
	0.555109322	4240		0.011564778	1.081633
	0.555610359	4260		0.011575216	1.086735
	0.556120932	4260		0.011585853	1.086735
	0.556697369	4270		0.011597862	1.089286
	0.557274818	4290		0.011609892	1.094388
	0.557774782	4290		0.011620308	1.094388
	0.558248222	4300		0.011630171	1.096939
	0.558747113	4310		0.011640565	1.09949
	0.559259772	4320		0.011651245	1.102041
	0.559773564	4330		0.011661949	1.104592
	0.560273528	4340		0.011672365	1.107143
	0.560792625	4350		0.01168318	1.109694
	0.561340332	4370		0.01169459	1.114796
	0.561847746	4370		0.011705161	1.114796
	0.562314808	4380		0.011714892	1.117347
	0.562816858	4390		0.011725351	1.119898
	0.563364625	4400		0.011736763	1.122449
	0.563888967	4420		0.011747687	1.127551
	0.564369857	4430		0.011757705	1.130102
	0.564886808	4430		0.011768475	1.130102
	0.565448344	4450		0.011780174	1.135204
	0.565979064	4460		0.01179123	1.137755
	0.566468418	4460		0.011801425	1.137755
	0.566986442	4470		0.011812218	1.140306
	0.567553282	4480		0.011824027	1.142857
	0.56813395	4490		0.011836124	1.145408
	0.569256961	4500		0.01185952	1.147959
	0.571753621	4530		0.011911534	1.155612
	0.573903143	4530		0.011956315	1.155612
	0.574903071	4540		0.011977147	1.158163
	0.575353146	4550		0.011986524	1.160714
	0.575778842	4560		0.011995393	1.163265
	0.57626605	4560		0.012005543	1.163265
	0.576745868	4570		0.012015539	1.165816
	0.577215016	4580		0.012025313	1.168367
	0.577699065	4590		0.012035397	1.170918
	0.578183115	4610		0.012045482	1.17602
	0.578664005	4610		0.0120555	1.17602
	0.579144835	4620		0.012065517	1.178571
	0.579640567	4630		0.012075845	1.181122
	0.580140531	4650		0.012086261	1.186224

	0.580613971	4650		0.012096124	1.186224
	0.58106935	4660		0.012105611	1.188776
	0.581533194	4670		0.012115275	1.191327
	0.582028925	4680		0.012125603	1.193878
	0.582498133	4700		0.012135378	1.19898
	0.582931221	4700		0.0121444	1.19898
	0.583374918	4710		0.012153644	1.201531
	0.58384198	4720		0.012163375	1.204082
	0.58432281	4730		0.012173392	1.206633
	0.584769726	4740		0.012182703	1.209184
	0.585235715	4750		0.012192411	1.211735
	0.585769653	4770		0.012203534	1.216837
	0.58626008	4770		0.012213752	1.216837
	0.586261153	4780		0.012213774	1.219388
	0.58658278	4790		0.012220475	1.221939
	0.587401152	4800		0.012237524	1.22449
	0.58813256	4810		0.012252762	1.227041
	0.588650584	4820		0.012263554	1.229592
	0.589134574	4830		0.012273637	1.232143
	0.589658976	4850		0.012284562	1.237245
	0.590172768	4850		0.012295266	1.237245
	0.590665281	4860		0.012305527	1.239796
	0.591200292	4870		0.012316673	1.242347
	0.592005968	4880		0.012333458	1.244898
	0.593694806	4890		0.012368642	1.247449
	0.595488727	4910		0.012406015	1.252551
	0.596538544	4920		0.012427886	1.255102
	0.597089469	4930		0.012439364	1.257653
	0.597480118	4940		0.012447502	1.260204
	0.597862244	4940		0.012455463	1.260204
	0.598295331	4950		0.012464486	1.262755
	0.598781466	4960		0.012474614	1.265306
	0.599272966	4980		0.012484853	1.270408
	0.599740028	4990		0.012494584	1.272959
	0.600220859	4990		0.012504601	1.272959
	0.60069114	5000		0.012514399	1.27551
	0.60113591	5010		0.012523665	1.278061
	0.60157007	5030		0.01253271	1.283163
	0.602017999	5030		0.012542042	1.283163
	0.602509499	5040		0.012552281	1.285714

Specimen 2

Specimen 2	**Specimen 2**

Highside		Lowside		Highside		Lowside	
Strain	Stress	Strain	Stress	Displacement	Force	Displacement	Force
mm/mm	N/mm2	mm/mm	N/mm2	mm	N	mm	N
0.000393	0.083333	0.000397	0.038265	0.038487766	160	0.019048369	150
0.0004	0.083333	0.000411	0.038265	0.039168186	160	0.019724542	150
0.000411	0.083333	0.000448	0.038265	0.040281698	160	0.021521658	150
0.000428	0.083333	0.000535	0.038265	0.041960988	160	0.025695469	150
0.00047	0.083333	0.000661	0.038265	0.046040323	160	0.031722654	150
0.000555	0.088542	0.0008	0.040816	0.054353978	170	0.038382493	160
0.000661	0.083333	0.000936	0.040816	0.064820349	160	0.044949982	160
0.00077	0.088542	0.001055	0.043367	0.07548628	170	0.050637487	170
0.000872	0.09375	0.001146	0.048469	0.085421897	180	0.054986443	190
0.000954	0.109375	0.001215	0.056122	0.093509451	210	0.058320608	220
0.001014	0.125	0.001266	0.061224	0.099332832	240	0.060771607	240
0.001054	0.135417	0.001309	0.066327	0.103263557	260	0.062828794	260
0.001086	0.145833	0.001352	0.068878	0.106415145	280	0.064872175	270
0.001118	0.15625	0.001393	0.071429	0.109563552	300	0.066886902	280
0.001151	0.15625	0.001441	0.07398	0.112843581	300	0.069164872	290
0.001183	0.161458	0.001501	0.07398	0.115913428	310	0.072027735	290
0.001217	0.166667	0.001576	0.076531	0.119242288	320	0.075627275	300
0.001253	0.166667	0.001649	0.079082	0.122755848	320	0.079149321	310
0.001292	0.171875	0.001711	0.079082	0.126603782	330	0.082131073	310
0.001336	0.177083	0.001767	0.081633	0.130907089	340	0.084830463	320
0.001376	0.182292	0.001827	0.086735	0.13481234	350	0.087702878	340
0.001412	0.1875	0.001884	0.091837	0.138389587	360	0.090448968	360
0.00145	0.192708	0.001935	0.091837	0.142077237	370	0.092878737	360
0.001489	0.197917	0.001984	0.096939	0.145874217	380	0.095221467	380
0.001527	0.203125	0.002034	0.096939	0.149687111	390	0.097608775	380
0.001565	0.208333	0.002088	0.09949	0.153402358	400	0.100220062	390
0.001599	0.213542	0.002147	0.102041	0.156714231	410	0.103047892	400
0.001634	0.21875	0.002205	0.104592	0.160100415	420	0.105859801	410
0.001667	0.223958	0.002262	0.107143	0.163363457	430	0.108569801	420
0.001696	0.234375	0.002316	0.109694	0.166250721	450	0.111188516	430
0.001725	0.239583	0.002373	0.112245	0.169004247	460	0.113923997	440
0.001754	0.244792	0.002427	0.114796	0.171891525	470	0.116502374	450
0.001786	0.244792	0.002479	0.117347	0.175027192	470	0.119014941	460
0.001814	0.25	0.002524	0.119898	0.177737191	480	0.121132635	470
0.001836	0.260417	0.002562	0.122449	0.179934502	500	0.122986004	480
0.001865	0.260417	0.002605	0.125	0.182737917	500	0.125062302	490
0.001893	0.265625	0.002652	0.127551	0.185527533	510	0.127292499	500
0.001918	0.270833	0.002699	0.130102	0.18798703	520	0.129558802	510
0.001945	0.28125	0.002748	0.132653	0.190652445	540	0.131916389	520
0.001974	0.28125	0.002795	0.135204	0.193480268	540	0.134149775	530
0.002006	0.28125	0.002839	0.137755	0.19663398	540	0.136285514	540
0.002039	0.291667	0.002885	0.140306	0.199865192	560	0.138465837	550
0.002069	0.296875	0.002933	0.145408	0.202776879	570	0.140768215	570

0.00209	0.302083	0.002977	0.147959	0.204821318	580	0.142875299	580
0.002107	0.307292	0.003013	0.147959	0.206503794	590	0.144625708	580
0.002129	0.317708	0.00305	0.15051	0.20859389	610	0.146396279	590
0.002156	0.322917	0.003091	0.153061	0.211263552	620	0.148362175	600
0.002183	0.322917	0.003133	0.155612	0.213916227	620	0.150398135	610
0.002209	0.328125	0.003177	0.158163	0.216519028	630	0.152474418	620
0.002234	0.333333	0.003222	0.160714	0.218979582	640	0.154642001	630
0.00226	0.338542	0.003267	0.163265	0.221466675	650	0.156807452	640
0.002283	0.34375	0.003309	0.165816	0.223740399	660	0.158825368	650
0.002304	0.348958	0.003352	0.168367	0.225765735	670	0.16088891	660
0.002325	0.354167	0.00339	0.170918	0.227807	680	0.162696645	670
0.002348	0.364583	0.003423	0.173469	0.230138049	700	0.164281458	680
0.002374	0.364583	0.003449	0.17602	0.232636809	700	0.165540397	690
0.002399	0.369792	0.00348	0.178571	0.235105857	710	0.16703923	700
0.002427	0.375	0.003528	0.181122	0.237836033	720	0.169331014	710
0.002454	0.380208	0.003574	0.186224	0.240461111	730	0.171567589	730
0.002472	0.385417	0.003608	0.186224	0.242299631	740	0.173196986	730
0.002489	0.390625	0.003637	0.188776	0.243916288	750	0.174589664	740
0.00251	0.401042	0.003672	0.191327	0.245968163	770	0.176240295	750
0.002538	0.401042	0.003716	0.196429	0.248690903	770	0.178386644	770
0.002567	0.40625	0.003767	0.196429	0.251561195	780	0.180798367	770
0.00259	0.40625	0.003809	0.19898	0.253864646	780	0.182838574	780
0.00261	0.416667	0.003844	0.19898	0.255747736	800	0.184497699	780
0.00263	0.427083	0.003872	0.204082	0.257705152	820	0.185833052	800
0.002653	0.432292	0.0039	0.209184	0.260024518	830	0.187182218	820
0.002674	0.432292	0.00393	0.209184	0.262054116	830	0.188641787	820
0.002693	0.4375	0.003967	0.211735	0.263936132	840	0.190393254	830
0.002716	0.447917	0.004006	0.214286	0.266153604	860	0.192272112	840
0.002739	0.453125	0.00404	0.216837	0.268431574	870	0.193917423	850
0.002765	0.453125	0.004074	0.219388	0.271003604	870	0.195555314	860
0.002789	0.458333	0.00411	0.221939	0.273354828	880	0.197290868	870
0.002809	0.463542	0.004149	0.227041	0.275259137	890	0.199161232	890
0.002823	0.46875	0.004187	0.227041	0.276652902	900	0.200955153	890
0.002838	0.479167	0.004224	0.229592	0.278132617	920	0.202742726	900
0.002862	0.479167	0.004257	0.232143	0.280439258	920	0.204348773	910
0.002889	0.484375	0.004287	0.234694	0.28310892	930	0.205761626	920
0.002913	0.484375	0.004318	0.239796	0.285514265	930	0.207285926	940
0.002934	0.489583	0.004352	0.239796	0.287547052	940	0.208890915	940
0.002954	0.5	0.004385	0.242347	0.289517194	960	0.210479975	950
0.002975	0.505208	0.00442	0.244898	0.291547835	970	0.212149709	960
0.002994	0.510417	0.004452	0.247449	0.293408632	980	0.213707998	970
0.003012	0.515625	0.004481	0.25	0.295178145	990	0.215107054	980
0.003032	0.520833	0.004511	0.252551	0.297140867	1000	0.216530517	990
0.003056	0.526042	0.004541	0.257653	0.299521804	1010	0.217955053	1010
0.003077	0.53125	0.004572	0.260204	0.301529109	1020	0.219454944	1020
0.003099	0.536458	0.004605	0.260204	0.303699851	1030	0.221052498	1020

0.003126	0.546875	0.00464	0.262755	0.306333423	1050	0.222725421	1030
0.003149	0.546875	0.004677	0.265306	0.308559388	1050	0.22447902	1040
0.003165	0.552083	0.00471	0.267857	0.310190916	1060	0.226064891	1050
0.003184	0.557292	0.004742	0.270408	0.312019885	1070	0.227600887	1060
0.003204	0.5625	0.004773	0.272959	0.313999563	1080	0.229112461	1070
0.003226	0.567708	0.004802	0.27551	0.31616503	1090	0.23050727	1080
0.003252	0.572917	0.004833	0.280612	0.318650007	1100	0.231972128	1100
0.003276	0.578125	0.004863	0.280612	0.321073383	1110	0.233407274	1100
0.003296	0.578125	0.004894	0.283163	0.323044598	1110	0.234892309	1110
0.003313	0.588542	0.004927	0.285714	0.324716449	1130	0.236493051	1120
0.003328	0.59375	0.004961	0.288265	0.326152653	1140	0.238139436	1130
0.003344	0.598958	0.005	0.290816	0.32773006	1150	0.239989623	1140
0.003364	0.609375	0.005037	0.293367	0.329644978	1170	0.24179098	1150
0.003387	0.609375	0.00507	0.295918	0.331918716	1170	0.243367314	1160
0.00341	0.614583	0.005104	0.298469	0.334174395	1180	0.244988218	1170
0.003432	0.619792	0.005135	0.306122	0.336301655	1190	0.246491298	1200
0.003456	0.625	0.005163	0.306122	0.338691086	1200	0.247802243	1200
0.003479	0.635417	0.00519	0.306122	0.340962678	1220	0.249130189	1200
0.003497	0.635417	0.005219	0.311224	0.342743874	1220	0.250533491	1220
0.003516	0.645833	0.005249	0.311224	0.344523996	1240	0.25194633	1220
0.003536	0.645833	0.005279	0.313776	0.346533418	1240	0.253410131	1230
0.003556	0.651042	0.005311	0.316327	0.348484457	1250	0.254932344	1240
0.003576	0.65625	0.005343	0.318878	0.350494951	1260	0.256470442	1250
0.003597	0.661458	0.005378	0.321429	0.35252133	1270	0.258155048	1260
0.003618	0.661458	0.005419	0.32398	0.354560465	1270	0.260109246	1270
0.00364	0.671875	0.005458	0.326531	0.356753528	1290	0.262006164	1280
0.003663	0.677083	0.005487	0.329082	0.358941287	1300	0.263398826	1290
0.003686	0.677083	0.005515	0.331633	0.361217141	1300	0.264718294	1300
0.003706	0.6875	0.005545	0.336735	0.363209546	1320	0.266147047	1320
0.003723	0.692708	0.005569	0.339286	0.364857018	1330	0.267300904	1330
0.003741	0.697917	0.005592	0.339286	0.366626531	1340	0.268393189	1330
0.003763	0.708333	0.005616	0.344388	0.368726164	1360	0.269553393	1350
0.003789	0.708333	0.005641	0.346939	0.371298164	1360	0.2707614	1360
0.003812	0.708333	0.005673	0.344388	0.373564482	1360	0.272313297	1350
0.003827	0.71875	0.005706	0.34949	0.375093043	1380	0.273906618	1370
0.003847	0.723958	0.005734	0.352041	0.376968712	1390	0.275247276	1380
0.003871	0.734375	0.00577	0.354592	0.37931779	1410	0.276954174	1390
0.003895	0.734375	0.005814	0.359694	0.381662637	1410	0.279087782	1410
0.003914	0.739583	0.005852	0.362245	0.38358289	1420	0.280881703	1420
0.003934	0.75	0.005884	0.359694	0.385490417	1440	0.282428324	1410
0.003954	0.755208	0.005913	0.364796	0.387524247	1450	0.283845425	1430
0.003976	0.755208	0.005943	0.369898	0.38966316	1450	0.285241276	1450
0.003998	0.760417	0.005966	0.369898	0.391793579	1460	0.286384523	1450
0.004019	0.765625	0.005987	0.372449	0.39382422	1470	0.287356853	1460
0.004042	0.770833	0.006012	0.375	0.396139354	1480	0.288572252	1470
0.004067	0.776042	0.006045	0.380102	0.398600966	1490	0.290171951	1490

0.00409	0.78125	0.006086	0.380102	0.400792956	1500	0.292132527	1490
0.004109	0.786458	0.00613	0.382653	0.402633607	1510	0.294245958	1500
0.004129	0.791667	0.006167	0.385204	0.404669553	1520	0.296012312	1510
0.004152	0.802083	0.006198	0.390306	0.40687111	1540	0.297502637	1530
0.004171	0.802083	0.006227	0.390306	0.408740401	1540	0.298912317	1530
0.004188	0.807292	0.006247	0.392857	0.41042605	1550	0.29986766	1540
0.004209	0.8125	0.006262	0.395408	0.41245988	1560	0.300579935	1550
0.004232	0.817708	0.006282	0.40051	0.414703876	1570	0.301545888	1570
0.004251	0.817708	0.006306	0.403061	0.416585922	1570	0.30268383	1580
0.00427	0.828125	0.006334	0.403061	0.41848281	1590	0.304045707	1580
0.004293	0.833333	0.006361	0.405612	0.420699239	1600	0.305332243	1590
0.004316	0.838542	0.006384	0.408163	0.423012227	1610	0.306448966	1600
0.004337	0.84375	0.00641	0.410714	0.425060928	1620	0.307672858	1610
0.004356	0.848958	0.006436	0.413265	0.426899433	1630	0.308941364	1620
0.004376	0.859375	0.006473	0.415816	0.428869575	1650	0.310726792	1630
0.004398	0.859375	0.006525	0.420918	0.431040347	1650	0.313195825	1650
0.004421	0.864583	0.006569	0.423469	0.43326205	1660	0.315318823	1660
0.004441	0.869792	0.006601	0.423469	0.435200363	1670	0.316856951	1660
0.004457	0.880208	0.006627	0.423469	0.436765015	1690	0.318075538	1660
0.004474	0.880208	0.006647	0.431122	0.438444287	1690	0.319039375	1690
0.004498	0.885417	0.006665	0.433673	0.440848589	1700	0.319943786	1700
0.004523	0.890625	0.006685	0.433673	0.443245441	1710	0.320863038	1700
0.004544	0.890625	0.006706	0.436224	0.445327044	1710	0.321870387	1710
0.004565	0.90625	0.006729	0.438776	0.447360873	1740	0.323007256	1720
0.004585	0.911458	0.006757	0.441327	0.449352235	1750	0.324312896	1730
0.004604	0.911458	0.006781	0.443878	0.451218367	1750	0.325482666	1740
0.004624	0.916667	0.006802	0.446429	0.45310995	1760	0.326479435	1750
0.004646	0.921875	0.006823	0.451531	0.455292374	1770	0.327520758	1770
0.004666	0.927083	0.006859	0.454082	0.457258284	1780	0.329223394	1780
0.004682	0.932292	0.006913	0.454082	0.458831429	1790	0.331810266	1780
0.0047	0.9375	0.006961	0.456633	0.460640222	1800	0.334124327	1790
0.004724	0.942708	0.006993	0.456633	0.462974459	1810	0.335666686	1790
0.004748	0.947917	0.007017	0.461735	0.46531719	1820	0.33683753	1810
0.004771	0.953125	0.007035	0.466837	0.467518717	1830	0.337697327	1830
0.00479	0.958333	0.007052	0.466837	0.469389081	1840	0.338475406	1830
0.004808	0.96875	0.007072	0.471939	0.47117877	1860	0.33946684	1850
0.00483	0.96875	0.007095	0.471939	0.473380327	1860	0.340570807	1850
0.004852	0.973958	0.007116	0.47449	0.475520283	1870	0.34156543	1860
0.004869	0.973958	0.007134	0.477041	0.477148622	1870	0.342434794	1870
0.004891	0.984375	0.007155	0.482143	0.479346991	1890	0.343429416	1890
0.004913	0.989583	0.007176	0.482143	0.481457263	1900	0.344452709	1890
0.004932	0.994792	0.007195	0.484694	0.483333975	1910	0.345365584	1900
0.004952	1	0.007217	0.487245	0.485281825	1920	0.346432388	1910
0.004977	1.005208	0.007242	0.489796	0.487720102	1930	0.347613841	1920
0.005003	1.005208	0.00728	0.492347	0.49026981	1930	0.349422634	1930
0.005024	1.015625	0.007334	0.494898	0.492400229	1950	0.352040291	1940

0.005044	1.026042	0.007383	0.497449	0.49434489	1970	0.35437876	1950
0.005066	1.03125	0.007417	0.502551	0.496424377	1980	0.355994374	1970
0.005086	1.03125	0.007442	0.5	0.498445481	1980	0.357212961	1960
0.005107	1.041667	0.007463	0.505102	0.500526011	2000	0.358238369	1980
0.005129	1.041667	0.007479	0.507653	0.502690375	2000	0.358986735	1990
0.005151	1.046875	0.007492	0.512755	0.504769862	2010	0.359632134	2010
0.005173	1.052083	0.00751	0.515306	0.506955504	2020	0.360501498	2020
0.005193	1.057292	0.007532	0.515306	0.508951128	2030	0.361536443	2020
0.005211	1.0625	0.00755	0.517857	0.510689855	2040	0.362423867	2030
0.005229	1.067708	0.00757	0.520408	0.512407362	2050	0.363372833	2040
0.005249	1.072917	0.00759	0.52551	0.514393389	2060	0.36431545	2060
0.005271	1.078125	0.007609	0.52551	0.51654613	2070	0.365255952	2060
0.005294	1.078125	0.007632	0.528061	0.518803954	2070	0.366341859	2070
0.005317	1.088542	0.007653	0.530612	0.521023512	2090	0.367365152	2080
0.005338	1.09375	0.007675	0.533163	0.52316457	2100	0.368378878	2090
0.005359	1.098958	0.007707	0.535714	0.525206864	2110	0.369941384	2100
0.005379	1.104167	0.007765	0.538265	0.527143061	2120	0.372726768	2110
0.005397	1.109375	0.007817	0.543367	0.528929591	2130	0.375218093	2130
0.005419	1.119792	0.007844	0.538265	0.531032383	2150	0.376492947	2110
0.005445	1.119792	0.007858	0.545918	0.533566177	2150	0.377205223	2140
0.005468	1.125	0.007875	0.55102	0.535854757	2160	0.378019392	2160
0.005488	1.135417	0.007898	0.55102	0.537823856	2180	0.37912336	2160
0.005508	1.135417	0.007918	0.553571	0.53981632	2180	0.380061716	2170
0.005527	1.140625	0.007931	0.556122	0.541680276	2190	0.380679518	2180
0.005547	1.145833	0.007945	0.558673	0.543611169	2200	0.381341875	2190
0.00557	1.151042	0.007966	0.563776	0.545875311	2210	0.382375777	2210
0.005594	1.15625	0.007989	0.563776	0.548163891	2220	0.383479744	2210
0.005614	1.161458	0.008005	0.566327	0.550174415	2230	0.384245068	2220
0.005635	1.166667	0.00802	0.568878	0.552225173	2240	0.384983897	2230
0.005658	1.171875	0.008039	0.57398	0.554499984	2250	0.385894656	2250
0.005679	1.177083	0.008058	0.571429	0.556574166	2260	0.386770397	2240
0.005698	1.182292	0.008074	0.576531	0.558373392	2270	0.387545288	2260
0.005718	1.1875	0.008093	0.579082	0.560359478	2280	0.388452858	2270
0.005741	1.192708	0.008115	0.581633	0.562640607	2290	0.389538765	2280
0.005763	1.197917	0.008149	0.584184	0.564784825	2300	0.391164988	2290
0.005785	1.203125	0.008204	0.586735	0.56692481	2310	0.393784761	2300
0.005809	1.208333	0.008254	0.589286	0.569319546	2320	0.396189064	2310
0.005835	1.213542	0.008285	0.589286	0.571782231	2330	0.397673041	2310
0.005856	1.223958	0.008306	0.596939	0.573854268	2350	0.398689955	2340
0.005871	1.229167	0.008319	0.59949	0.575352073	2360	0.399324715	2350
0.005889	1.229167	0.008331	0.602041	0.577123702	2360	0.399903238	2360
0.005913	1.229167	0.008341	0.607143	0.579442024	2360	0.400356501	2380
0.005938	1.239583	0.008351	0.607143	0.581941843	2380	0.40085116	2380
0.005962	1.244792	0.008375	0.607143	0.584323823	2390	0.401998639	2380
0.005984	1.25	0.008401	0.609694	0.586439431	2400	0.403258622	2390
0.006005	1.260417	0.008421	0.612245	0.58848387	2420	0.404224604	2400

0.006027	1.260417	0.008437	0.614796	0.590636551	2420	0.404981434	2410
0.006047	1.265625	0.00845	0.619898	0.592640698	2430	0.405616224	2430
		0.008465	0.619898			0.406306207	2430
		0.008483	0.622449			0.407164931	2440
		0.008504	0.625			0.408203095	2450
		0.008523	0.627551			0.409096867	2460
		0.008539	0.630102			0.409882367	2470
		0.008557	0.635204			0.410720974	2490
		0.00858	0.635204			0.411824912	2490
		0.008629	0.637755			0.414207995	2500
		0.008688	0.640306			0.417047501	2510
		0.008726	0.642857			0.418842494	2520
		0.008747	0.645408			0.419833928	2530
		0.00876	0.65051			0.420494169	2550
		0.008772	0.653061			0.42105782	2560
		0.008786	0.655612			0.421709597	2570
		0.008803	0.655612			0.422531188	2570
		0.00882	0.658163			0.42336446	2580
		0.008836	0.660714			0.424114943	2590
		0.008852	0.663265			0.424912125	2600
		0.008867	0.665816			0.42561698	2610
		0.008881	0.668367			0.426306933	2620
		0.008899	0.673469			0.4271487	2640
		0.008918	0.673469			0.428052038	2640
		0.008936	0.67602			0.428915054	2650
		0.008951	0.678571			0.429636866	2660
		0.008967	0.681122			0.430428743	2670
		0.008985	0.686224			0.431292802	2690
		0.009002	0.686224			0.432083607	2690
		0.009017	0.688776			0.432800114	2700
		0.009041	0.691327			0.433945477	2710
		0.009093	0.693878			0.436459094	2720
		0.00915	0.696429			0.439188212	2730
		0.009184	0.693878			0.440836728	2720
		0.009202	0.704082			0.441688031	2760
		0.009215	0.706633			0.442312211	2770
		0.009228	0.709184			0.442963958	2780
		0.009244	0.711735			0.443712324	2790
		0.009256	0.711735			0.444280237	2790
		0.009266	0.716837			0.444765329	2810
		0.009281	0.716837			0.445470154	2810
		0.009297	0.719388			0.446236551	2820
		0.009312	0.721939			0.446956247	2830
		0.009328	0.72449			0.447737515	2840
		0.009345	0.727041			0.448572934	2850
		0.009362	0.732143			0.449383914	2870

	0.009377	0.732143		0.450079173	2870
	0.009393	0.737245		0.450883806	2890
	0.009409	0.737245		0.451619416	2890
	0.009422	0.739796		0.452257395	2900
	0.009435	0.742347		0.452892154	2910
	0.009447	0.744898		0.453472793	2920
	0.009463	0.75		0.454242378	2940
	0.009483	0.75		0.455163777	2940
	0.009503	0.752551		0.456138223	2950
	0.009543	0.757653		0.458064824	2970
	0.009604	0.757653		0.461003065	2970
	0.009648	0.757653		0.463081479	2970
	0.009668	0.762755		0.464076102	2990
	0.009681	0.767857		0.464668423	3010
	0.009695	0.767857		0.465343535	3010
	0.00971	0.770408		0.466086566	3020
	0.009723	0.772959		0.466710746	3030
	0.009735	0.778061		0.467256337	3050
	0.009749	0.778061		0.46796754	3050
	0.009766	0.780612		0.468782783	3060
	0.009781	0.783163		0.469491869	3070
	0.009794	0.785714		0.470109642	3080
	0.009806	0.790816		0.470675439	3100
	0.009819	0.790816		0.47131446	3100
	0.009835	0.793367		0.472087234	3110
	0.009852	0.795918		0.472910941	3120
	0.009869	0.798469		0.473700702	3130
	0.009885	0.80102		0.474458605	3140
	0.009898	0.803571		0.475093395	3150
	0.009911	0.808673		0.475708008	3170
	0.009925	0.808673		0.47640115	3170
	0.00994	0.811224		0.477117658	3180
	0.009953	0.813776		0.477738649	3190
	0.009967	0.818878		0.47841695	3210
	0.009986	0.818878		0.479335129	3210
	0.010024	0.821429		0.481133312	3220
	0.010084	0.82398		0.484008908	3230
	0.010129	0.826531		0.486203015	3240
	0.010152	0.831633		0.487303793	3260
	0.010165	0.834184		0.487940699	3270
	0.010177	0.834184		0.48851496	3270
	0.010193	0.836735		0.489276052	3280
	0.010208	0.839286		0.489996821	3290
	0.010221	0.844388		0.490630537	3310
	0.010233	0.846939		0.491198421	3320
	0.010243	0.84949		0.491680354	3330

	0.010256	0.84949		0.492308766	3330
	0.010274	0.852041		0.493165404	3340
	0.010289	0.852041		0.493855357	3340
	0.010301	0.859694		0.494447678	3370
	0.010314	0.859694		0.495090961	3370
	0.010328	0.862245		0.495738477	3380
	0.01034	0.864796		0.496325463	3390
	0.010351	0.867347		0.49686259	3400
	0.010364	0.869898		0.497470826	3410
	0.010377	0.872449		0.498073757	3420
	0.010391	0.875		0.49876374	3430
	0.010406	0.877551		0.499500424	3440
	0.010421	0.880102		0.500222206	3450
	0.010433	0.882653		0.500782728	3460
	0.010445	0.885204		0.501365483	3470
	0.01046	0.887755		0.502083063	3480
	0.010474	0.890306		0.502765596	3490
	0.010488	0.892857		0.503402472	3500
	0.010503	0.895408		0.504165709	3510
	0.01054	0.897959		0.505919278	3520
	0.010604	0.90051		0.508972168	3530
	0.010651	0.890306		0.511261821	3490
	0.010673	0.908163		0.512293577	3560
	0.010685	0.910714		0.512859344	3570
	0.010697	0.913265		0.513442099	3580
	0.01071	0.913265		0.514062047	3580
	0.010722	0.918367		0.51466924	3600
	0.010732	0.918367		0.515146911	3600
	0.010744	0.923469		0.51570946	3620
	0.010758	0.923469		0.516393065	3620
	0.010771	0.92602		0.51700449	3630
	0.010784	0.928571		0.517616987	3640
	0.010796	0.931122		0.518227339	3650
	0.010808	0.933673		0.518788874	3660
	0.01082	0.936224		0.519372702	3670
	0.010835	0.938776		0.520065844	3680
	0.01085	0.941327		0.520783424	3690
	0.010862	0.943878		0.521366179	3700
	0.010874	0.946429		0.521934092	3710
	0.010886	0.94898		0.522504151	3720
	0.010899	0.954082		0.523146331	3740
	0.010912	0.954082		0.523767292	3740
	0.01092	0.959184		0.524168551	3760
	0.010923	0.959184		0.524300218	3760
	0.010938	0.961735		0.52502203	3770
	0.010959	0.964286		0.526014507	3780

	0.010975	0.966837		0.526778758	3790
	0.010986	0.971939		0.52731061	3810
	0.010998	0.971939		0.527896523	3810
	0.011011	0.97449		0.528517544	3820
	0.011022	0.979592		0.529065251	3840
	0.011035	0.979592		0.529687285	3840
	0.011049	0.982143		0.530333757	3850
	0.011062	0.984694		0.530965328	3860
	0.011085	0.987245		0.532069266	3870
	0.011143	0.989796		0.534874856	3880
	0.011199	0.982143		0.537568927	3850
	0.011228	0.997449		0.538962662	3910
	0.011242	1		0.539638817	3920
	0.011254	1.002551		0.540183365	3930
	0.011265	1.007653		0.540713072	3950
	0.011275	1.005102		0.541190743	3940
	0.011284	1.007653		0.54161638	3950
	0.011294	1.012755		0.542104721	3970
	0.011307	1.012755		0.542750061	3970
	0.011319	1.017857		0.543324351	3990
	0.01133	1.017857		0.543827534	3990
	0.01134	1.020408		0.544334888	4000
	0.011352	1.022959		0.544903874	4010
	0.011366	1.02551		0.545590639	4020
	0.011379	1.028061		0.546188295	4030
	0.01139	1.030612		0.546714783	4040
	0.011403	1.030612		0.547356963	4040
	0.011418	1.035714		0.548061848	4060
	0.011428	1.040816		0.548539519	4080
	0.011437	1.040816		0.548961997	4080
	0.01145	1.043367		0.549594641	4090
	0.011464	1.045918		0.55025804	4100
	0.011476	1.048469		0.550840795	4110
	0.011485	1.05102		0.551288784	4120
	0.011496	1.053571		0.551784515	4130
	0.011509	1.056122		0.552415013	4140
	0.011521	1.061224		0.553000987	4160
	0.011534	1.063776		0.553637862	4170
	0.011547	1.061224		0.554238677	4160
	0.011555	1.068878		0.554661155	4190
	0.011566	1.066327		0.555173874	4180
	0.01158	1.071429		0.555829883	4200
	0.011592	1.076531		0.556416869	4220
	0.011604	1.076531		0.556978405	4220
	0.011614	1.081633		0.557490051	4240
	0.011624	1.081633		0.557962418	4240

	0.011635	1.084184		0.558466613	4250
	0.011647	1.086735		0.559058964	4260
	0.01166	1.089286		0.559693694	4270
	0.011674	1.091837		0.560355008	4280
	0.011685	1.096939		0.560893238	4300
	0.011696	1.09949		0.561419725	4310
	0.011719	1.09949		0.562494993	4310
	0.011774	1.102041		0.565156162	4320
	0.011829	1.102041		0.567814171	4320
	0.011859	1.112245		0.569218516	4360
	0.011871	1.112245		0.569825709	4360
	0.01188	1.114796		0.570239723	4370
	0.01189	1.114796		0.570739686	4370
	0.011902	1.119898		0.571284235	4390
	0.011912	1.119898		0.571792662	4390
	0.011923	1.122449		0.572297931	4400
	0.011934	1.125		0.572819114	4410
	0.011946	1.127551		0.573414624	4420
	0.011956	1.132653		0.57390821	4440
	0.011966	1.132653		0.57435298	4440
	0.011976	1.135204		0.574858248	4450
	0.011987	1.137755		0.5753901	4460
	0.011999	1.140306		0.575945258	4470
	0.012009	1.142857		0.576447368	4480
	0.01202	1.145408		0.576983392	4490
	0.012033	1.147959		0.577589512	4500
	0.012042	1.155612		0.578032136	4530
	0.01205	1.153061		0.578422785	4520
	0.01206	1.155612		0.578864396	4530
	0.012071	1.155612		0.57942909	4530
	0.012085	1.160714		0.58007127	4550
	0.012097	1.165816		0.580638111	4570
	0.012107	1.165816		0.581116855	4570
	0.012116	1.168367		0.58157438	4580
	0.012127	1.170918		0.582083881	4590
	0.012137	1.17602		0.582566857	4610
	0.012147	1.17602		0.583079576	4610
	0.012159	1.178571		0.583627284	4620
	0.01217	1.181122		0.584176123	4630
	0.012181	1.183673		0.584684551	4640
	0.012191	1.188776		0.585185587	4660
	0.012202	1.188776		0.585701466	4660
	0.012212	1.191327		0.586170673	4670
	0.012221	1.193878		0.586620748	4680
	0.012232	1.196429		0.587119639	4690
	0.012242	1.19898		0.587602615	4700

	0.012253	1.201531		0.588139713	4710
	0.012265	1.204082		0.588712931	4720
	0.012275	1.206633		0.589199126	4730
	0.012285	1.209184		0.589669347	4740
	0.012296	1.211735		0.5902192	4750
	0.012308	1.216837		0.590760589	4770
	0.012317	1.216837		0.591208518	4770
	0.012327	1.219388		0.591673493	4780
	0.012338	1.221939		0.592222273	4790
	0.012347	1.227041		0.592678726	4810
	0.012357	1.22449		0.593152106	4800
	0.012369	1.229592		0.593696654	4820
	0.01238	1.232143		0.594234884	4830
	0.01239	1.234694		0.594738007	4840
	0.012413	1.237245		0.595845163	4850
	0.012474	1.237245		0.598758996	4850
	0.012528	1.247449		0.601332009	4890
	0.012553	1.247449		0.60253787	4890
	0.012563	1.25		0.603043199	4900
	0.012573	1.25		0.603494287	4900
	0.012583	1.255102		0.60396564	4920
	0.01259	1.255102		0.604338229	4920
	0.012599	1.257653		0.604753256	4930
	0.012611	1.257653		0.605334938	4930

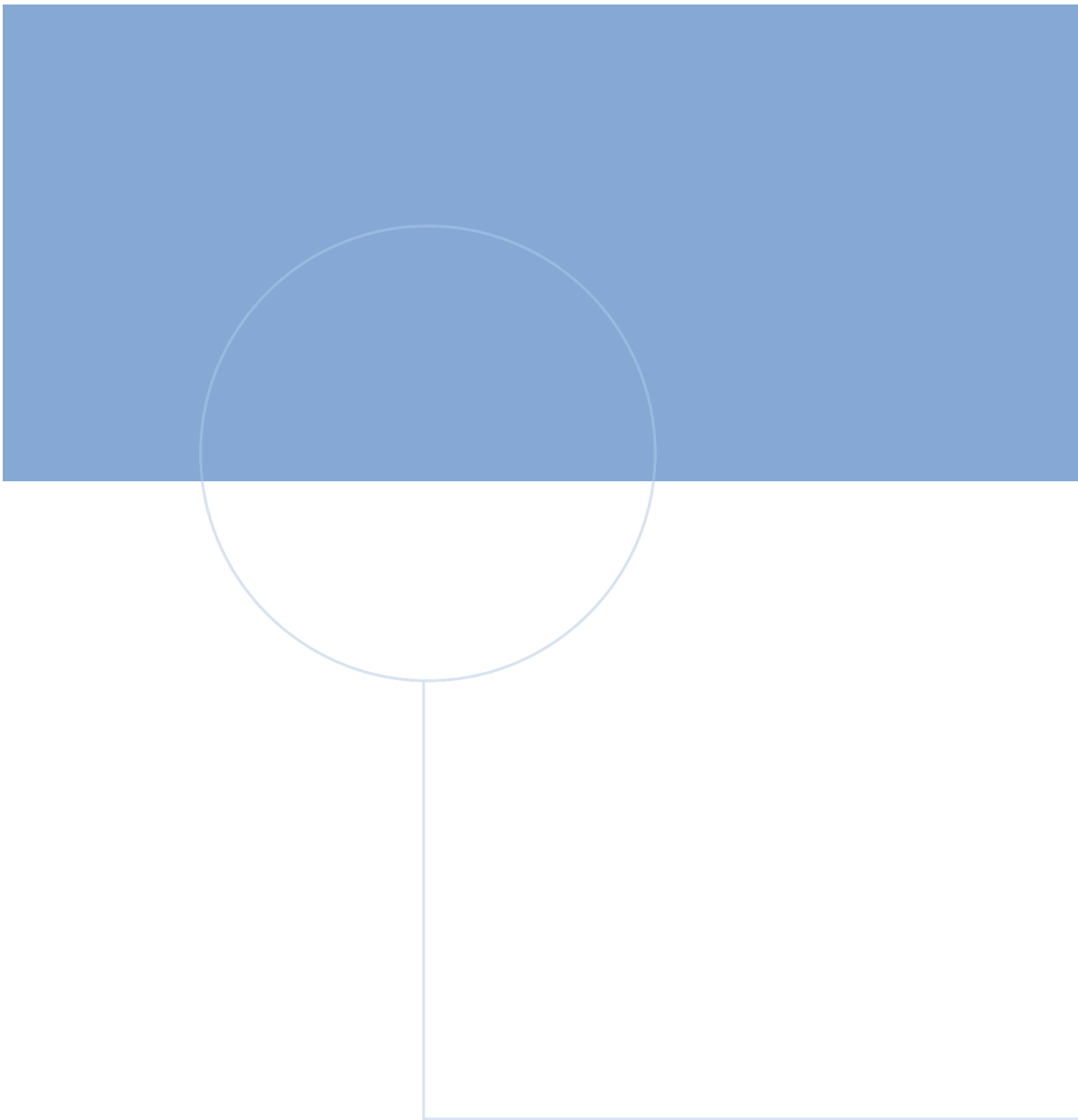

NTNU

Norwegian University of
Science and Technology